

ELECTRICAL CHARACTERIZATION OF CARBON BLACK FILLED RUBBER

by

Donald R. Parris

thesis submitted to the Faculty of the
Virginia Polytechnic Institute and State University
in partial fulfillment of the requirements for the degree of
Master of Science
in
Materials Engineering

APPROVED:

L.C. Burton, chairman

T.C. Ward

G.L. Wilkes

January 1986
Blacksburg, Virginia

ELECTRICAL CHARACTERIZATION OF CARBON BLACK FILLED RUBBER

by

Donald R. Parris

L.C. Burton, chairman

Materials Engineering

(ABSTRACT)

DC resistance and AC conductance and capacitance have been measured under various conditions in an effort to electrically characterize and make electrical-mechanical correlations for 15 carbon black filled rubber samples.

Resistance, conductance and capacitance have been monitored as functions of uniaxial compressive stress, time, temperature, and mechanical and thermal history. Capacitance and conductance have also been monitored as functions of frequency under various degrees of compressive loading and before and after specific heat treatments.

A direct relationship has been found between sample conductance and capacitance under any thermal and/or mechanical condition. This is in agreement with previous theories of conduction network formation and percolation. Various conduction mechanisms have been enumerated and an equivalent circuit of a network of lumped R-C "microelements" has been qualitatively described. Stress, relaxation, frequency, and temperature dependences of the macroscopic parameters meas-

ured (conductivity and capacitance) are discussed in terms of this model.

ACKNOWLEDGEMENTS

The author wishes to extend his most sincere appreciation to his committee chairman, Professor Larry C. Burton, who provided the opportunity, the tools, and the advice and direction to complete this endeavor. Also, thanks are due to the other committee members, Professor G.L. Wilkes and Professor T.C. Ward. for their help and inspiration.

Special thanks go to Hee Young Lee for his help and advice on the many experimental problems encountered.

TABLE OF CONTENTS

1.0 INTRODUCTION 1

2.0 LITERATURE REVIEW 4

2.1 CARBON BLACK 5

2.2 CARBON BLACK - POLYMER COMPOSITES 7

2.3 CONDUCTION MECHANISMS 8

2.4 EFFECT OF MIXING ON ELECTRICAL CONDUCTIVITY . . . 9

2.5 EFFECT OF VULCANIZATION ON ELECTRICAL CONDUCTIVITY 12

2.6 EFFECT OF STRESS, STRAIN, TIME AND TEMPERATURE ON
ELECTRICAL CONDUCTIVITY 13

 2.6.1 STRESS 15

 2.6.2 TIME 15

 2.6.3 TEMPERATURE 19

2.7 DIELECTRIC PROPERTIES 20

2.8 FREQUENCY DEPENDENCE OF THE POLARIZATION 22

2.9 DIELECTRIC MEASUREMENTS ON CARBON BLACK FILLED RUB-
BER 25

2.10 THERMAL CONDUCTIVITY 26

3.0 EXPERIMENTAL METHODS AND MATERIALS 28

3.1 RESISTANCE AS A FUNCTION OF TIME (STATIC) 35

3.2 RESISTANCE DURING AND AFTER COMPRESSIVE LOADING . 36

3.3 RESISTANCE AND STRESS RELAXATION 37

3.4	THERMAL RELIEF	39
3.5	CURRENT - VOLTAGE RELATIONSHIPS	39
3.6	CAPACITANCE AND CONDUCTANCE AS FUNCTIONS OF FRE- QUENCY	40
3.7	CAPACITANCE AND CONDUCTANCE DURING AND AFTER COMPRESSIVE LOADING	40
3.8	CAPACITANCE AND CONDUCTANCE TRENDS WITH MECHANICAL HISTORY	41
3.9	THERMOELECTRIC EFFECT	42
3.10	THERMAL CONDUCTIVITY	42
4.0	RESULTS AND DISCUSSION	45
4.1	RESISTANCE AS A FUNCTION OF TIME (STATIC)	45
4.2	RESISTANCE DURING AND AFTER COMPRESSIVE LOADING	47
4.3	RESISTANCE AND STRESS RELAXATION	58
4.4	TEMPERATURE EFFECTS	60
4.5	THERMAL RELIEF	64
4.6	CURRENT - VOLTAGE RELATIONSHIPS	67
4.7	CAPACITANCE AND CONDUCTANCE AS FUNCTIONS OF FRE- QUENCY	68
4.8	CAPACITANCE AND CONDUCTANCE DURING AND AFTER COMPRESSIVE LOADING	68
4.9	CAPACITANCE AND CONDUCTANCE TRENDS WITH MECHANICAL HISTORY	78
4.10	EQUIVALENT CIRCUIT MODEL	89
4.11	THERMOELECTRIC EFFECT	94

4.12 THERMAL CONDUCTIVITY	96
5.0 CONCLUSIONS AND RECOMMENDATIONS	100
APPENDIX A. RESISTANCE "SIGNATURES"	105
BIBLIOGRAPHY	115
VITA	119

LIST OF ILLUSTRATIONS

Figure 1.	Resistivity as a function of carbon black concentration	6
Figure 2.	Various properties as a function of mixing	11
Figure 3.	Resistivity as a function of vulcanization time	14
Figure 4.	Resistivity as a function of elongation	16
Figure 5.	Dielectric constant as a function of frequency	24
Figure 6.	Dielectric constant as a function of frequency	27
Figure 7.	Carbon black filled rubber sample with brass electrodes	29
Figure 8.	Apparatus for testing electrical behavior	38
Figure 9.	Apparatus for measuring thermal conductivity	44
Figure 10.	Standardized load profile for testing electrical response	48
Figure 11.	Resistance response to a standardized load profile (NAT14)	51
Figure 12.	Resistance response to a standardized load profile (NAT15)	52
Figure 13.	Resistance response to a standardized load profile (NAT18)	53
Figure 14.	Resistance response to a standardized load profile (NAT38)	54
Figure 15.	Resistance response to a standardized load profile (NAT42)	55
Figure 16.	Resistance and stress as functions of temperature	61
Figure 17.	Capacitance versus frequency at various temperatures	65
Figure 18.	Conductance versus frequency at various temperatures	66

Figure 19. Capacitance versus frequency for "virgin" samples	69
Figure 20. Conductance versus frequency for "virgin" samples	70
Figure 21. Capacitance and conductance versus pressure (sample NAT1)	72
Figure 22. Capacitance and conductance versus pressure (sample NAT42)	73
Figure 23. Capacitance versus pressure at 100Hz for all samples	74
Figure 24. Conductance versus pressure at 100Hz for all samples	75
Figure 25. Capacitance versus conductance for several pressures at 100Hz	76
Figure 26. Capacitance versus frequency for NAT14 in various "states"	79
Figure 27. Conductance versus frequency for NAT14 in various "states"	80
Figure 28. Capacitance versus frequency for NAT15 in various "states"	81
Figure 29. Conductance versus frequency for NAT15 in various "states"	82
Figure 30. Capacitance versus frequency for NAT18 in various "states"	83
Figure 31. Conductance versus frequency for NAT18 in various "states"	84
Figure 32. Capacitance versus frequency for NAT38 in various "states"	85
Figure 33. Conductance versus frequency for NAT38 in various "states"	86
Figure 34. Capacitance versus frequency for NAT42 in various "states"	87
Figure 35. Conductance versus frequency for NAT42 in various "states"	88

Figure 36. Capacitance versus frequency for "virgin" and degraded samples	90
Figure 37. Capacitance versus frequency for "virgin" and degraded samples	91
Figure 38. Conductance versus frequency for "virgin" and degraded samples	92
Figure 39. Capacitance versus frequency for "virgin" and degraded samples	93
Figure 40. Equivalent circuit for carbon black filled rubber	95
Figure 41. Resistance response to a standardized load profile (NAT25A)	105
Figure 42. Resistance response to a standardized load profile (NAT1)	106
Figure 43. Resistance response to a standardized load profile (NAT16)	107
Figure 44. Resistance response to a standardized load profile (NAT41)	108
Figure 45. Resistance response to a standardized load profile (NAT44)	109
Figure 46. Resistance response to a standardized load profile (NAT43)	110
Figure 47. Resistance response to a standardized load profile (NAT57)	111
Figure 48. Resistance response to a standardized load profile (NAT60)	112
Figure 49. Resistance response to a standardized load profile (NAT61)	113
Figure 50. Resistance response to a standardized load profile (NAT22A)	114

LIST OF TABLES

Table 1.	Sample compositions	30
Table 2.	Sample compositions (cont.)	31
Table 3.	Sample compositions (cont.)	32
Table 4.	Sample compositions (cont.)	33
Table 5.	Carbon black filled rubber sample properties	34
Table 6.	Sample resistances original and at 15 months with no mechanical	46
Table 7.	Pressure test samples and some corresponding data (reference 64)	49
Table 8.	Carbon black filled rubber sample resistances at two temperatures	62
Table 9.	Thermal conductivity values for all samples	98

1.0 INTRODUCTION

Tracked military vehicles such as tanks, armored personnel carriers, self-propelled artillery and certain recovery vehicles utilize rubber pads on their tracks for the purpose of damping vibration, reducing noise, and preventing unnecessary damage to the built-up surfaces such as concrete, asphalt and macadam over which these vehicles must often travel. These rubber pads generally consist of a crosslinked elastomer using sulfur as a crosslinking agent and zinc oxide as an accelerator. Additionally, reinforcing fillers (carbon black), processing aids, antidegradants, and other diluents are added to form the final vulcanizate. The molded product is then bonded to a steel backing plate and bolted to the track of the vehicle.

The United States Army's Tank and Automotive Command (TACOM) is currently conducting a systematic, in-depth study for improving the field-service life of these track pad materials. The scope of the work described in this thesis was designed to assist the TACOM study by determining if electrical measurements would be useful in this task. The goals of this specific study are:

1. To determine if electrical measurements can be used to distinguish between various types of rubbers of different

compositions and/or between various track pads of the same composition that have different manufacturers and/or service histories;

2. To obtain more fundamental information about the electrical properties of the carbon black filled rubber and, if possible, to correlate these with mechanical properties;
3. To make recommendations as to the feasibility of electrical measurements toward improving the reliability of track pad rubber, and make recommendations for future work.

The electrical parameters of carbon black that have been measured here are resistance and capacitance and their dependence on pressure, temperature, time, and mechanical history. Other physical properties such as thermal conductivity and expansion are monitored either quantitatively or qualitatively as necessary. None of these parameters is well understood theoretically, since each depends on complicated processes in the carbon black-rubber composite.

The author believes that electrical properties as measured in this study are very sensitive indicators of the "state" of the carbon black-rubber composite at any time. Character-

istic responses and trends in electrical and electro-mechanical behavior have been identified.

2.0 LITERATURE REVIEW

Many studies have been done on carbon black filled elastomers. There are many types of carbon blacks and elastomers available to form these composites. The original purpose of creating such a composite was to increase the strength and durability of an elastomer while still retaining sufficient elastomeric behavior. Carbon black has long been used as a reinforcing agent in these composites (1,2) because of its low cost, ready availability, and phenomenal reinforcing ability.

Most rubbers have long been appreciated as good electrical insulators (non-conductors) with resistivities in the range of 10^{13} - 10^{16} ohm-cm (3). Carbon black would be classified as a moderately good conductor with resistivities in the range of 10^3 - 10^6 ohm-cm. A composite of the two would therefore have a resistivity that is a function of the relative concentrations of each. The relation between carbon black concentration in an elastomer and the composite resistivity for a particular carbon black filled sample can be seen in Figure 1. The weight percent of carbon black at which the transition from high to low resistivity occurs is a function of carbon black and polymer type and extent of mixing but this relation is clearly non-linear. The addition of about 20 weight percent carbon black reduces the composite

resistivity by about 90% of its total change in resistivity between 0 and 100 weight percent carbon black. The reason why this occurs can be better understood by looking further into the physical nature of these composites.

2.1 CARBON BLACK

Carbon black is typically made of solid or hollow spheres of partly graphitized carbon which are most always fused together in clusters of branched, irregular shape (2,5). These clusters are referred to as aggregates or agglomerates. The carbon black particles (spheres) may be as small as 140 angstroms in diameter or as large as 3000 angstroms (6), and the agglomerates may contain up to around several hundred of these particles (5). Carbon black is typically formed by subjecting oil droplets to extremely high temperatures (2). The processing conditions determine the particle and agglomerate size and structure.

Gas molecules are easily adsorbed onto the carbon black surface and thus the effective surface area can be determined. This measurement will be roughly inversely proportional to the carbon black particle size. Surface area can be determined by adsorbing nitrogen or cetyltrimethylammonium bromide (CTAB) molecules (7,8), but the ASTM standard test uses iodine adsorption for surface area assessment (9).

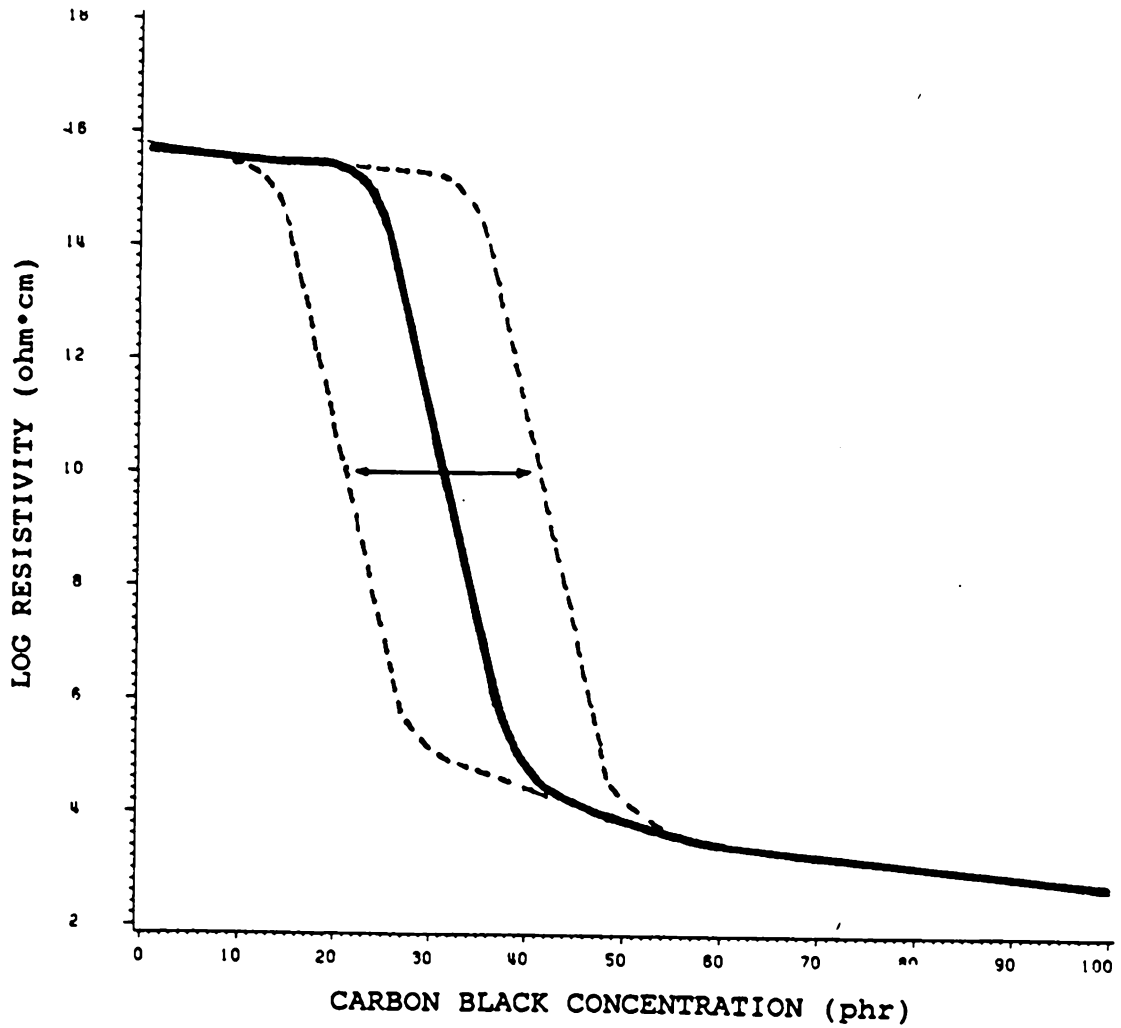


Figure 1. Resistivity as a function of carbon black concentration. The weight percent of carbon black at which the transition from high to low resistivity occurs is a function of carbon black and polymer type and extent of mixing.

The carbon black structure is related to how many particles make up an agglomerate and their three dimensional arrangement. This feature is quantified by adding a vehicle such as linseed oil or dibutyl phthalate (DBP) to a quantity of carbon black to the point where the mixture changes form a crumbly powder to a stiff paste, and then to a soft ball (5). At this point it is believed that the vehicle has filled the voids within and between the agglomerates and these voids are a function of the degree of agglomerate structure (10,11).

2.2 CARBON BLACK - POLYMER COMPOSITES

When carbon black is introduced into a supporting media the agglomerates may flocculate under the influence of London-Van der Waals forces (12,13). These processes are governed by the viscosity of the media; however, given sufficient time and/or mobility a network of interconnected carbon black agglomerates can be formed. It is this network formation that is used to explain the onset of conduction in a carbon black-polymer composite at the low carbon black loadings observed (4).

The volume of carbon black at which the change in conductance occurs most rapidly is sometimes called the percolation threshold. The percolation threshold for real mixtures of conducting particles in an insulating matrix as

statistically determined by Kirkpatrick (14), if insulating and conducting regions have on average a similar shape, is 25 volume percent. Bueche (15) has applied Flory's theory of gel formation (16) to model this effect of sudden onset of conduction ("gelation") at a certain level of carbon black ("crosslink") content.

Hollow carbon black spheres (17,18) have been found to reach their percolation threshold at lower loadings than their solid sphere counterparts. This is because these agglomerates can have the same external dimensions, which are critical for network formation, at a lower density due to their porosity.

2.3 CONDUCTION MECHANISMS

DC conduction will be a direct function of the conducting paths formed by inter-agglomerate contacts across a sample. The number of contacts and the resulting extent of "network" formation are functions of the particle size (19), and the agglomerate size (14), size distribution (20), and structure.

Electron micrographs of carbon black filled rubber at low loadings have shown that even though there isn't enough carbon black present to form a continuously connected network of agglomerates, there is a measurable conductivity. This has suggested that electronic charge must tunnel through the polymer between the carbon black agglomerates and that the

conduction here is controlled by this effect (13,18,21,22). Others have investigated electron hopping as a conduction mechanism (23). The distance between particles and agglomerates is an important parameter here and has been evaluated by Oono (24) using a Fraunhofer diffraction technique.

In addition to the possible variations in physical dispersion of the carbon black in a rubber and the corresponding conduction mechanisms, the presence of a thin immobilized or second "phase" polymer layer on the carbon black agglomerate surface has been suggested in separate studies by Kaufman (25) and Pliskin and Tokita (26).

It is certain that many conduction processes can take place in these mixtures, any one of which may be predominant in given circumstances. Each type of conduction responds differently to variations in applied voltage and temperature. In addition, the matrix will expand or contract with the same variations, which much complicates differentiating and identifying each effect.

2.4 EFFECT OF MIXING ON ELECTRICAL CONDUCTIVITY

DC conductivity as a function of mixing time has been thoroughly documented for rubber-carbon black systems (4,27-31). Carbon blacks are blended into an elastomer matrix in a mill which ultimately reduces the elastomer's molecular

weight and the agglomerates' size by as much as 50% or more depending on variables such as time, temperature, speed, and shear force of mixing (5,32,33). The mixing action also favors formation of bonded polymer at the carbon black surface (33,34,35). Thus, with more thorough mixing, an initially conductive carbon black network may be destroyed by agglomerate breakup and polymer adherence at the interface which would serve to insulate agglomerates from one another and inhibit reformation of the inter-agglomerate contacts (21,33,36).

A typical plot of various properties versus mixing time for a carbon black filled rubber is shown in Figure 2 (37). The curves shown here are for a particular carbon black filled elastomer, but the same trends are expected for other carbon black filled elastomers.

Note how the moduli and dispersion curves level off after a few minutes while the resistivity continues to rise sharply. This has been shown as evidence that resistivity during mixing is not related to mechanical properties (37). In reality the resistivity during mixing is thought to be a measure of "micro"-dispersion which cannot be seen optically (31,37) and even though it may be a poor indicator of the modulus, it may correlate with some other important mechanical property such as "time to failure" in a cyclically loaded sample.

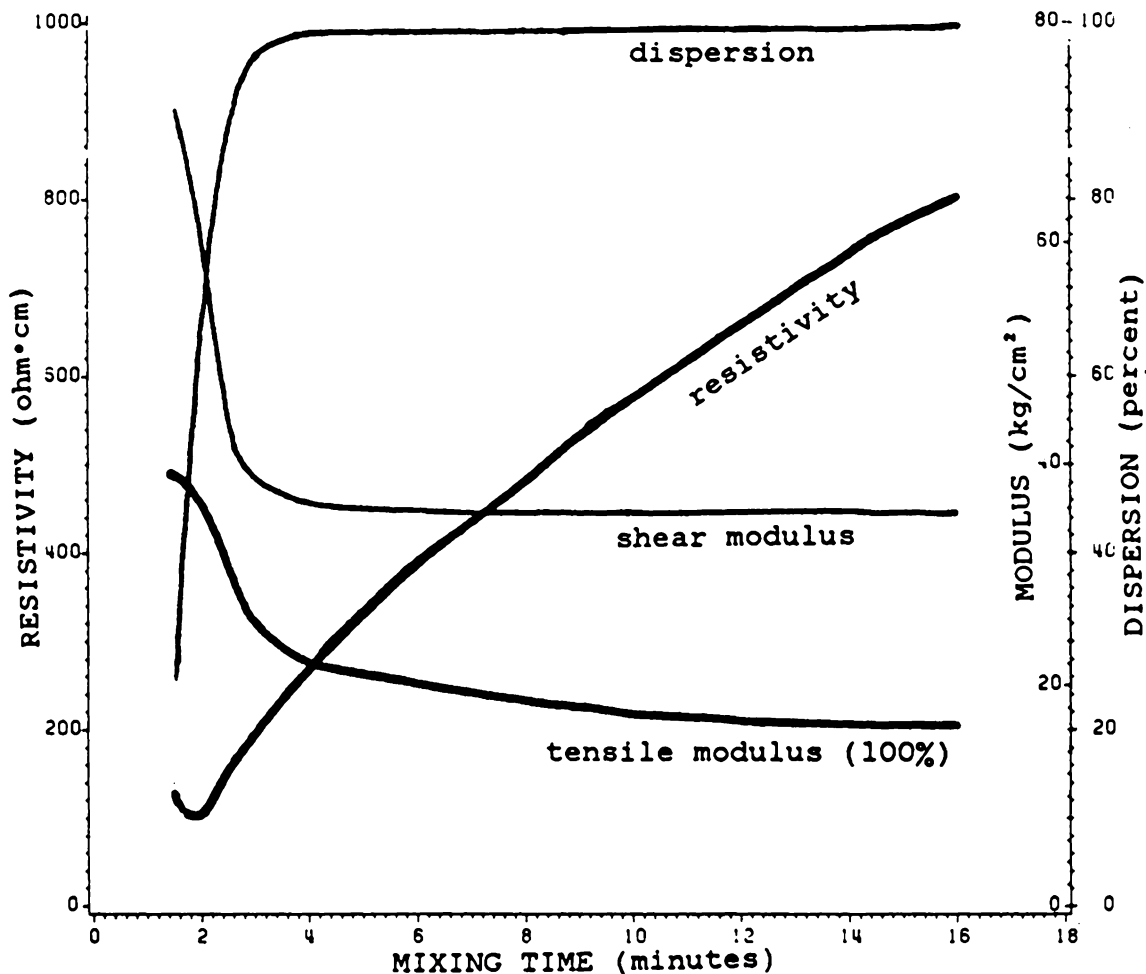


Figure 2. Various properties as a function of mixing. These curves are for a particular carbon black filled elastomer, but the same trends are expected for other carbon black filled elastomers.

Hess, Swor and Micek (38) have reported that for an 80 phr carbon black filled SBR, an improvement in dispersion by tripling the total mixing energy approximately doubled the characteristic fatigue life under cyclic load.

2.5 EFFECT OF VULCANIZATION ON ELECTRICAL CONDUCTIVITY

Mixing of a rubber formulation is understandably done at a lower than vulcanization temperature and the dispersion as measured by electrical resistance increases with increasing mixing. As the mixture temperature is later increased for vulcanization to occur, the electrical resistance will decrease with time at temperature. A plot of this effect for three samples with 60 phr carbon black but with different mixing procedures is shown in Figure 3, (4). This process is thought to be the result of re-formation of the inter-agglomerate network which was broken down on mixing. Here the attractive forces between agglomerates are the same, but the agglomerates' mobility has been increased thermally. Thus the extent of network re-formation will depend on the extent of previous network breakdown and the time at the elevated temperature that the agglomerates have to orient before the polymer matrix "gels".

Another possibility is that during vulcanization there may be a reaction in which sulfur becomes a chemical bond between the carbon black surface and the polymer chains. This would

facilitate transfer of electrons to the polymer and thus reduce resistivity (30).

2.6 EFFECT OF STRESS, STRAIN, TIME AND TEMPERATURE ON ELECTRICAL CONDUCTIVITY

Bulgin (27) performed the first systematic study on the effects of strain, time, and temperature on carbon black filled elastomers. This work gave rise to the basic logic behind these composites' behavior. The general results are:

1. The thermal coefficient of resistance (TCR) of the composite is most often not equal to the TCR of the conductive carbon black filler. Thus the conduction between carbon black entities may be controlled by the thermal expansion of the matrix.
2. The effect of uni- or bi-directional tensile strain is to disrupt the conductive carbon black network by orienting their statistical distribution and thus raise the composite's resistivity. After removal of this strain at the same temperature the network structure will "re-form".
3. The rate of network "re-formation" can be accelerated with higher temperatures.

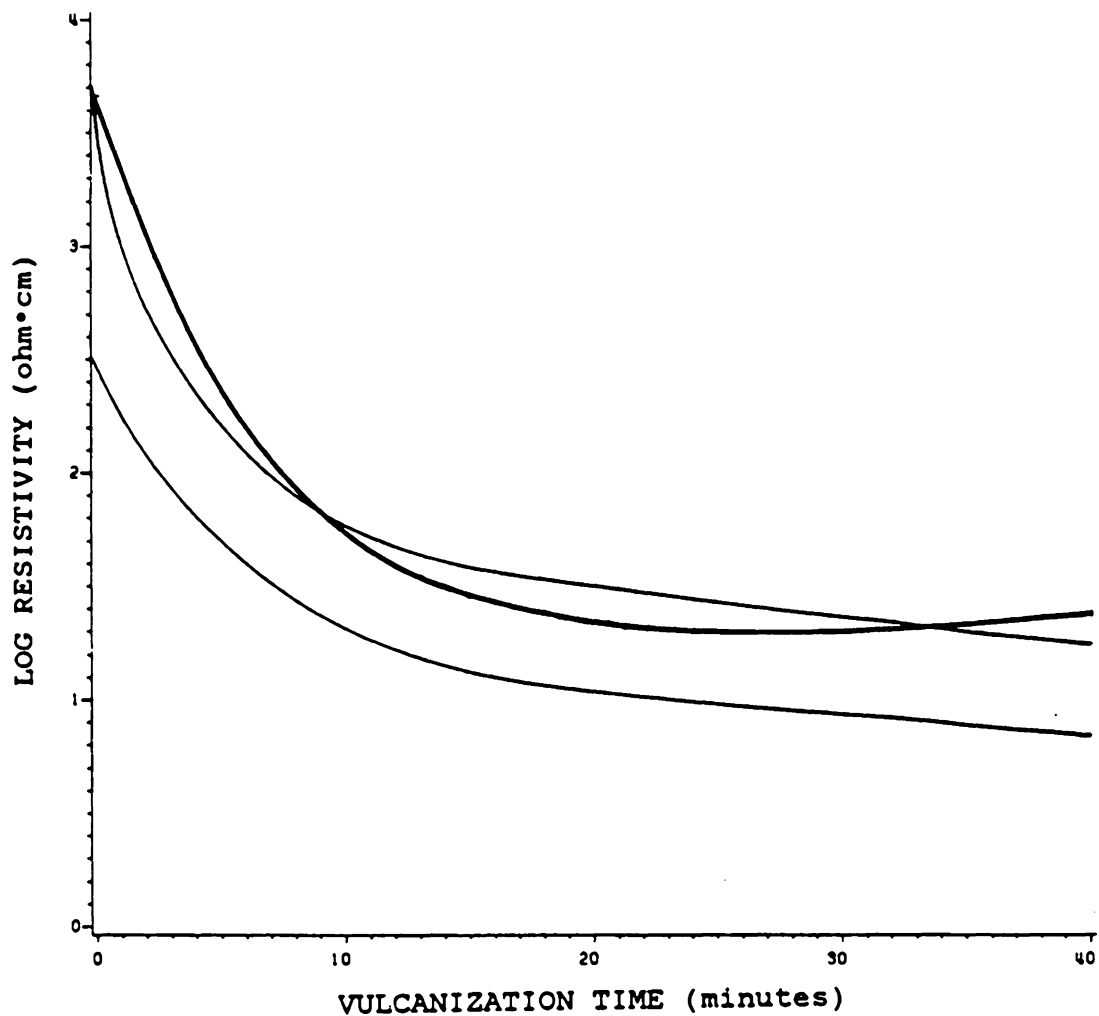


Figure 3. Resistivity as a function of vulcanization time. Three natural rubber samples with 60 phr carbon black and different mixing procedures are shown (reference 4).

2.6.1 STRESS

The effect of tensile stress on electrical conductivity of carbon black filled rubbers has been studied and reported (4,39,40). A typical response is shown in Figure 4 (40). Here as a piece of carbon black filled rubber is stretched, the resistance initially increases, reaches a maximum, and then decreases. This behavior is thought to be due to the breakup of the conducting network at lower elongations followed by the formation of another conducting network at higher elongations (4,39-42). It must be remembered that this is a three dimensional problem and as the elastomer is stretched in one direction it will simultaneously retract in the other two directions. The transverse resistance during elongation was also monitored in reference 40, showing the same trends as the longitudinal resistance.

A decrease in electrical resistance with applied hydrostatic pressure has been reported by Sodolski, et.al. for a carbon black filled polyester (43).

2.6.2 TIME

Time dependent behavior for carbon black filled vulcanizates has been widely investigated in stress relaxation studies (13,38,44-52).

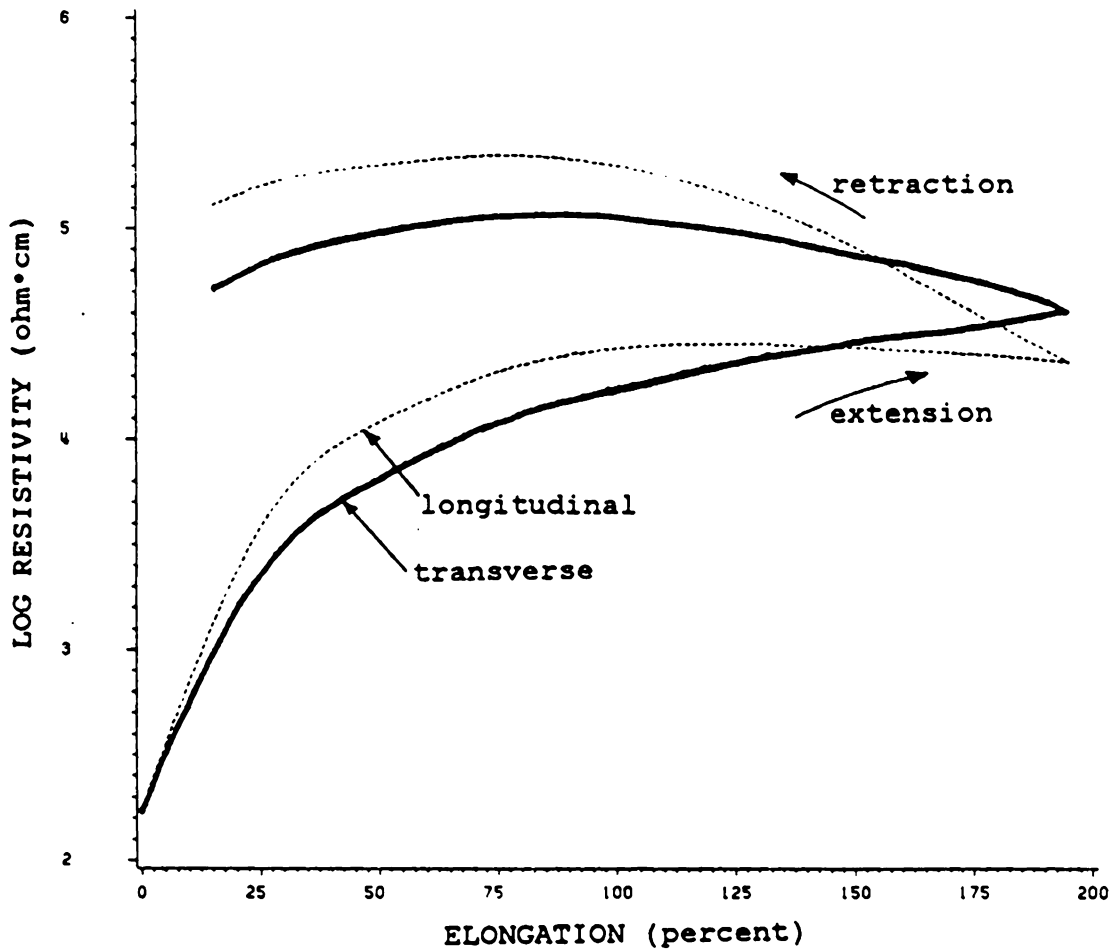


Figure 4. Resistivity as a function of elongation. This sample's resistivity was measured in the longitudinal and transverse directions during extension and retraction.

In early investigations Gent (44) found that for both unfilled and carbon black filled natural rubber vulcanizates linear plots were obtained of stress versus log (time). The slope of such plots was independent of strain for the unfilled vulcanizates up to levels at which stress induced crystallization occurred. The slopes of the plots for filled vulcanizates were dependent upon strain and were greater than those from the unfilled vulcanizates at the same strain. Gent proposed a similarity in viscoelastic mechanisms for filled and unfilled vulcanizates.

In later investigations Cotten and Boonstra (45) and Voet, Sircar and Cook (46) plotted log (stress) versus log (time) to get a linear relationship. This implied a power law relationship

$$\sigma(t) = at^{-n}$$

between stress and time which was further investigated.

Bartenev (47) has modeled stress relaxation in carbon black filled natural rubber vulcanizates. He proposed the existence of discrete elementary relaxation mechanisms and has provided a method to differentiate between these mechanisms when they are present. Mechanisms which he proposed are; relaxation of free segments of chain molecules, relaxation of elements of the supramolecular structure, relaxation of the carbon black filler network and chemical crosslink relaxation. Bartenev also considers and treats the possibility of a spectrum of relaxation mechanisms.

Payne (48,49,50) has observed in dynamic mechanical measurements on carbon black filled rubbers that at high carbon black loadings and at low strain amplitudes the magnitude of the modulus is very strongly dependent upon strain amplitude. He attributed this dependence to the existence within the carbon black filled vulcanizate of a structure which is progressively destroyed as the stress increases. He also concluded that because there was no frequency dependence of dynamic modulus that re-formation of the structure occurred very rapidly. MacKenzie and Scanlan (51) further reinforced this rapid re-formation conclusion by performing tensile stress relaxation experiments on pre-strained carbon black filled natural rubber samples. No significant differences in stress relaxation was found for the pre-strained samples versus the non pre-strained samples. However, their shortest time between pre-straining and testing was 1 minute and they considered that the vulcanizate may have been able to recover within this period. (NOTE - approximately 10% strain was used in these studies)

Meier, Kuster and Mandell (52) have measured stress relaxation at various temperatures and applied time-temperature superposition to produce stress relaxation master curves.

2.6.3 TEMPERATURE

Temperature dependence of the conductivity of a carbon black filled rubber is a function of the response of the rubber and/or the carbon black and/or the physical state of the conductive network in the matrix. Positive and negative temperature coefficients of resistivity (PTC & NTC) have been found for carbon black filled polymers (13).

PTC behavior is generally explained by the fact that the thermal expansion of the rubber is known to be at least 50 times larger than that of carbon black (53). Thus when the composite is heated the rubber matrix expansion causes the conductive network to be reduced by breakage of inter-agglomerate contacts and by increasing the distances between agglomerates.

NTC behavior can be attributed to several mechanisms. As pure carbon black can act as a semiconductor, so might carbon black in a carbon black-polymer composite. An increase in temperature would free more electrons and conductivity would increase. If the conductivity is controlled by tunnelling or hopping then an increase in temperature would give the charge carriers more energy which would effectively lower the barrier thickness or height.

2.7 DIELECTRIC PROPERTIES

A dielectric material is characterized by a dielectric constant which relates the electric flux density D to the electric field E by the relationship;

$$D = \epsilon E = K\epsilon_0 E$$

where ϵ is the product of ϵ_0 (permittivity of free space) and K (relative dielectric constant).

If a potential is applied across a vacuum, new charges arrive at each electrode surface. The charge per unit area of each surface is then

$$Q/A = \epsilon_0 V/d .$$

When a dielectric material replaces the vacuum at the same potential difference, more charges arrive at the surfaces. The charge of each surface is then

$$Q'/A = \epsilon_0 K V/d .$$

If we let P equal the amount of excess charge over that of the vacuum then

$$P = Q'/A - Q/A = E (\epsilon - \epsilon_0) .$$

P is accordingly called the polarized surface charge density.

When an electric field is applied the opposite charges attract one another and the polarizable entities become polarized. For each entity there will then be equal and opposite charges, q , separated by a distance δ . This constitutes an induced dipole with a dipole moment of

$$\mu = q\delta.$$

If N is equal to the number of polarizable entities per unit volume, then $N\mu$ equals the total charge per unit area and is equal to the polarized surface charge density P .

For low electric fields it can be assumed that the dipole moment is proportional to the local electric field E' :

$$\mu = \alpha E'$$

where α is a constant called the polarizability.

Derivations of the local electric field E' are presented in references 54 and 55. Here the relation between E' and the macroscopic field E and the polarized surface charge density P is shown to be

$$E' = E + P/3\epsilon_0$$

An important assumption in this derivation is that the material of interest is homogeneous. This is clearly not the case in carbon black filled rubbers.

Rearranging $Q'/A = \epsilon_0 K V/d$ we can get

$$Q' = \epsilon_0 K A V/d$$

Thus Q' is proportional to V by $\epsilon_0 K A/d$ which is the capacitance (C)

$$C = \epsilon_0 K A/d$$

Capacitance is an easily measured macroscopic property which is proportional to the dielectric constant of the material assuming all other variables to be constant.

When an insulating material is placed in an electric field it becomes polarized due to the relative displacement of positive and negative electric charges in the material.

The total polarization in any material is made up of different components, according to the nature of the charges of displacement. Electronic polarization is due to the relative displacement of the electrons and nuclei of the atoms. Atomic polarization is due to the relative displacement of the atoms in a molecule, involving the stretching, twisting, or bending of chemical bonds. In an ionic solid the corresponding effect is the relative displacement of the ions. Orientation polarization occurs only in dipolar materials. It is due to a perturbation of the thermal motion of the dipoles, which tend to rotate into positions more favorable to the electric field. Interfacial or Maxwell-Wagner polarization occurs in heterogeneous materials where one component has a higher conductivity than the other.

2.8 FREQUENCY DEPENDENCE OF THE POLARIZATION

For any type of polarization, if the applied electric field is alternating at a sufficiently low frequency, the polarization will also alternate. With increasing frequency, the polarization will eventually have difficulty in following the field and will not have time to attain its full value before the field reverses. Here there will be a loss, or ab-

sorption, of electrical energy which causes heating in the dielectric. A simple mechanical analogy is a pendulum of length " δ ". A short δ will be able to follow a certain maximum frequency and all lower frequencies. As δ increases, its maximum "response" frequency decreases. A plot of dielectric constant ("response") versus frequency for a model dielectric possessing all four types of polarization ("length") can be seen in Figure 5, (56).

Each polarizable entity in a material can be characterized by its ability to respond to an alternating field. This is often measured as a relaxation time (τ) which characterizes the rate of build-up or decay of the polarization when an electric field is applied or removed.

The frequency dependence of the relative permittivity (dielectric constant) ϵ' and dielectric loss factor ϵ'' are described by the Debye equations (57,58).

$$\epsilon' = \epsilon_{\infty} + \frac{\epsilon_s - \epsilon_{\infty}}{1 + \omega^2 \tau^2}$$

$$\epsilon'' = (\epsilon_s - \epsilon_{\infty}) \frac{\omega \tau}{1 + \omega^2 \tau^2}$$

where ϵ_s and ϵ_{∞} are the permittivities at frequencies below and above the absorption, respectively, and ω is the frequency

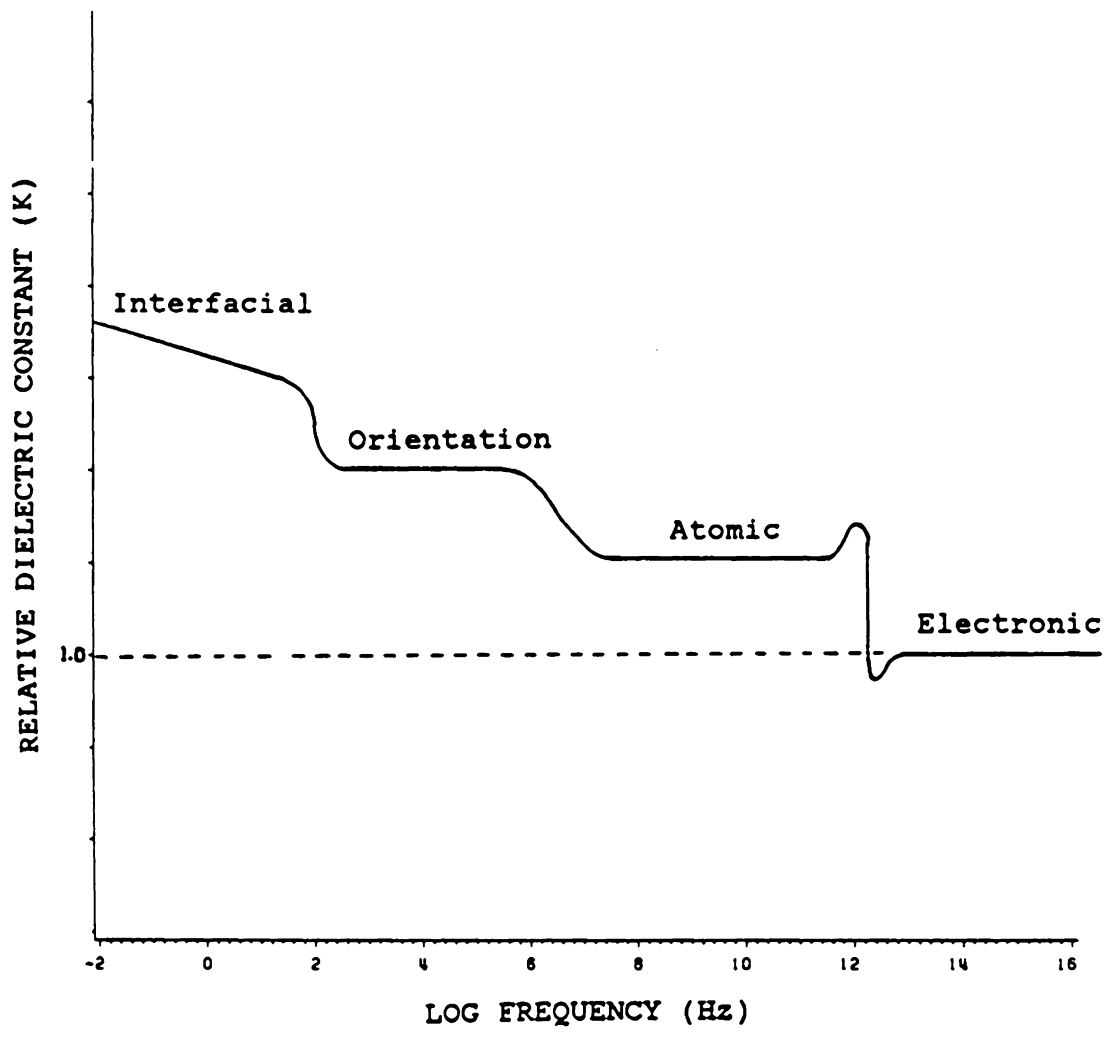


Figure 5. Dielectric constant as a function of frequency. This is a generic curve for a model dielectric exhibiting all four types of polarization.

in radians per second. These equations are generally for a dielectric with one characteristic relaxation time, but can be applied separately to each relaxation mechanism if there is more than one.

2.9 DIELECTRIC MEASUREMENTS ON CARBON BLACK FILLED RUBBER

The dielectric properties of carbon black filled rubber have been measured by Lukomskaya and Dogadkin (59) under no load conditions.

The inclusion of carbon black into a rubber vulcanizate gives rise to a complex dielectric behavior. The dielectric properties arise from the following components:

1. Normal dipole loss from the sulfur-rubber chains,
2. Conductivity losses due to direct conduction paths of linked carbon agglomerates in the matrix,
3. Maxwell-Wagner losses due to the conducting carbon particles in a non-conducting matrix and
4. "Structural" losses characterized by a loss which is independent of temperature and frequency at a given carbon black loading.

The losses in number 4 above are a function of the actual structure formed by the carbon black in the mixture and give rise to a high frequency dielectric constant ϵ' which is larger than the high frequency dielectric constant of the unfilled sulfur vulcanizate.

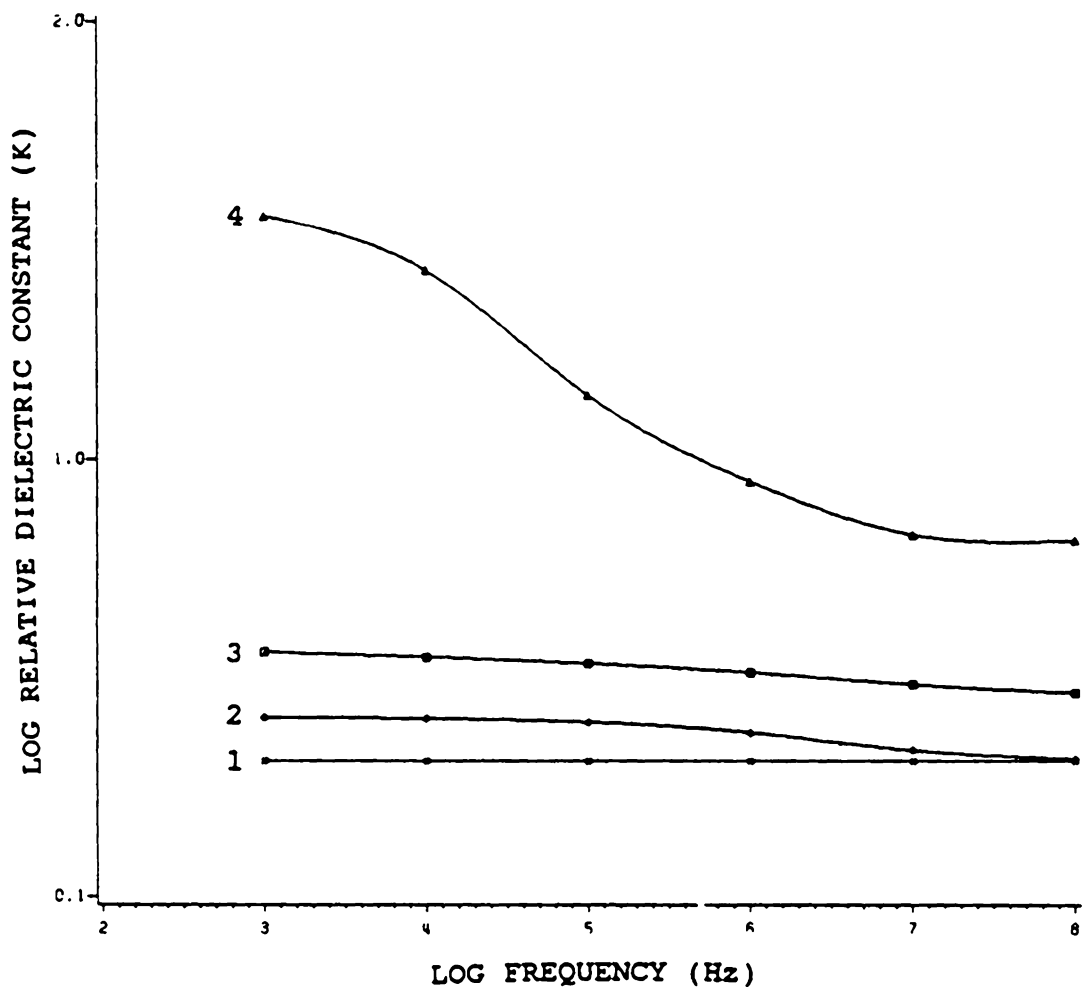
The dielectric constant as a function of frequency is plotted in Figure 6 for Hevea rubber samples which have been unvulcanized, vulcanized without carbon black, and vulcanized with different loadings of carbon black (60). Carbon black addition is shown to greatly increase the dielectric constant at all frequencies, but its effect is greatest at lower frequencies.

Lukomskaya and Dogadkin (59) have reviewed work in this area and have outlined a method of separating the dielectric properties into the conductivity, Maxwell-Wagner, "structural" and dipolar contributions, and have illustrated the method for experimental systems.

2.10 THERMAL CONDUCTIVITY

The thermal conductivity for many materials is related to the electrical conductivity as electrons are often the major carriers of electrical charge and thermal energy.

The thermal conductivity of vulcanized pure natural rubber at room temperature has been reported to be $\approx .0015\text{J/cm s K}$ (61).



- STATE 1 - pale crepe rubber (unvulcanized)
- STATE 2 - 100 phr pale crepe rubber, 6 phr sulfur, (vulcanized)
- STATE 3 - 100 phr pale crepe rubber, 1 phr stearic acid, acid, 10 phr carbon black, 5 phr Kadox, 0.5 phr Captax, 3 phr sulfur, (vulcanized)
- STATE 4 - 100 phr pale crepe rubber, 1 phr stearic acid, 40 phr carbon black, 5 phr Kadox, 1 phr Captax, 3 phr sulfur, (vulcanized)

Figure 6. Dielectric constant as a function of frequency before and after vulcanization and carbon black addition (reference 60).

3.0 EXPERIMENTAL METHODS AND MATERIALS

Carbon black filled rubber samples used in this study were obtained from the U.S. Army Materials Research and Development Laboratory in Fort Belvoir, Virginia. Supplied were two sample types each of 15 different carbon black filled rubber compositions. One sample type, for electrical measurements, was 0.5" X 1" X 1" in dimension with brass plates bonded onto each face during vulcanization to serve as electrical contacts (see Figure 7). It has been found that this type of contact has the minimum attainable contact resistance for such a carbon black filled composite (4). Two samples of each composition were provided. One of these samples was mechanically tested, one was kept as a control. The other sample type was for thermal conductivity measurement and these were 0.075" X 2" X 2" in dimension. Two samples of each composition were also provided here and both were used in thermal conductivity measurements. Sample compositions are listed in Tables 1-4. Sample mechanical properties as measured at Ft. Belvoir, VA (62) are listed in Table 5.

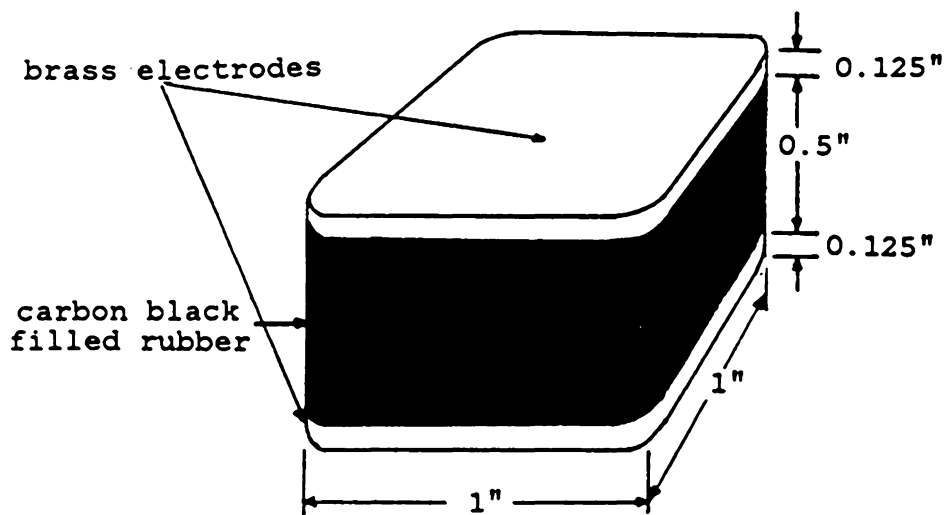


Figure 7. Carbon black filled rubber sample with brass electrodes

Table 1. Sample compositions

INGREDIENT	NAT25A	NAT14	NAT1	NAT15
RUBBER	NR	NR	NR	NR
CARBON BLACK TYPE	N-110	N-110	N-110	N-110
CARBON BLACK QTY. (PHR)	45	45	45	45
SULFUR (PHR)	0.75	1.5	2.5	5.0
ZINC OXIDE (PHR)	4.0	4.0	4.0	4.0
STEARIC ACID	2.0	2.0	2.0	2.0
AGERITE RESIN D	0.5	0.5	0.5	0.5
AGERITE WHITE	0.5	0.5	0.5	0.5
ANTOZITE 2	3.0	3.0	3.0	3.0
SANTOCURE	0.8	0.8	0.8	0.8

Table 2. Sample compositions (cont.)

INGREDIENT	NAT16	NAT18	NAT41
RUBBER	NR	NR	NR
CARBON BLACK TYPE	N-220	N-234	N-299
CARBON BLACK QTY. (PHR)	45	45	45
SULFUR (PHR)	2.5	2.5	2.5
ZINC OXIDE (PHR)	4.0	4.0	4.0
STEARIC ACID	2.0	2.0	2.0
AGERITE RESIN D	0.5	0.5	0.5
AGERITE WHITE	0.5	0.5	0.5
ANTOZITE 2	3.0	3.0	3.0
SANTOCURE	0.8	0.8	0.8

Table 3. Sample compositions (cont.)

INGREDIENT	NAT42	NAT44	NAT43	NAT38
RUBBER	NR	NR	NR	NR
CARBON BLACK TYPE	N-326	N-330	N-351	N-472
CARBON BLACK QTY. (PHR)	45	45	45	45
SULFUR (PHR)	2.5	2.5	2.5	2.5
ZINC OXIDE (PHR)	4.0	4.0	4.0	4.0
STEARIC ACID	2.0	2.0	2.0	2.0
AGERITE RESIN D	0.5	0.5	0.5	0.5
AGERITE WHITE	0.5	0.5	0.5	0.5
ANTOZITE 2	3.0	3.0	3.0	3.0
SANTOCURE	0.8	0.8	0.8	0.8

Table 4. Sample compositions (cont.)

INGREDIENT	NAT57	NAT61	NAT60	NAT22A
RUBBER	NR	NR	NR	NR
CARBON BLACK TYPE	N-110/ XE-2	N-110/ XE-2	N-220	N-110
CARBON BLACK QTY. (PHR)	30/10	30/10	60	45
SULFUR (PHR)	2.5	0.4	0.7	0.4
ZINC OXIDE (PHR)	4.0	4.0	5.0	4.0
STEARIC ACID	2.0	2.0	2.0	2.0
AGERITE RESIN D	0.5	0.5	2.0	0.5
AGERITE WHITE	0.5	0.5	0.5	----
ANTOZITE 2	3.0	----	----	5.0
SANTOCURE	0.8	----	----	----
SANTOFLEX 13	----	1.5	----	1.5
VANOX MTI	----	0.5	----	0.5
NOVOR 924	----	4.2	7.5	4.2
TM TM MONEX	----	1.5	1.6	1.5
SANTOCURE NS	----	0.10	0.14	0.08
VULCANOX ZMB	----	----	2.0	----

Table 5. Carbon black filled rubber sample properties

SAMPLE	TENSILE STRENGTH (psi)	200% MODULUS (psi)	ELONGATION AT BREAK (%)	HARDNESS, IHRD, (deg)	BLOW OUT TIME, TIME AT PRESSURE, (min/psi)
NAT25A	3643	573	597	64	6.3/265
NAT14	3334	606	510	67	40.6/142
NAT1	3870	712	503	71	29/142
NAT15	3482	1049	453	73	11.6/265
NAT16	3476	881	440	70	8.9/265
NAT18	3811	865	493	71	10.6/265
NAT41	3717	1197	453	70	64.9/142
NAT42	3800	897	507	66	15.9/265
NAT44	3513	1093	430	65	15.8/265
NAT43	3713	1207	447	66	15.9/265
NAT38	3253	880	490	----	68/142
NAT57	4017	870	510	69	61.1/142
NAT60	3613	1980	353	----	9.5/265
NAT61	3508	642	567	----	5.0/265
NAT22A	3412	592	596	76	77.3/142

The experiments performed in this study in an attempt to evaluate and correlate the electrical properties of the supplied rubber samples are listed below;

1. RESISTANCE AS A FUNCTION OF TIME (STATIC)
2. RESISTANCE DURING AND AFTER COMPRESSIVE LOADING
3. RESISTANCE AND STRESS RELAXATION
4. THERMAL RELIEF
5. CURRENT - VOLTAGE RELATIONSHIPS
6. CAPACITANCE AND CONDUCTANCE AS FUNCTIONS OF FREQUENCY
7. CAPACITANCE AND CONDUCTANCE DURING AND AFTER COMPRESSIVE LOADING
8. CAPACITANCE AND CONDUCTANCE TRENDS WITH MECHANICAL HISTORY
9. THERMOELECTRIC EFFECT
10. THERMAL CONDUCTIVITY

These measurements are now described in greater detail.

3.1 RESISTANCE AS A FUNCTION OF TIME (STATIC)

Many electrical response experiments were to be performed monitoring resistance as a function of some other parameter. It was desired to determine beforehand if the rubber resistance changed with time by itself (statically). These measurements were made with a FLUKE 8012A Digital Volt Meter (DVM).

3.2 RESISTANCE DURING AND AFTER COMPRESSIVE LOADING

As was previously stated, studies of electrical resistance during extension of carbon black filled rubbers have shown characteristic responses. That response has been explained in terms of breakup and realignment of the conductive network inside the composite.

This study is interested in electrical behavior of the carbon black filled rubber under compressive loading, as that is how these materials are loaded in use on a tracked vehicle.

For this experiment a pressure and temperature apparatus was assembled (see Figure 8) in which to test the samples. A HEWLETT-PACKARD 0-10 volt power supply which was used to apply a potential across each sample. A KEITHLEY logarithmic picoammeter was used to measure the resulting current. A copper-constantan thermocouple was taped directly to the sample, which was placed into a 2" diameter metal chamber with steel disks above and below. The sample's electrical leads went through a hole in the side of the chamber to the power supply. The chamber was wrapped in heating tape regulated by a POWERSTAT variable autotransformer to control sample temperature. This apparatus was then placed on a REVERE 0-500 lb. load cell in a GREENERD 2 ton arbor press. A COLE-PARMER 2-pen chart recorder was used to simultaneously

record sample pressure from the load cell and sample current from the logarithmic picoammeter.

3.3 RESISTANCE AND STRESS RELAXATION

High polymers are known to display both perfect solid-like (elastic solid) and perfect liquid like (Newtonian liquid) behavior depending upon the time scale of measurement or the temperature to which they are subjected. Perfect solid or liquid behavior will generally occur at the extremes of stress or strain application rates (either instantaneously fast or infinitely slow). At intermediate application rates an elastomer will display both an elastic and a viscous response. Accordingly, an applied stress will cause an immediate (elastic) and a time dependent (viscous) strain response and vice versa. The rate of stress or strain application is an important parameter here.

It was found that the electrical resistance of the samples in this study was similarly dependent on time after load application or removal. This behavior was first recorded in experiments described previously in section 3.2 and was subsequently measured using the same apparatus only with a longer experimental time frame. Constant strain could also be applied to record stress relaxation.

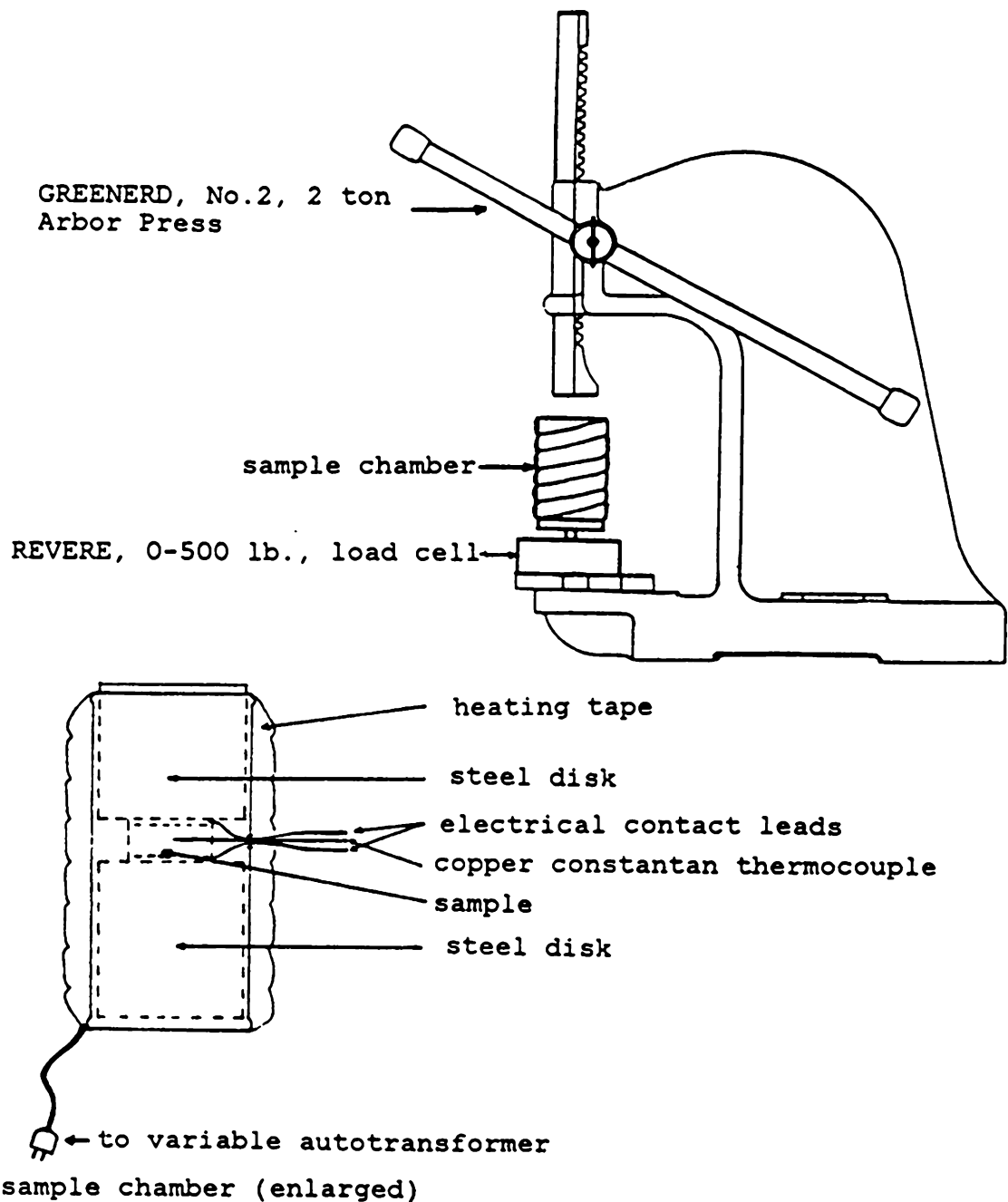


Figure 8. Apparatus for testing electrical behavior of sample under variable pressure and temperature.

3.4 THERMAL RELIEF

It was found in preliminary studies that the resistance increased during compressive loading and then after pressure removal went through a relaxation very similar to a Maxwell-Kelvin model (63). The resistance decreases significantly immediately after load removal and this relaxation becomes slower with time. The relaxing resistance, at room temperature, could easily take several weeks or months to approach its original value but it was found that the rate of this process could be increased thermally. At 70°C, the resistance of a previously compressed sample would approach its original value in less than 1 hour.

It was necessary that each experiment was begun with all samples in some equivalent microstructural state. It was hoped that reproducing their original or minimum resistance would accomplish this. This "thermal restoration" has henceforth been used extensively on all experimental samples to restore them to an "equilibrium" state.

3.5 CURRENT - VOLTAGE RELATIONSHIPS

Current-voltage behavior was monitored by applying voltages from 0-100 volts across each sample with a HP6116A DC power supply and measuring the resultant current with a DVM.

3.6 CAPACITANCE AND CONDUCTANCE AS FUNCTIONS OF FREQUENCY

Capacitance and conductance as functions of frequency from 100 Hz to 10 MHz were measured at room temperature for all thermally relieved samples. A HP4192A Impedance Analyzer was used for these measurements.

3.7 CAPACITANCE AND CONDUCTANCE DURING AND AFTER COMPRESSIVE LOADING

Capacitance and conductance during and after compressive loading were next measured for samples NAT 1 and NAT 42. These samples were chosen because they represented a wide range in static resistances and in resistance response to compressive stress (See Table 6 and Figures 11 - 15)

Here the sample was placed in the metal sample chamber which was mounted on an arbor press (see section 3.2). A 0-500 lb. load cell was used to monitor the sample pressure and a HP4192A Impedance Analyzer was used to monitor capacitance and conductance. A constant mid-frequency of 10 kHz was chosen and a pressure of 150 psi was applied, held for \approx 60 seconds, and released. Concurrent with pressure application and removal, the capacitance and conductance were simultaneously recorded on a 2-pen chart recorder.

Additionally, all samples were thermally relieved for 1 hour at 70°C, allowed to slow cool to room temperature, and

then their capacitance and conductance at 100Hz was measured at increasing compressive stress levels from 0 to 200 psi in 40 psi increments.

3.8 CAPACITANCE AND CONDUCTANCE TRENDS WITH MECHANICAL HISTORY

During this set of experiments, capacitance and conductance as a function on frequency were monitored for select samples as a function of previous or concurrent compressive stress and thermal recovery.

The HP4192A Impedance Analyzer was used to monitor capacitance and conductance versus frequency. The arbor press and load cell were used to apply and monitor sample pressure (see section 3.2). All samples were thermally relieved for 1 hour at 70°C and allowed to slow cool to room temperature prior to testing.

The NAT 18A sample was chosen to be tested under various conditions because its capacitance and conductance versus frequency curves had the most "structure" of all samples tested (see Figures 19 and 20). (Here the term "structure" refers to this sample having the greatest discontinuity in the measured property over the measured frequency range.)

3.9 THERMOELECTRIC EFFECT

Thermoelectric measurements were made on each Fort Belvoir sample in order to determine the sign of the charge carrier. Due to the thermoelectric effect, when one surface of a conductor is heated, the charge carriers are given extra energy (kT). These energized carriers will travel away from the heat source, creating a slight potential difference across the sample, the polarity of the cold side being the charge of the carrier.

All samples were tested using a soldering iron as the heat source and a DVM to measure the polarity.

3.10 THERMAL CONDUCTIVITY

The thermal conductivity of all samples was measured to determine if any relationship existed between the thermal and electrical conductivities.

The apparatus used to measure this property is shown schematically in Figure 9. Here a central copper block is heated by four heaters at a known current and voltage (Power = current X voltage). Identical rubber samples are placed on each side of the central block and further sandwiched between copper plates. Both sides of each rubber sample were coated with OMEGATHERM 201 thermally conductive paste ($K \approx 16$) to allow for good interfacial heat transfer. Copper-constantan

thermocouples were installed near the center of the copper pieces about 0.0625" above and below each rubber sample. To minimize heat loss, the edges of the copper blocks were painted silver and a cardboard insulating sleeve was made and used. This apparatus was then sandwiched between identical materials to allow for equal heat transfer in both directions. The apparatus was placed between aluminum and rubber plates respectively. A 10 lb. weight was placed on top for better interfacial surface contact, and an aluminum foil cover surrounded the setup to reduce the effect of varying room temperatures and air currents.

Samples were installed, and the apparatus was completed. The central block was heated to 100-120°C and allowed to stabilize for a particular heater I-V setting. The input power was measured ($P=IV$) and the ΔT across both samples was measured. Several different I-V combinations were used for each sample and an average thermal conductivity was determined over an approximate 25°C temperature range. The resulting ΔT across each sample was measured and recorded.

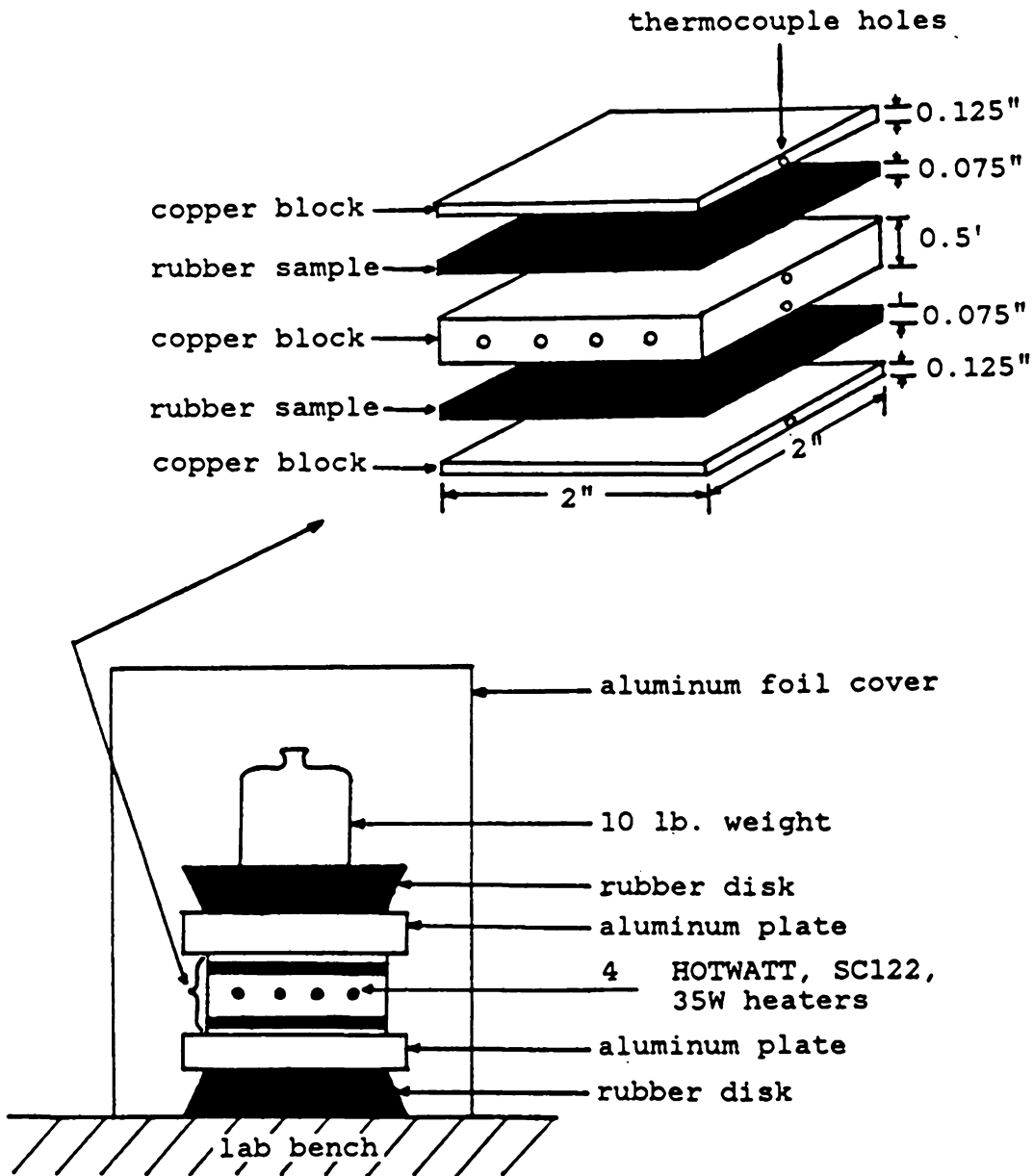


Figure 9. Apparatus for measuring thermal conductivity

4.0 RESULTS AND DISCUSSION

4.1 RESISTANCE AS A FUNCTION OF TIME (STATIC)

Resistances for "virgin" samples as recieved in August 1984 are listed in Table 6. It was found that over a 3 day period, all resistances remained constant and thus concluded that the possible change over the short term due to storage would be negligible.

The sample resistances for the same set of samples after 15 months are also listed in Table 6. These samples have been thermally cycled up to 5 times in other experiments, but have not been mechanically stressed. Here one can see that most sample resistances have changed by less than a factor of two. Thus we conclude that the sample resistance changes with time are also relatively negligible over the long term when compared with resistances changes observed during experimentation.

Table 6. Sample resistances at 0 and 15 months with no mechanical history

SAMPLE	RESISTANCE ORIGINAL (OHMS)	RESISTANCE AT 15 MONTHS (OHMS)
NAT25A	293	875
NAT14	77	85
NAT1	59	106
NAT15	33	40
NAT16	277	299
NAT18	170	2200
NAT41	228	394
NAT42	774	1600
NAT44	31300	39000
NAT43	14900	15000
NAT38	28	31
NAT60	91000	68400
NAT57	5.1	5.9
NAT22A	308	298

4.2 RESISTANCE DURING AND AFTER COMPRESSIVE LOADING

From preliminary studies it was found that the resistance increased upon compressive loading and then decreased on load removal. In an effort to systematically characterize each rubber sample in this study, a standardized resistance versus pressure test was devised. All samples were thermally relieved for 1 hour at 70°C and allowed to slow cool to room temperature prior to testing.

The load profile as shown in Figure 10 was then applied; an increasing pressure "ramp" (constant load rate) from 0 to 150 psi in 30 seconds; a constant 150 psi stress for 40 seconds; a decreasing pressure "ramp" from 150 to 0 psi in 30 seconds; a constant 0 psi stress for 80 seconds; an instantaneous load to 150 psi; a constant 150 psi stress for 60 seconds; an instantaneous load removal; and finally a constant 0 psi stress for =80 seconds. It is relevant to note here that 150 psi corresponds with approximately 10% compressive strain in these samples.

Samples measured here are listed in Table 7. Five typical resistance responses to the applied load profile are shown in Figures 11-15. Resistance responses for the remaining samples are located in Appendix A.

All samples responded uniquely to the applied load profile. All but one sample, NAT60, showed a resistance increase

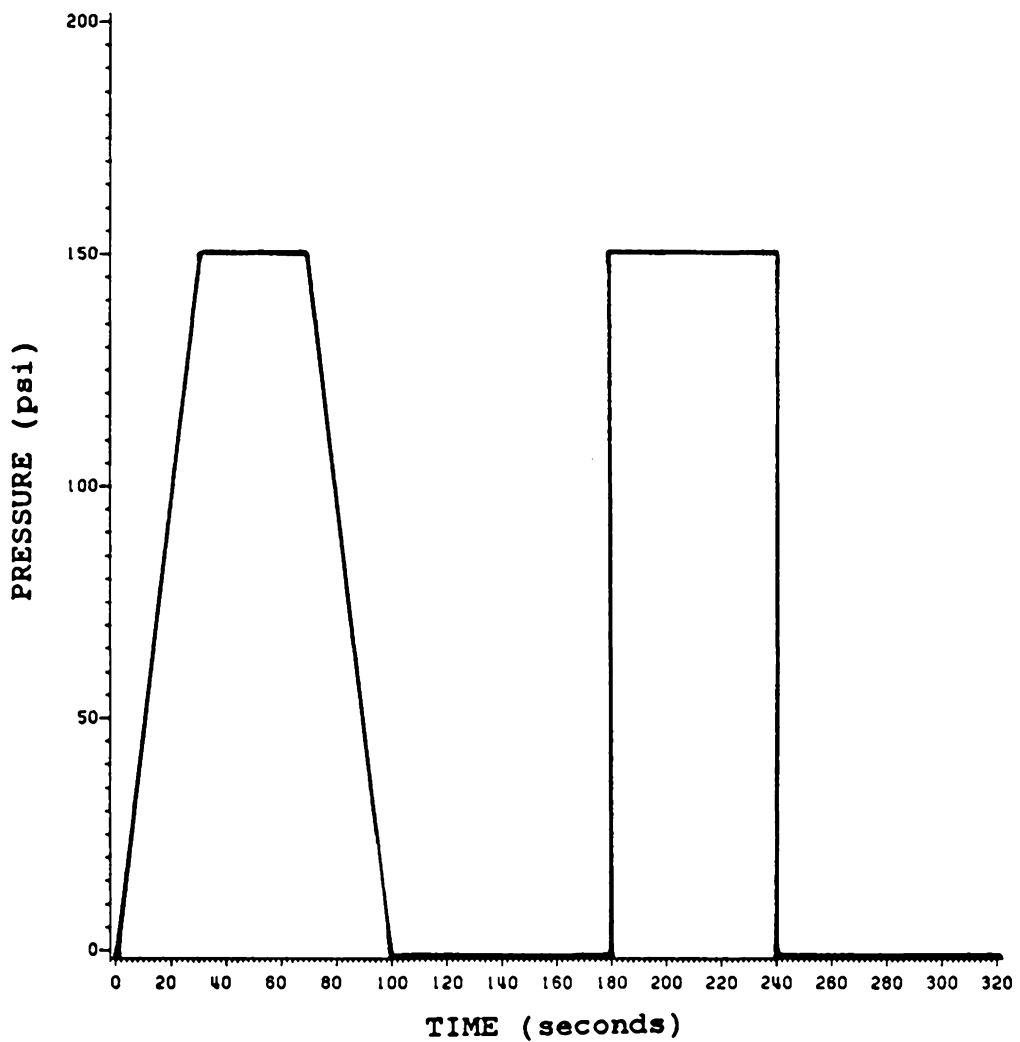


Figure 10. Standardized load profile for testing electrical response

Table 7. Pressure test samples and some corresponding data (reference 64)

SAMPLE	CARBON BLACK TYPE	IODINE #	DBP ABSORPTION
NAT25A	N-110	145	113
NAT14	N-110	145	113
NAT1	N-110	145	113
NAT15	N-110	145	113
NAT16	N-220	121	114
NAT18	N-234	120	125
NAT41	N-299	107	124
NAT42	N-326	82	71
NAT44	N-330	82	102
NAT43	N-351	67	120
NAT38	N-472	250	178
NAT57	N-110 and XE-2	145 and unknown	113 and unknown
NAT60	N-110	145	113
NAT61	N-110 and XE-2	145 and unknown	113 and unknown
NAT22A	N-110	145	113

on pressure application followed by an eventual decrease on pressure removal.

The results, except for NAT60, can be explained in a fashion which is consistent with Bulgin's theory of conductive network behavior. A statistical network is formed and secured in place during vulcanization. An applied uniaxial compressive stress reduces the conductive network by orienting the conductive elements and disrupting their statistical distribution of orientations. One can see that as pressure is linearly applied, the resistance response is very non-linear. Such a response is reasonable because the elements of the conductive network have a finite size of contact or conducting area and they also have a finite attractive force or possibly a bond between them. Thus at small stresses the inter-particle contacts may not be broken or they may be moved very little so that the effect of a decrease in their conduction area is small. However, at larger stresses the inter-particle contacts may be severed and the previously "sound" agglomerates themselves may be broken. Also at larger stresses the distances that the contact areas move from one another may be large and have a significant effect.

At a constant 150 psi stress, each sample's resistance decreases slightly. As pressure is removed, either slowly or instantly, the samples will first exhibit a resistance increase followed by an eventual decrease. The magnitude of

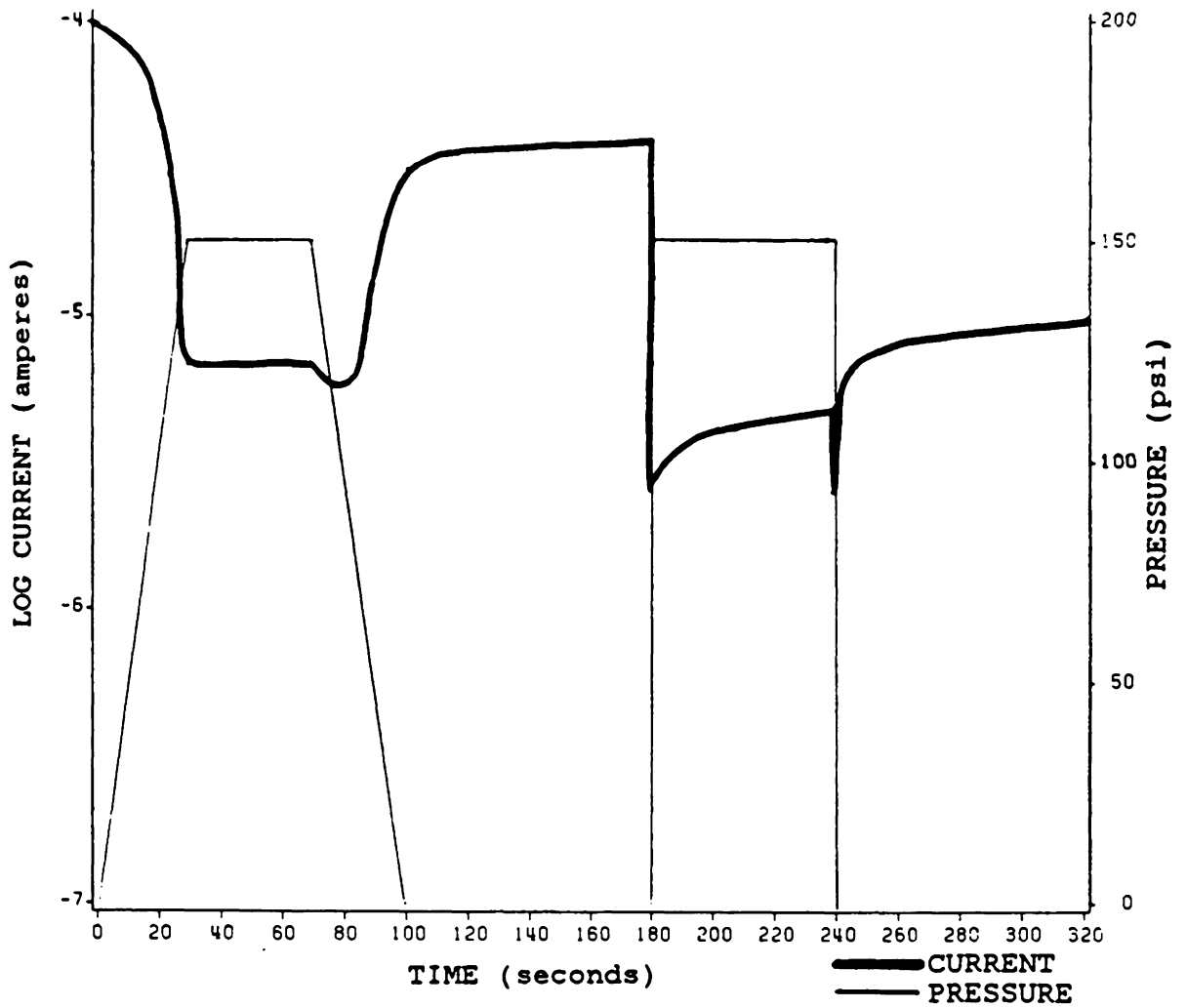


Figure 11. Resistance response to a standardized load profile (NAT14)

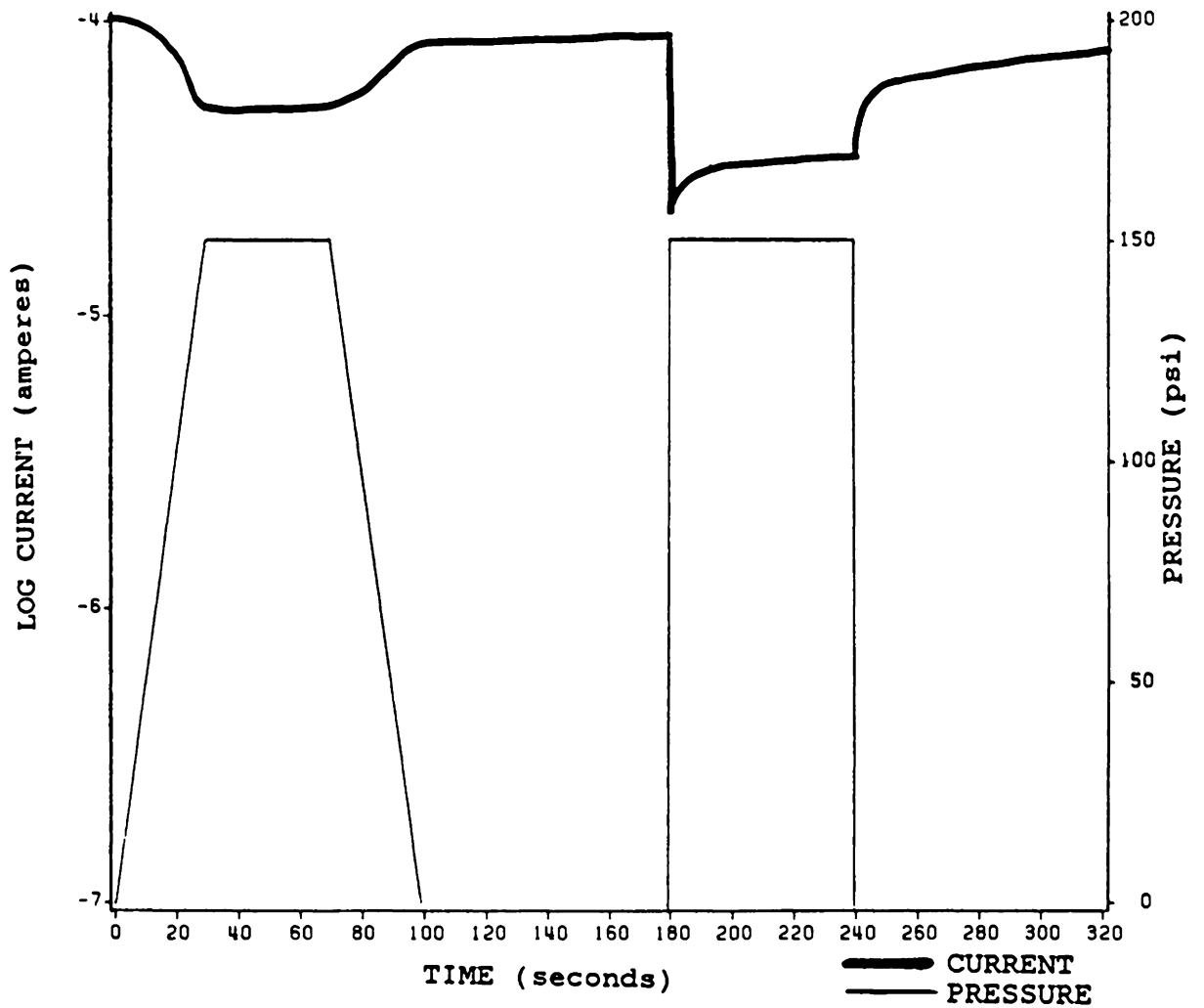


Figure 12. Resistance response to a standardized load profile (NAT15)

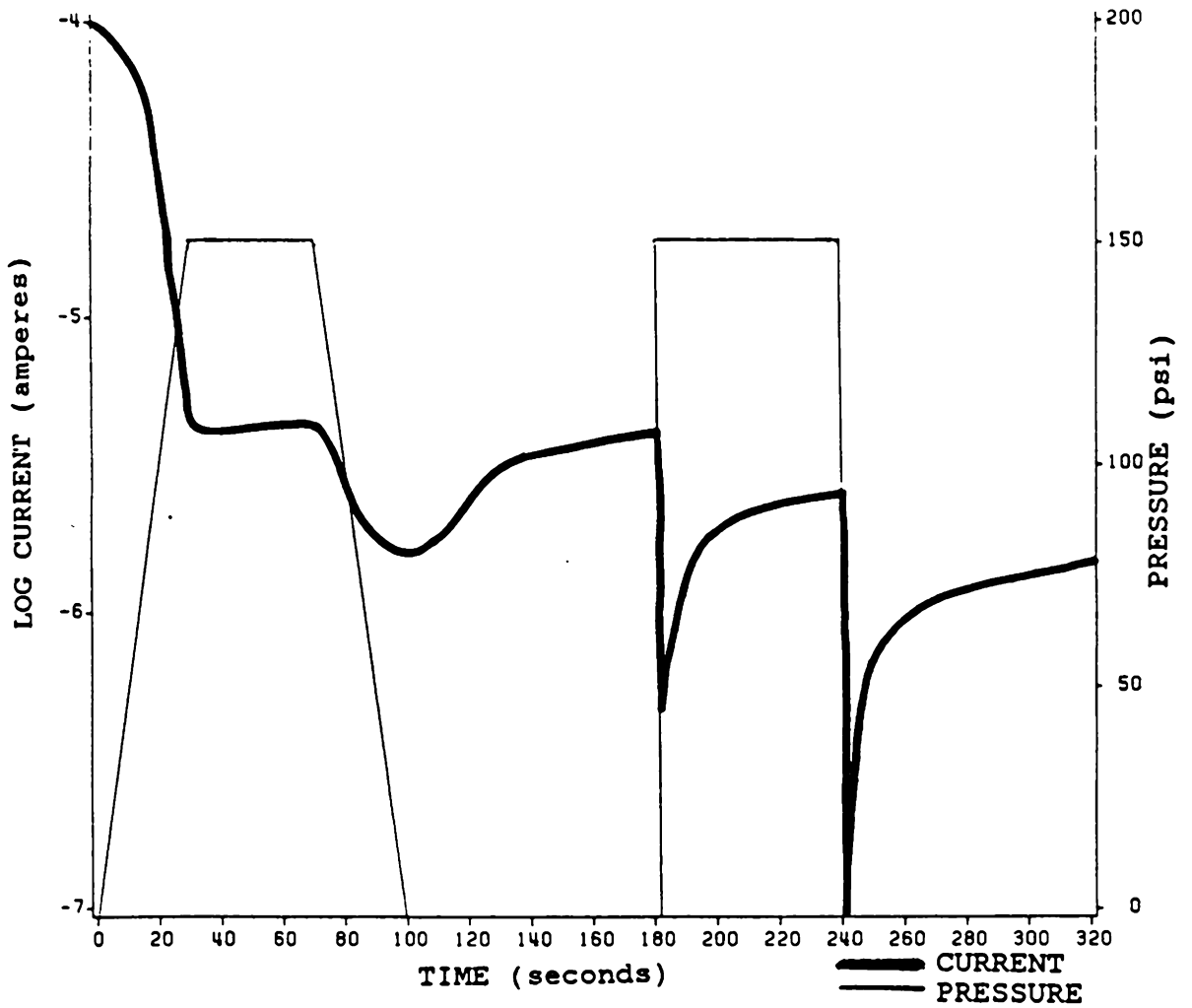


Figure 13. Resistance response to a standardized load profile (NAT18)

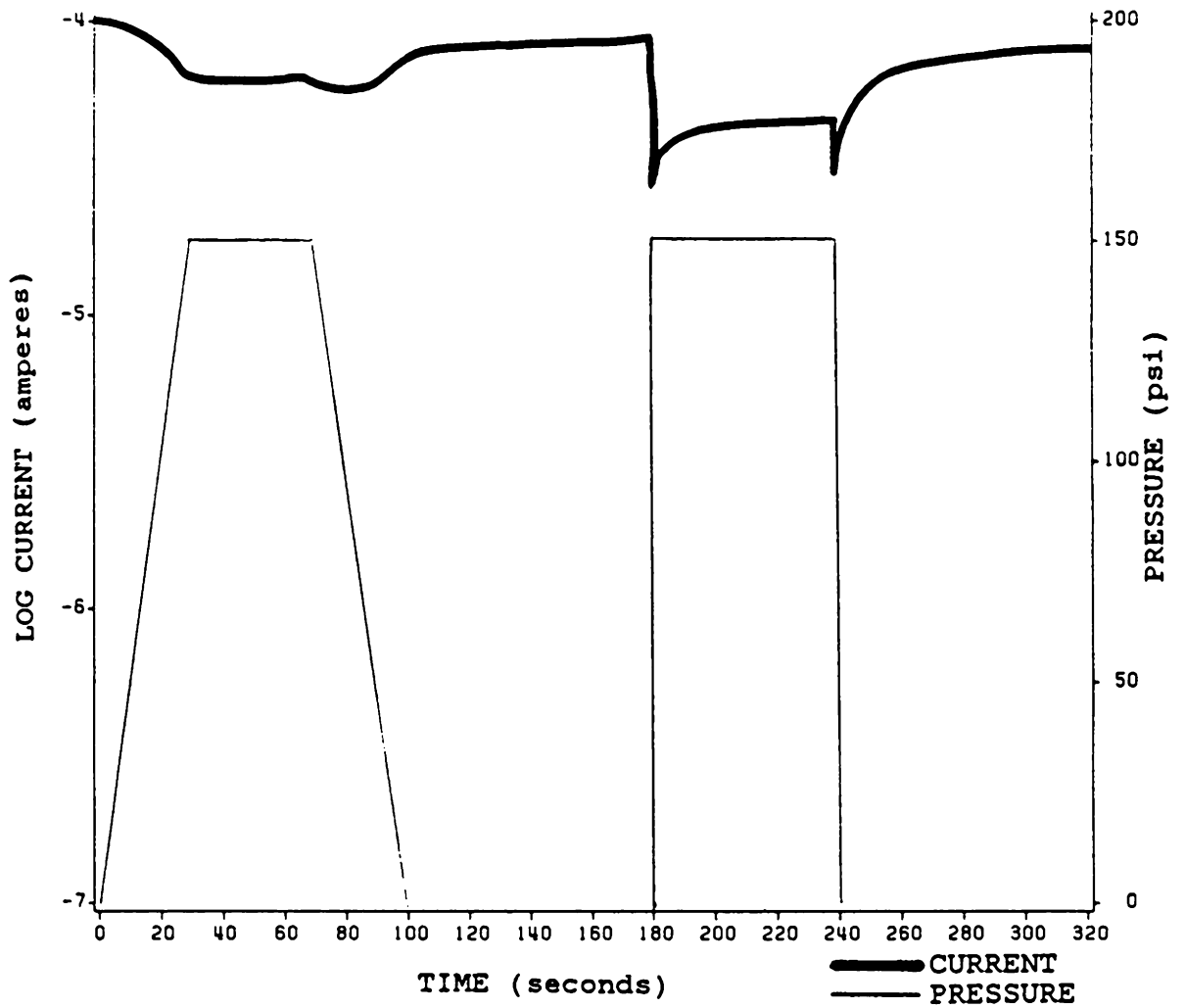


Figure 14. Resistance response to a standardized load profile (NAT38)

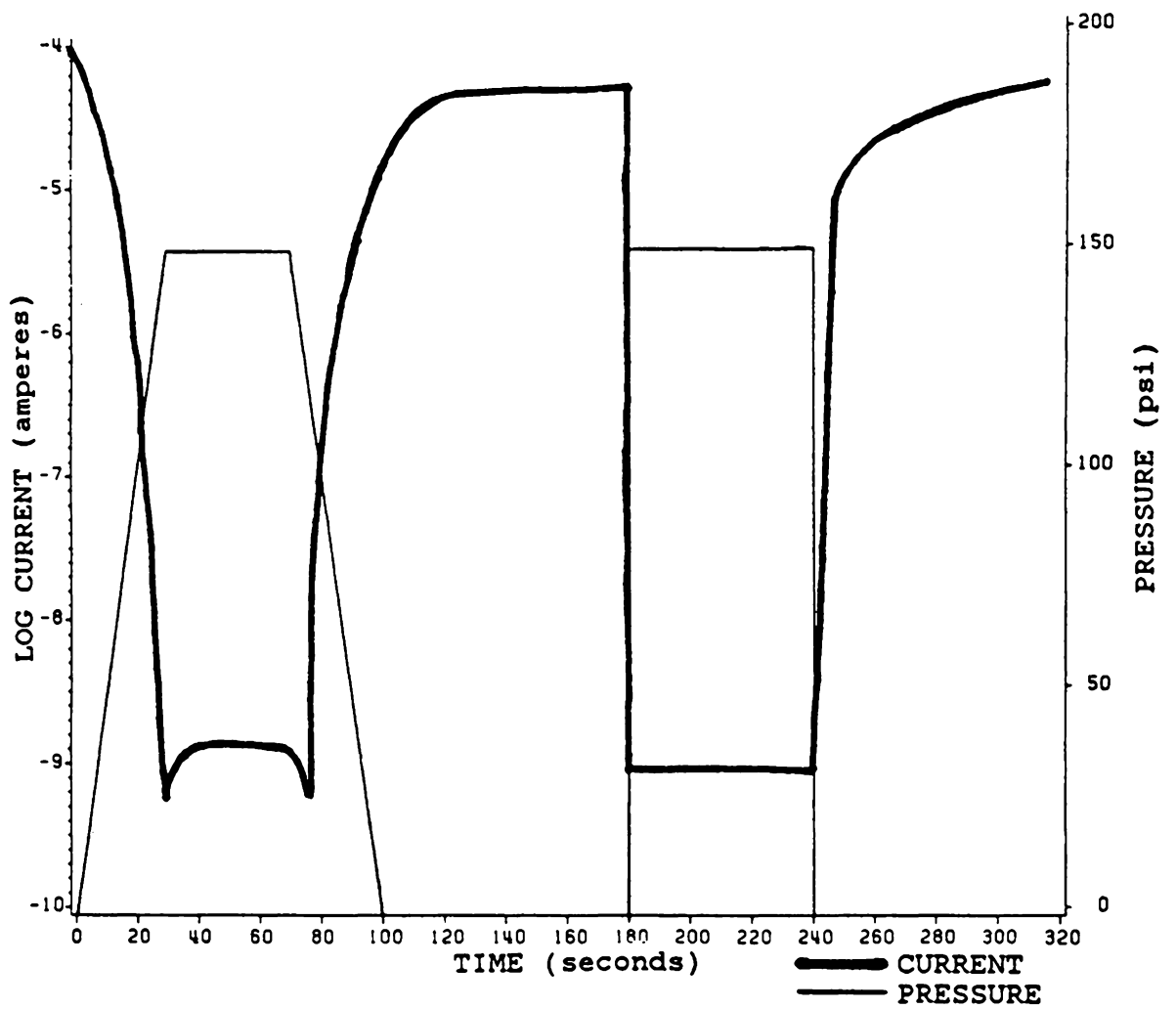


Figure 15. Resistance response to a standardized load profile (NAT42)

the resistance increase upon pressure removal appears to be related to the magnitude of the resistance relaxation during constant 150 psi stress. A larger decrease in resistance during constant 150 psi stress results in a larger increase in resistance upon pressure removal. It seems that the polymer matrix during relaxation at constant stress allows some conductive elements to realign in a fashion that adds to the existing conductive network. This addition is subsequently destroyed on pressure removal where the matrix then relaxes under no pressure and the original conductive network re-forms.

The response of the series of increasing sulfur content (NAT25A,NAT14,NAT1,NAT15) indicates that a higher sulfur content (more highly crosslinked system) allows less resistance relaxation under pressure and thus less resistance increase on pressure removal. From these observations it is evident that the resistance relaxation is linked to the relaxing abilities (modulus) of the polymer matrix.

The series of N-300 carbon black filled rubbers (NAT42,NAT43,NAT44) responded uniquely during constant rate loading in that they would reach a maximum in resistance before the maximum load was applied. Their maximum resistance would then decrease slightly to a constant level regardless of additional pressure. This response was reversed for constant rate pressure removal. This response suggests that the original conductive network is disrupted during pressure ap-

plication to a point where a new network is formed and becomes dominant. Why this new network is not pressure sensitive is not clear, however the value of the resistance here may be the minimum resistance attainable for close packed, rubber coated, carbon black particles.

Generally, all samples filled with same N-series of carbon blacks responded similarly to the standard load test. The most notable exception was NAT18 of the N-200 series (NAT16, NAT18, NAT41). This sample seems to have an extreme sensitivity to matrix strains, the conductive network being disrupted on pressure application and even more on pressure removal. Even though samples NAT16 and NAT41 have the largest difference in particle sizes and structures their behavior is very similar. NAT18 does have a combination of a small particle size and a high degree of structure. This may result in a more fragile agglomerate which is more easily broken with matrix strains. One must remember also that the effect of mixing would be to mechanically "equalize" all types of carbon black agglomerates as they would be broken down until they could withstand the level of stress in the mixer.

From observing the increasing sulfur content series it is obvious that sulfur plays an important role in the resistance response. There also correlations possible between resistance response and the particle size (iodine #)⁻¹ and agglomerate structure (DBP #).

As one goes from the N-100 series to the N-200 series carbon black filled rubbers, the general trend is that the carbon black particle size increases (64) (See Table 7). The magnitude of the initial sample resistance (See Table 6) and the resistance change upon 150 psi pressure application also increases with this particle size trend. At equal loadings, the initial resistance for larger particle sizes is larger because there are less particles and agglomerates to form the conductive network. Each inter-particle or inter-agglomerate contact is therefore much more critical to the conductive network existence. Thus a larger particle size carbon black may act analogously to a smaller particle size carbon black at a lower loading level.

4.3 RESISTANCE AND STRESS RELAXATION

Viscoelastic materials with a single relaxation mechanism can be described by the Maxwell equation:

$$\sigma(t) = \sigma_0 \exp(-t/\tau),$$

where τ is the relaxation time. A complex relaxation process may be separated into elementary processes, each having its own relaxation time. Stress relaxation in a cross-linked rubbery polymer is a complex function which was suggested by Bartenev (47) to be separable into elementary relaxation processes where

$$\sigma(t) = \sum_{n=0}^{\infty} \sigma \exp(-t/\tau)$$

for x relaxation processes.

This approach was attempted for samples NAT25A, NAT14, NAT1, and NAT15 (listed in order of increasing sulfur content). All samples were strained to 10% and stress and resistance were recorded as a function of time.

In order for this method to work, the sample relaxation must be monitored until only the last and slowest mechanism is active. In other words, until a plot of $\ln \sigma$ versus t becomes linear. For measurements made for 120 seconds this was found not to happen, and although subsequent equations developed for these relaxations (stress and resistance) were accurate to within $\pm 1\%$, the intervals over which the equations were formulated probably did not represent discrete mechanisms.

The same procedure was again tried monitoring resistance and stress relaxation for 300 seconds with the same results. Finally a test for 100 hours was performed on sample NAT1 only. Again it was found on a $\ln \sigma$ versus t plot that no truly linear regions exist even after this length of time. A spectrum of relaxation times could probably be defined but it was decided to look for other electrical-mechanical correlations.

4.4 TEMPERATURE EFFECTS

It was found in two separate experiments on the same sample that both PTC and NTC responses could be exhibited, depending on the "state" of the sample.

In one experiment, several thermally relieved samples were simply heated from room temperature to 75°C and their resistance values were recorded at both temperatures. These values are listed in Table 8. All samples' resistances decreased by at least 50% in a NTC response.

In another test the sample NAT1, from the previous section, had been held at 10% strain and room temperature for about 100 hours. At this point, the rate of change of the stress and the resistance was very slow. Taking this "state" as "near" equilibrium, the temperature was then increased to observe the effects. The resistance and stress did change with temperature and would stabilize at any constant temperature. A plot of resistance and stress versus temperature is shown in Figure 16.

The kinetic theory of elasticity predicts that a rubber network should behave under uniaxial strain according to the relation

$$\sigma = \nu kT (\alpha - \alpha^{-2})$$

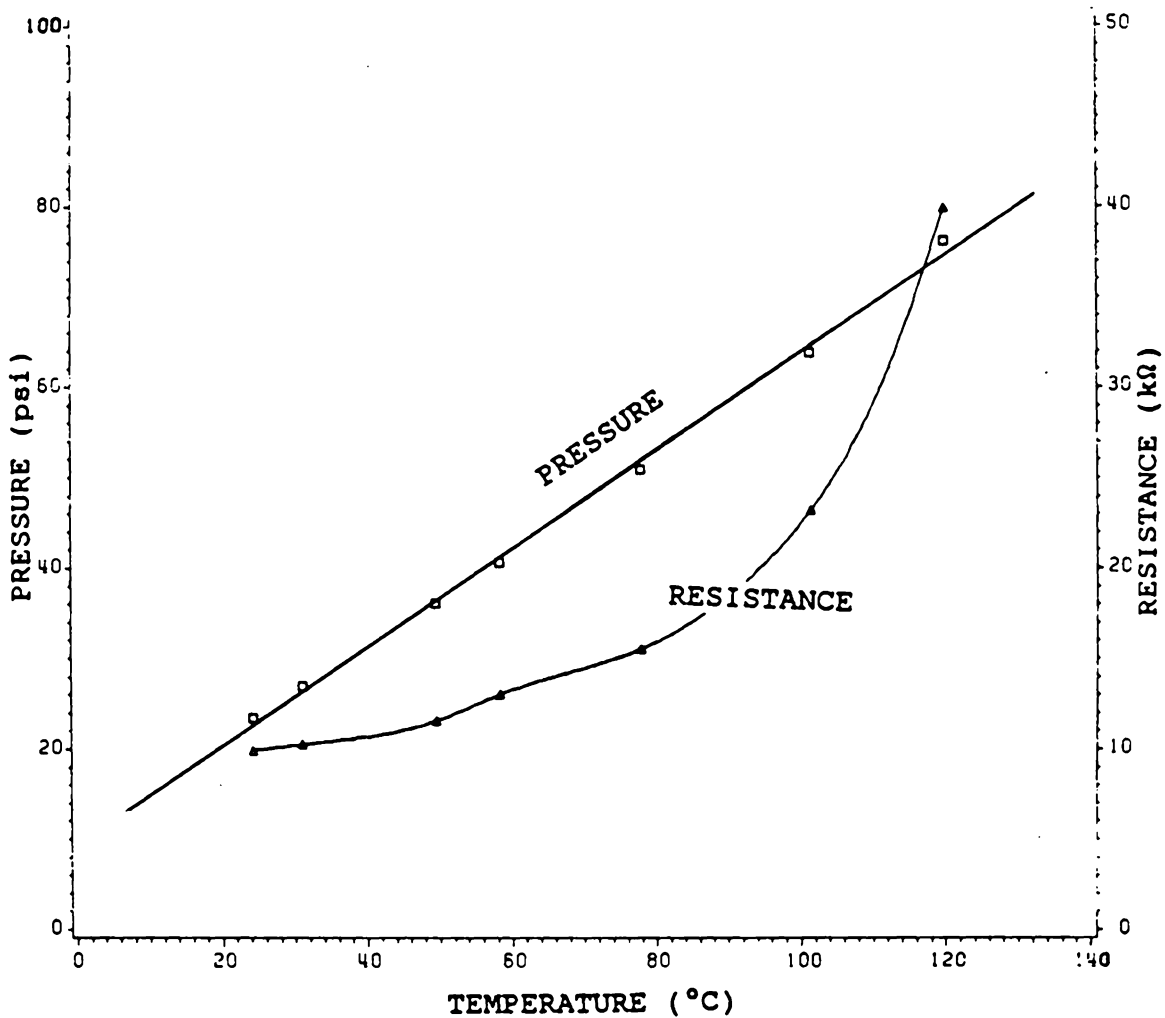


Figure 16. Resistance and stress as functions of temperature: (sample NAT1 under constant 10% strain)

Table 8. Carbon black filled rubber sample resistances at two temperatures

SAMPLE	RESISTANCE AT 24°C (OHMS)	RESISTANCE AT 75°C (OHMS)
NAT14	2020	568
NAT1	33900	13900
NAT15	238	131
NAT16	4100	1550
NAT41	4020	1343
NAT42	73600	9910
NAT38	206	94
NAT22A	2500	100

where

ν = number of effective network chains per unit volume

α = extension ratio (L/L_0)

and k = Boltzman's constant

Accordingly, for rubbers filled with carbon black

$$\sigma = (\nu_r + \nu_f) kT (\alpha - \alpha^{-2})$$

where

ν_r = ordinary network chains in the rubber

ν_f = additional chains produced by bonds to the filler

As predicted and shown in Figure 16, a plot of σ versus T is linear, but we also observe a nonlinear PTC resistance response.

The fact that different temperature coefficients can be seen indicates that it is the "state" of the conductive network, not semiconducting or space charge effects, that controls the conductivity. As the conductive network is formed at the vulcanization temperature it is probably disrupted to some extent by thermal contraction upon cooling. When such a sample is heated under no load, the original high temperature network is allowed to "re-form" and thus the NTC response. When a uniaxial load is applied to a sample the conductive network is disrupted. If the temperature of that sample is then increased, it will attempt to expand in all

three directions, but the restraint in one direction will have the same effect as an increased load and thus a PTC resistance response is observed.

Conductance and capacitance were also monitored as a function of frequency under no load conditions at various temperatures for sample NAT18. These results are plotted in Figures 17 and 18. Here the effect of increasing temperature is to increase both conductance and capacitance at low frequencies. There is no monotonic trend at higher frequencies, but it is interesting to note that the capacitance and conductance curves for each temperature are positioned the same relative to the other temperatures.

4.5 THERMAL RELIEF

As was mentioned in the literature review and described in the methods and materials section, the resistance relaxation rate after stress removal was found to be very temperature dependent. For example sample NAT1 in one experiment had an initial resistance (R_0) of 135Ω which increased to 377Ω after 60 psi was applied and released. The resistance was reduced to 160Ω after 30 minutes at 70°C then to 114Ω after 1 hour at 70°C and cooled to room temperature. All other samples behaved similarly. A standard "thermal relief" procedure of 1 hour at 70°C followed by a slow cool to room

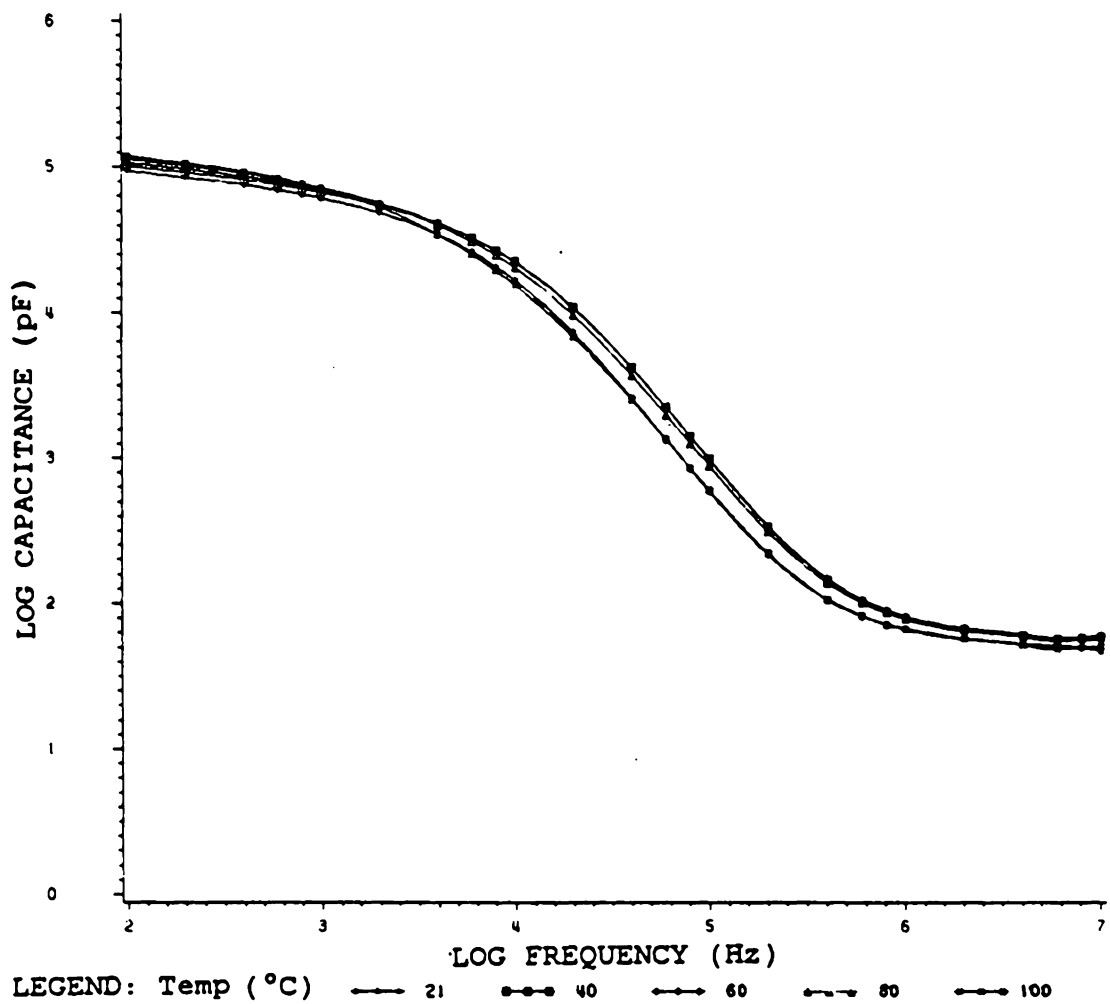


Figure 17. Capacitance versus frequency at various temperatures

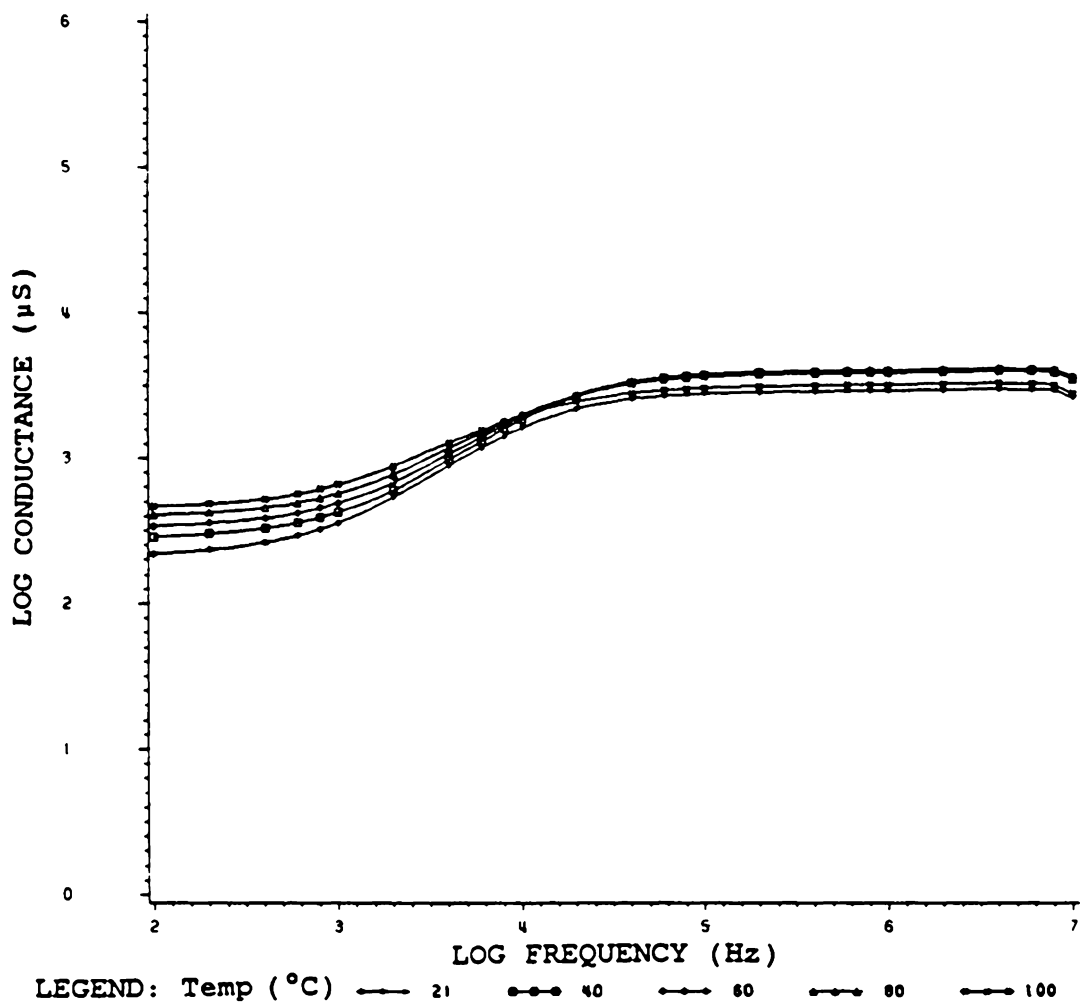


Figure 18. Conductance versus frequency at various temperatures

temperature was used to restore samples to an "equilibrium" condition.

It was found by accident that the cooling rate after the thermal treatment could significantly affect the final sample resistance. In all cases observed, the final resistance was higher for faster cooling rates. In terms of the network model here it could be theorized that the thermal shock of a faster cooling rate would result in higher stresses which could cause inter-agglomerate contact breakage that might not occur at slower cooling rates.

4.6 CURRENT - VOLTAGE RELATIONSHIPS

All samples responded ohmically to voltages from 0 to 100 volts ($E = 0$ to ≈ 80 V/cm.). This implies that inter-agglomerate contact is the dominant conduction mechanism here. Space charge limited conduction mechanisms (tunnelling and hopping) would respond super-ohmically if they were dominant. Such super-ohmic responses have been reported in references 36, 65, and 66 but those experiments used higher fields (≈ 700 V/cm.) or lower carbon black loadings (≈ 15 phr) where the conductive network is not yet formed. Subsequently, in either case, the space charge limited currents were the dominant conduction mechanism. The same result is possible in samples measured here at higher fields and thus the other conduction mechanisms are not ruled out.

4.7 CAPACITANCE AND CONDUCTANCE AS FUNCTIONS OF FREQUENCY

Capacitance and conductance as functions of frequency from 100Hz to 10MHz for "virgin" thermally relieved samples at room temperature are plotted in Figures 19 and 20. These curves are similar in shape for all samples except for sample NAT18. NAT18 exhibits the most drastic change in capacitance and conductance over this frequency range. This sample was also very different from all other samples in its resistance response to the applied load profile in section 4.2. Samples not shown here could not be measured because their capacitance and conductance values were out of range on the HP4192A Impedance Analyzer.

4.8 CAPACITANCE AND CONDUCTANCE DURING AND AFTER COMPRESSIVE LOADING

As noted earlier, a unique resistance response was recorded for each sample under the applied load profile (section 4.2). This section addresses the possibility of an additional unique capacitance response to a compressive load and its implications.

Two samples, NAT1 and NAT42, were first installed in the pressure test apparatus (section 3.2) and their capacitance and conductance were recorded as 150 psi was instantly applied, held for 60 and 80 seconds, respectively, and in-

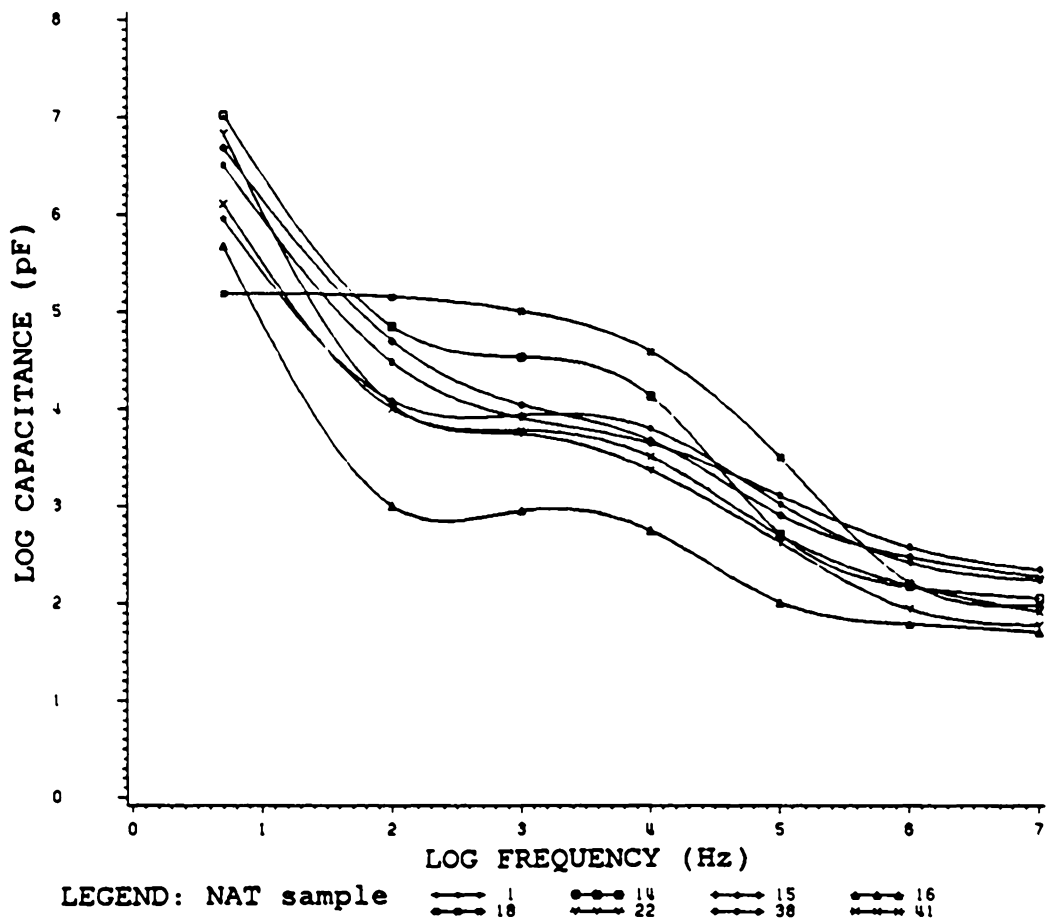


Figure 19. Capacitance versus frequency for "virgin" samples

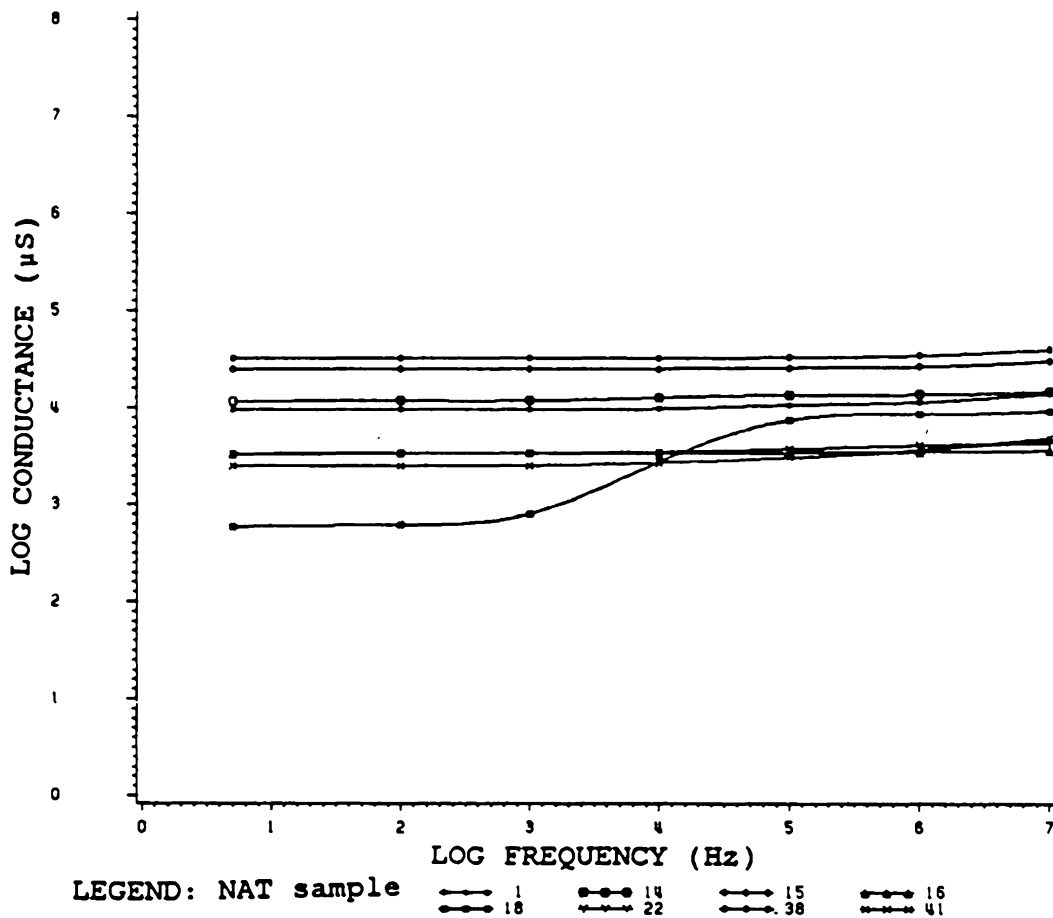


Figure 20. Conductance versus frequency for "virgin" samples

stantly removed. Their subsequent responses are plotted in Figures 21 and 22. This response is somewhat surprising because the capacitance and conductance curves have the same shape. The mechanism for capacitance and conductance changes with physical strains is therefore evidently the same. This means that any theory of conductive network behavior should also be consistent with the capacitive behavior.

All samples were next thermally relieved and measured for capacitance and conductance at a constant low frequency of 100Hz under compressive loads from 0 to 200 psi. Immediately after any pressure application the electrical response reaches a maximum or minimum and then begins to relax. Accordingly, each measurement in this test was taken about 10 seconds after pressure application. The results are plotted in Figures 23 and 24. A definite trend of decreasing capacitance and conductance with increasing pressure can be seen here. When the logarithm of capacitance is plotted versus the logarithm of conductance, ($\ln C$ vs. $\ln G$) for all samples at all pressures, (Figure 25) a trend common to all samples is observed. This trend does not depend on carbon black type or quantity.

Five samples (NAT14,15,18,38,&42) which encompass the range of compositions and electrical behavior were next thermally relieved and measured for capacitance and conductance as a function of frequency at room temperature in various identical "states" of mechanical and thermal his-

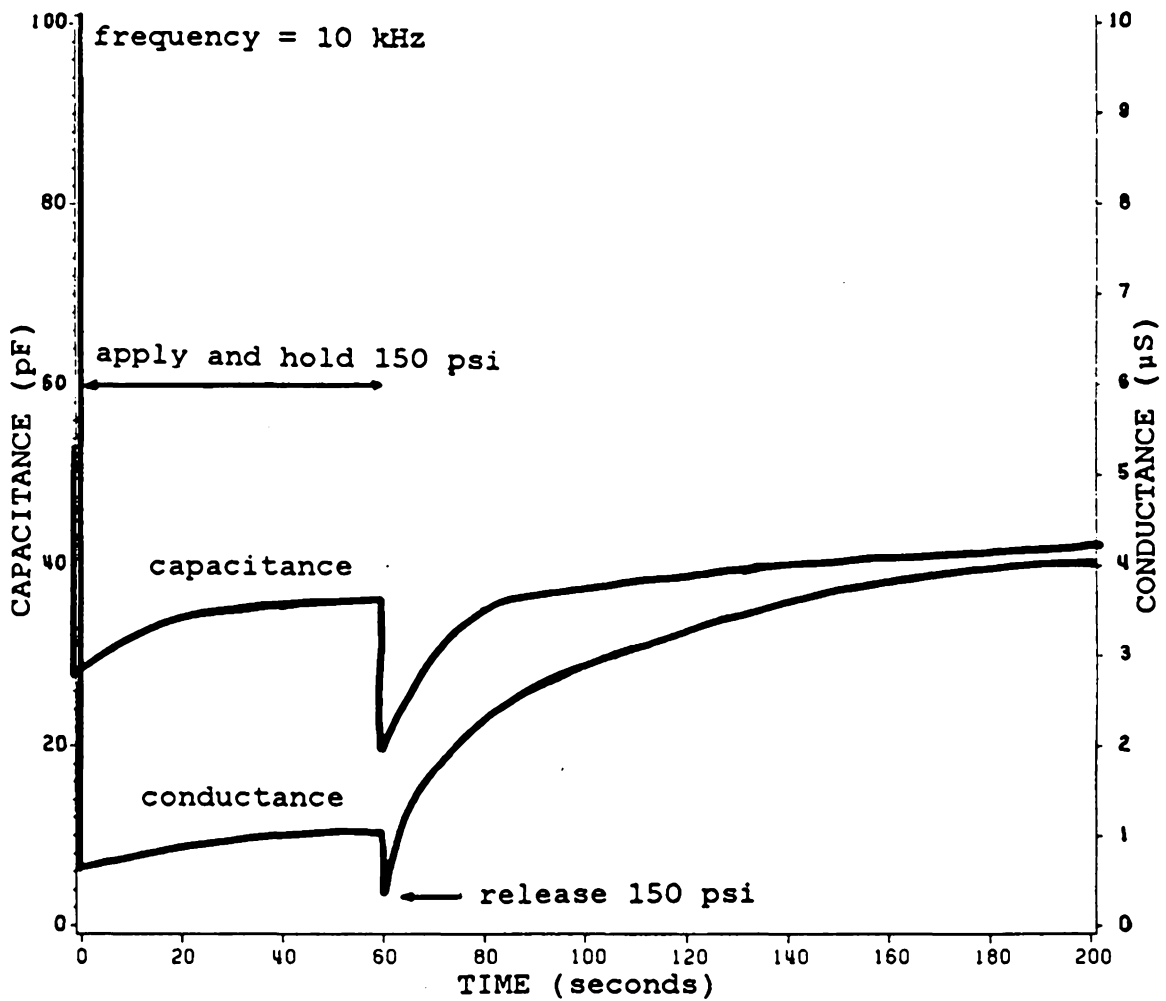


Figure 21. Capacitance and conductance versus pressure (NAT1)

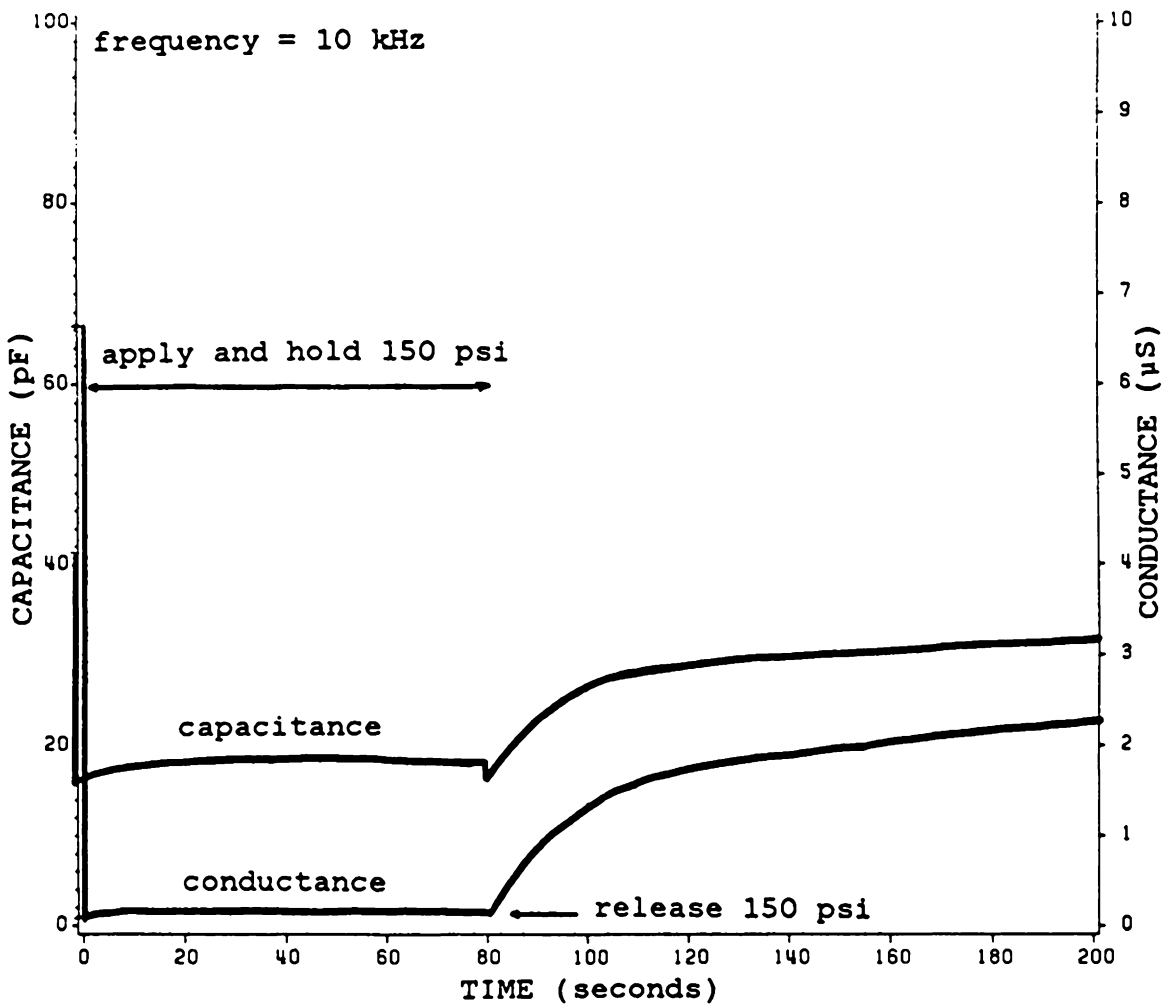


Figure 22. Capacitance and conductance versus pressure (NAT42)

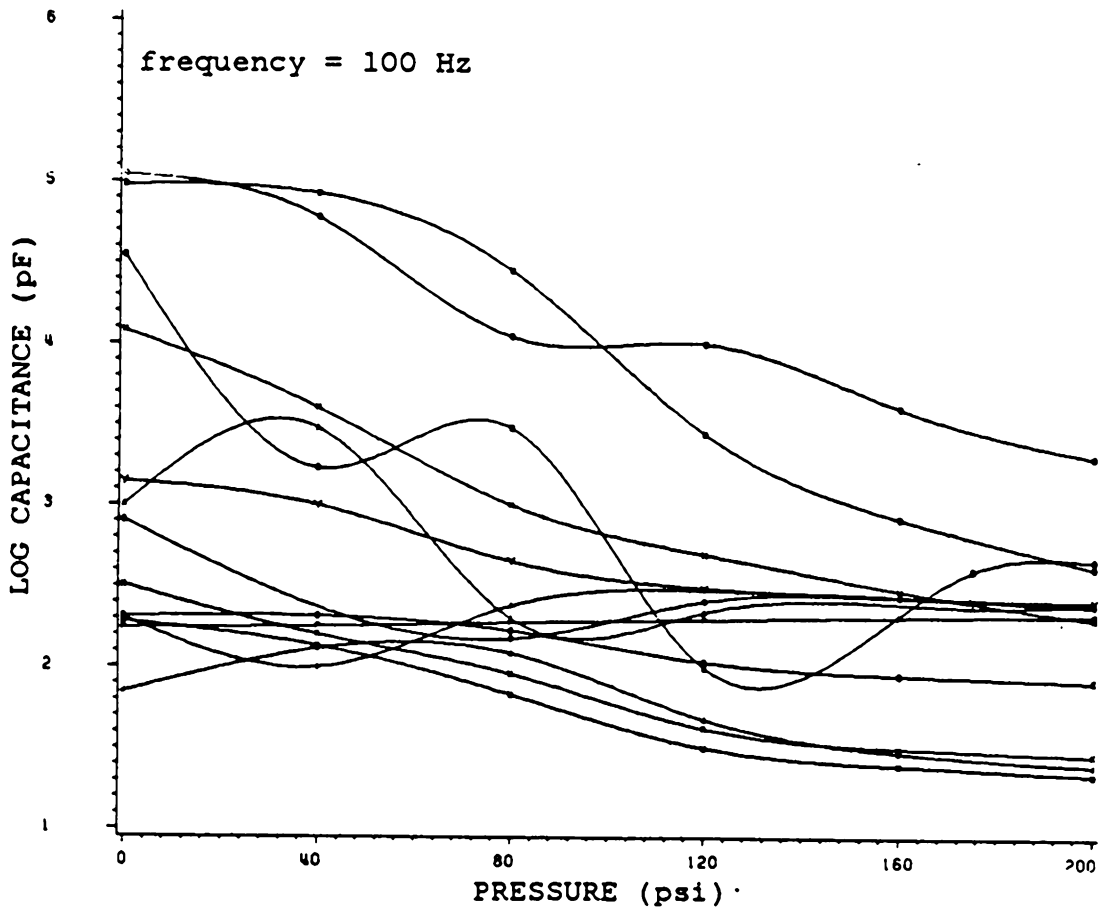


Figure 23. Capacitance versus pressure at 100Hz for all samples. The general trend of decreasing capacitance with increasing pressure can be seen here.

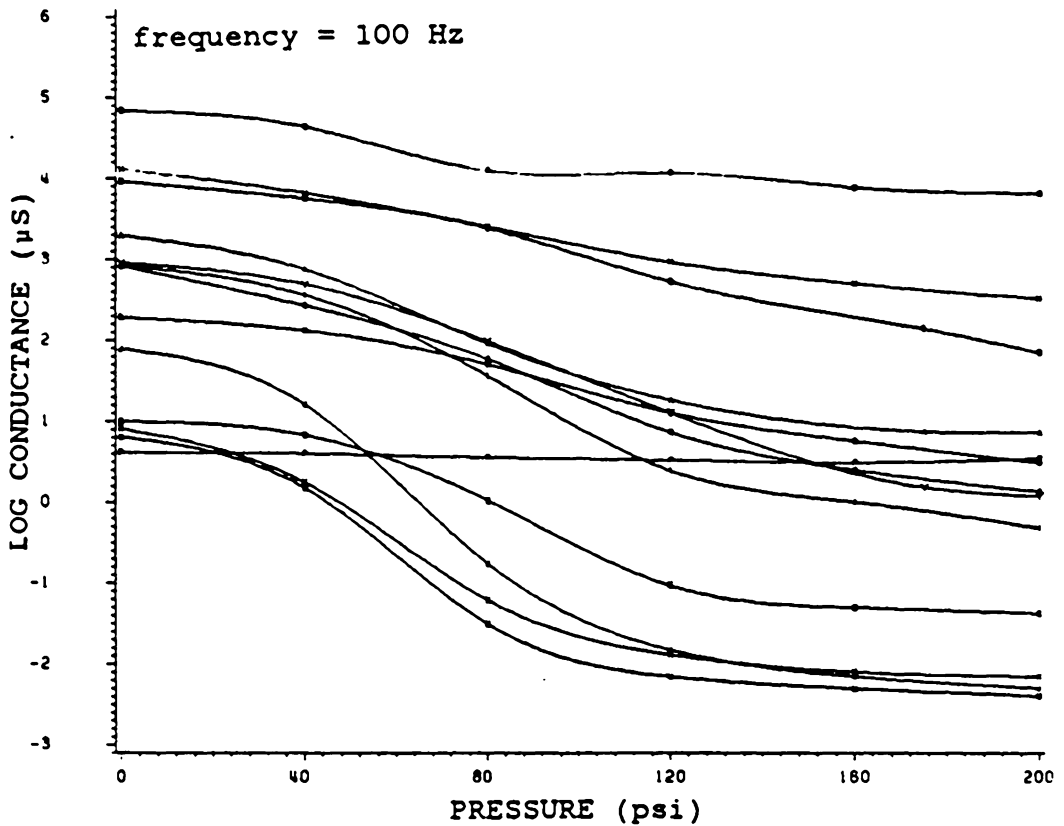


Figure 24. Conductance versus pressure at 100Hz for all samples. The general trend of decreasing conductance with increasing pressure can be seen here.

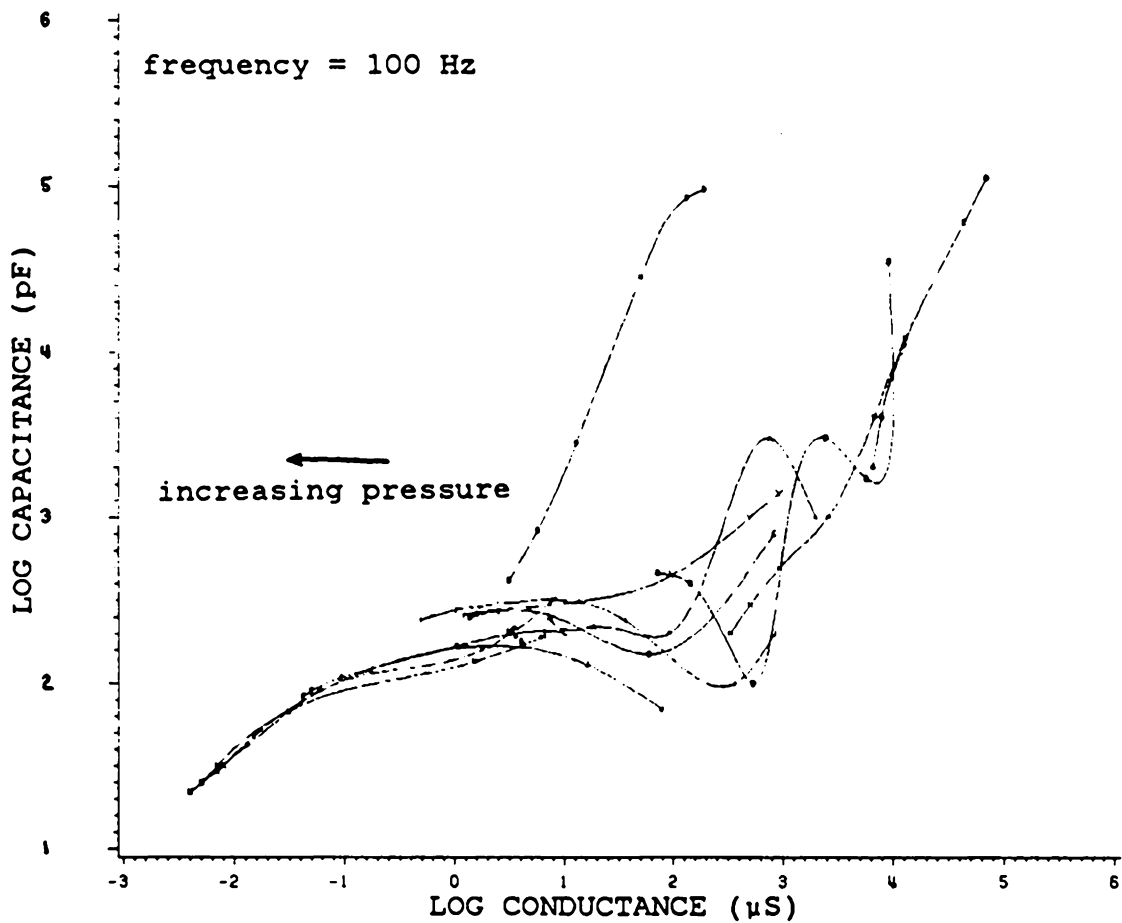


Figure 25. Capacitance versus conductance for several pressures at 100Hz. Curves for all samples are shown here and a trend common to all samples is evident.

tories. Measurements were made for five "states" which are listed below.

1. After initial thermal relief
2. 10 minutes after 150 psi application and removal
3. After sitting overnight
4. After 10 minutes at 70°C
5. After 50 additional minutes at 70°C

The responses for each sample can be seen in Figures 26 - 35. The effect of sulfur can be seen between samples NAT14 (1.5 phr sulfur) and NAT15 (5.0 phr sulfur). The total change in capacitance and conductance is greater for the less sulfur, less crosslinked, less bound, sample NAT14. The magnitude of the capacitance and conductance values is greater for the higher sulfur sample.

Sample NAT42, which had one of the greatest changes under pressure also exhibits the largest range of conductivity from "state" 1 to "state" 5. However, its capacitance changes very little at any frequency in any "state".

Sample NAT38 has a response similar to NAT14 and NAT15 as it also behaved similarly in the resistance response to the applied load profile (section 3.2). In the load profile tests, the magnitude and shape of the NAT38 response was more like that of NAT15 than NAT14. The same is true for NAT38 in

this test also. Additionally NAT38 has a larger capacitance and conductance at all frequencies than NAT14 or NAT15.

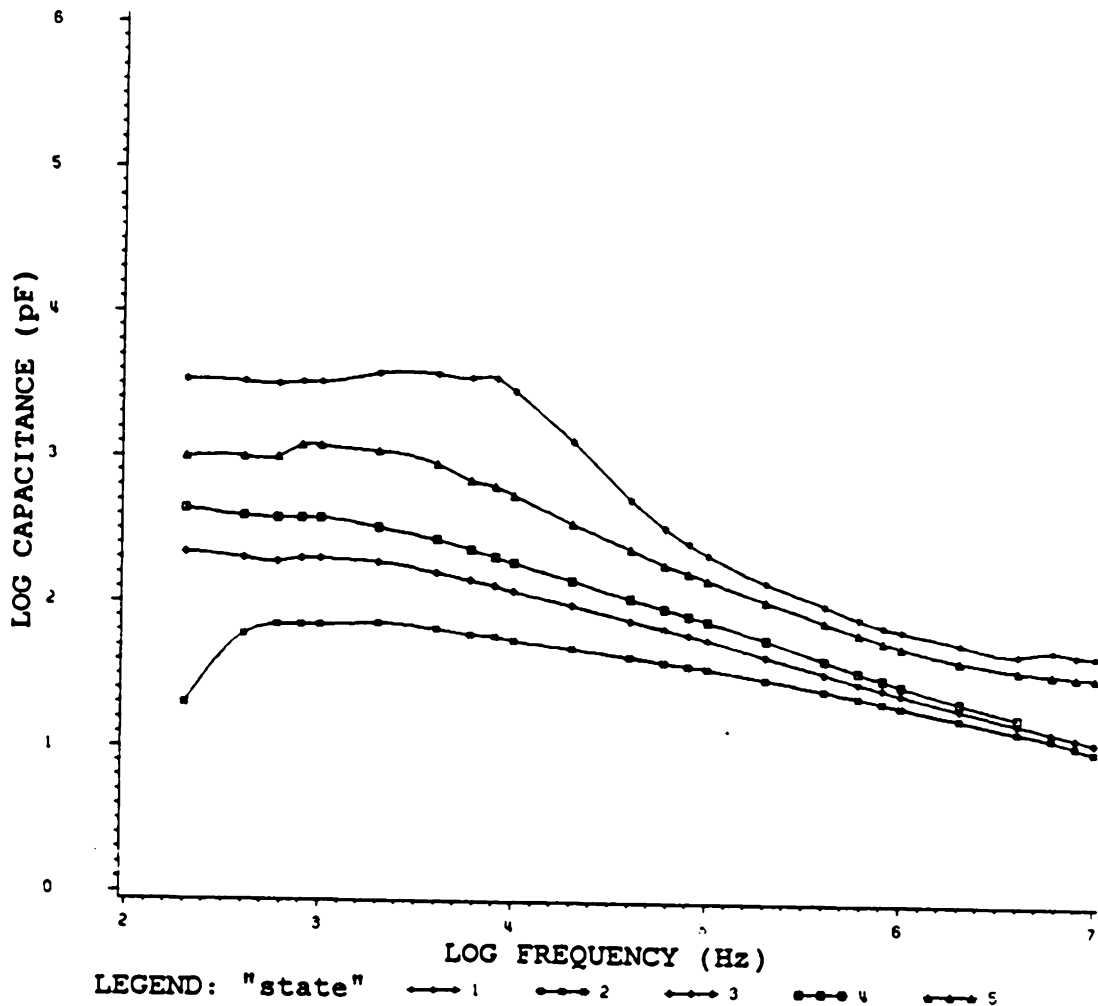
The response of sample NAT18 is again very different from any other sample. It also seems to have the smoothest response curves found.

There is a general trend observable across all samples for this experiment which is that after pressure application and removal, the capacitance and conductance curves are lowered. (again C follows G) The capacitance is most greatly affected at low frequencies and the conductance is more equally affected at all frequencies.

As the frequency is lowered, the response of the "larger" polarizable entities is observed. After pressure application and removal it appears that there are less of these entities present. This could indicate that the "large" entities are carbon black structures which are broken into smaller structures with pressure. With time and/or temperature, these structures "re-form" and the carbon black filled rubber regains its original properties.

4.9 CAPACITANCE AND CONDUCTANCE TRENDS WITH MECHANICAL HISTORY

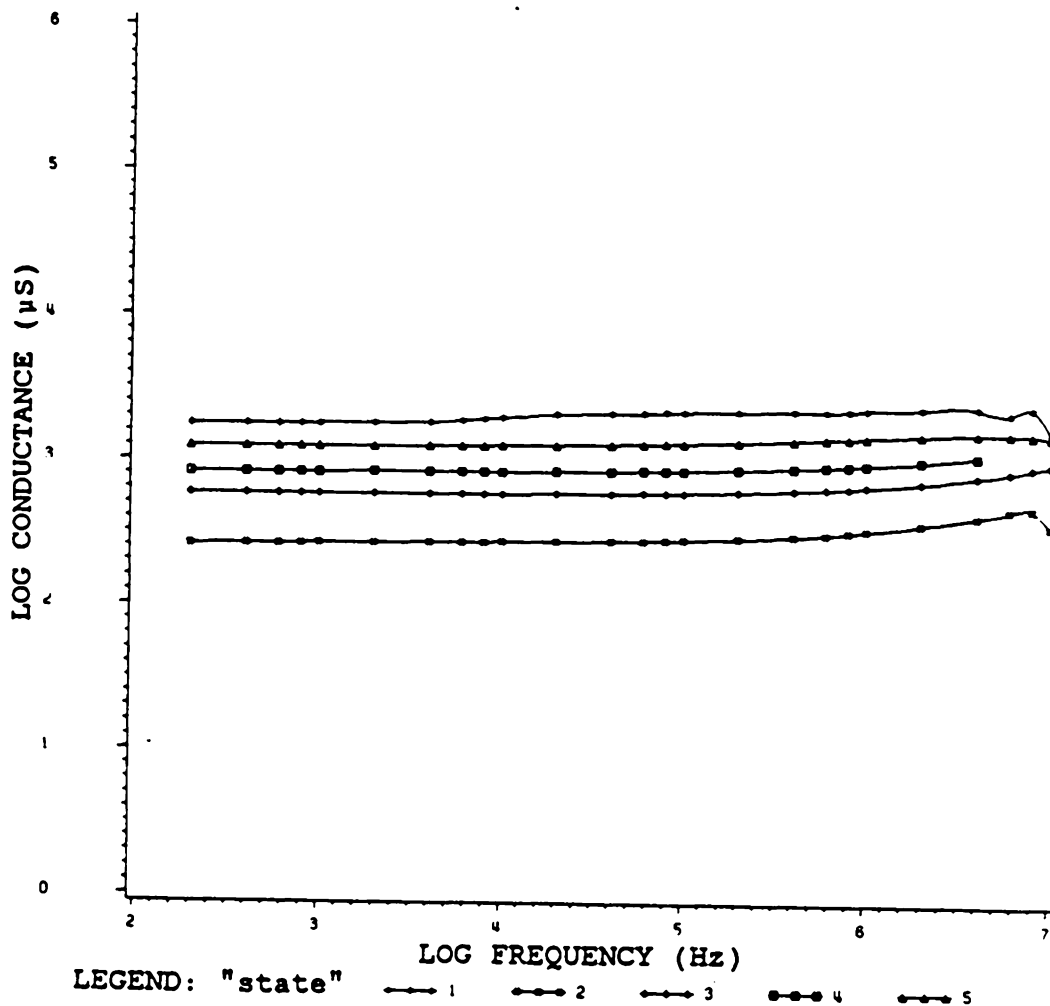
Capacitance and conductance as a function of frequency for 8 "virgin" and 8 identical mechanically degraded samples have been measured and plotted in Figures 36 - 39. The "virgin"



"state"

- 1 - thermally relieved
- 2 - 10 min. after 150 psi compression and release
- 3 - after sitting overnight
- 4 - after 10 min. at 70°C and cooled to room temp.
- 5 - after 50 additional min. at 70°C and cooled to room temp.

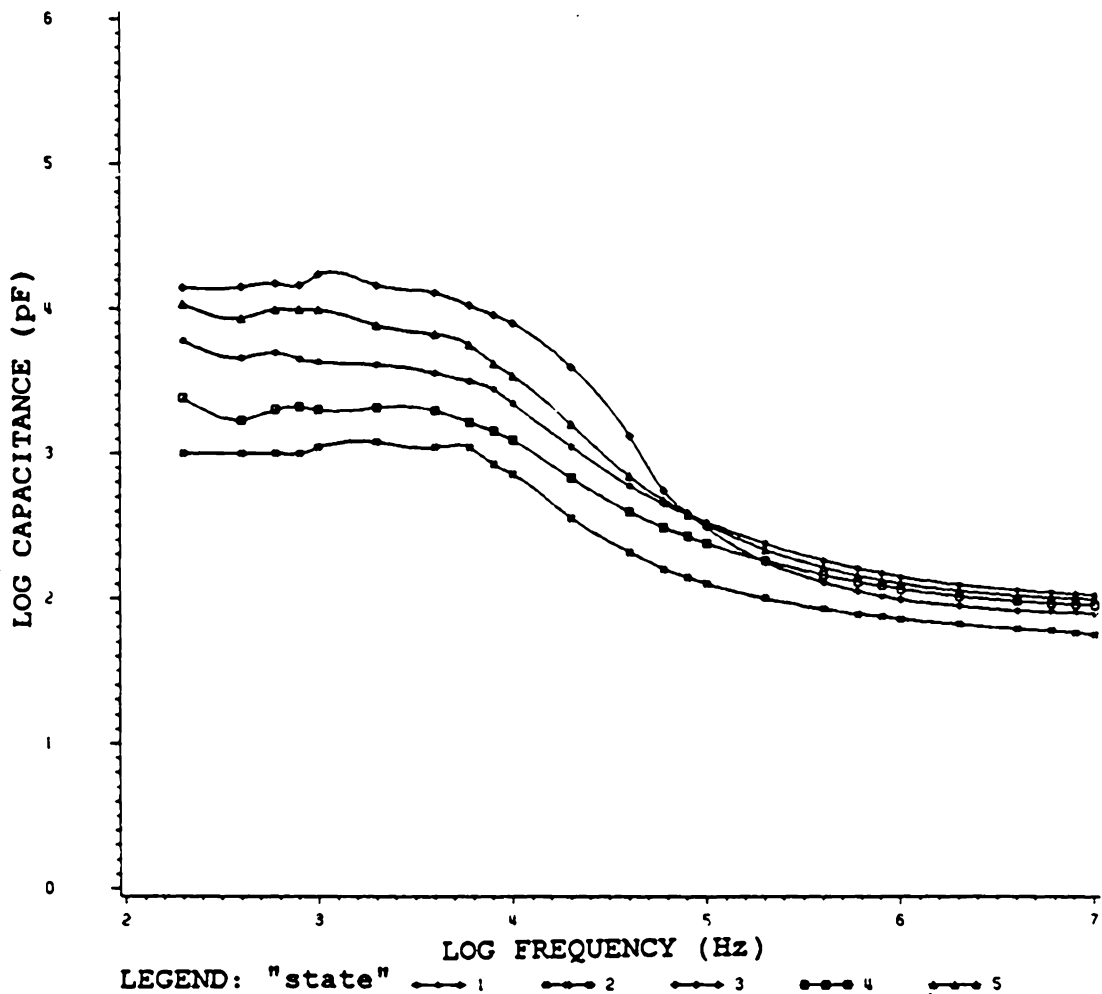
Figure 26. Capacitance versus frequency for NAT14 in various "states"



"state"

- 1 - thermally relieved
- 2 - 10 min. after 150 psi compression and release
- 3 - after sitting overnight
- 4 - after 10 min. at 70°C and cooled to room temp.
- 5 - after 50 additional min. at 70°C and cooled to room temp.

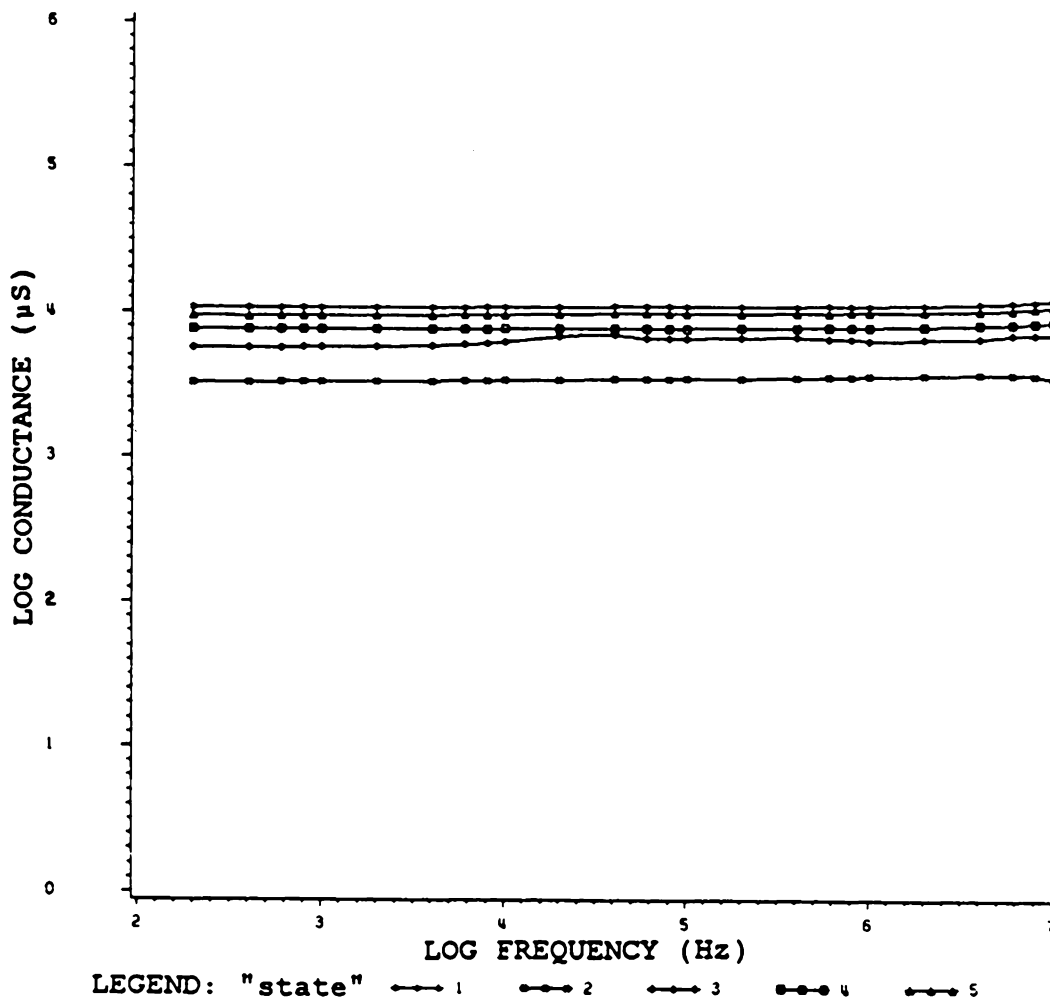
Figure 27. Conductance versus frequency for NAT14 in various "states"



"state"

- 1 - thermally relieved
- 2 - 10 min. after 150 psi compression and release
- 3 - after sitting overnight
- 4 - after 10 min. at 70°C and cooled to room temp.
- 5 - after 50 additional min. at 70°C and cooled to room temp.

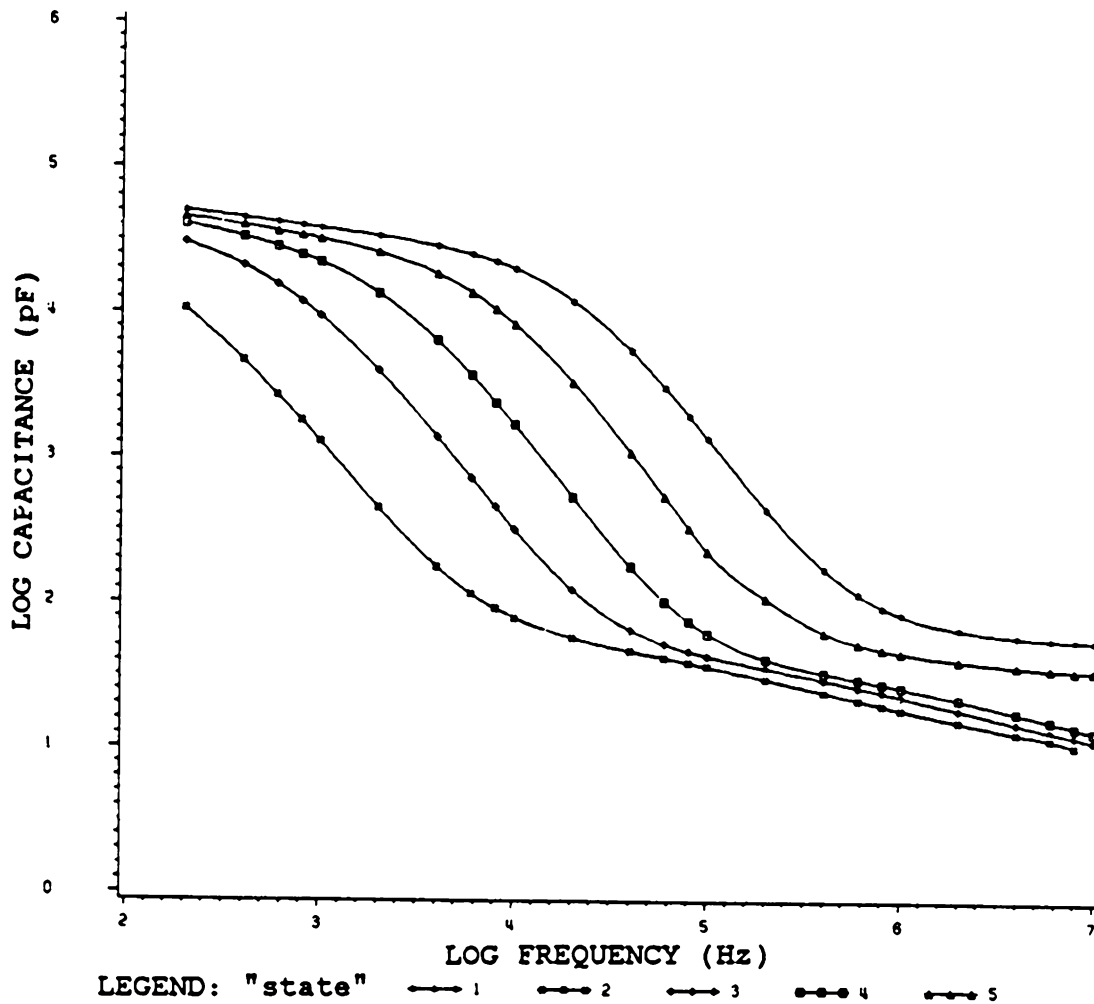
Figure 28. Capacitance versus frequency for NAT15 in various "states"



"state"

- 1 - thermally relieved
- 2 - 10 min. after 150 psi compression and release
- 3 - after sitting overnight
- 4 - after 10 min. at 70°C and cooled to room temp.
- 5 - after 50 additional min. at 70°C and cooled to room temp.

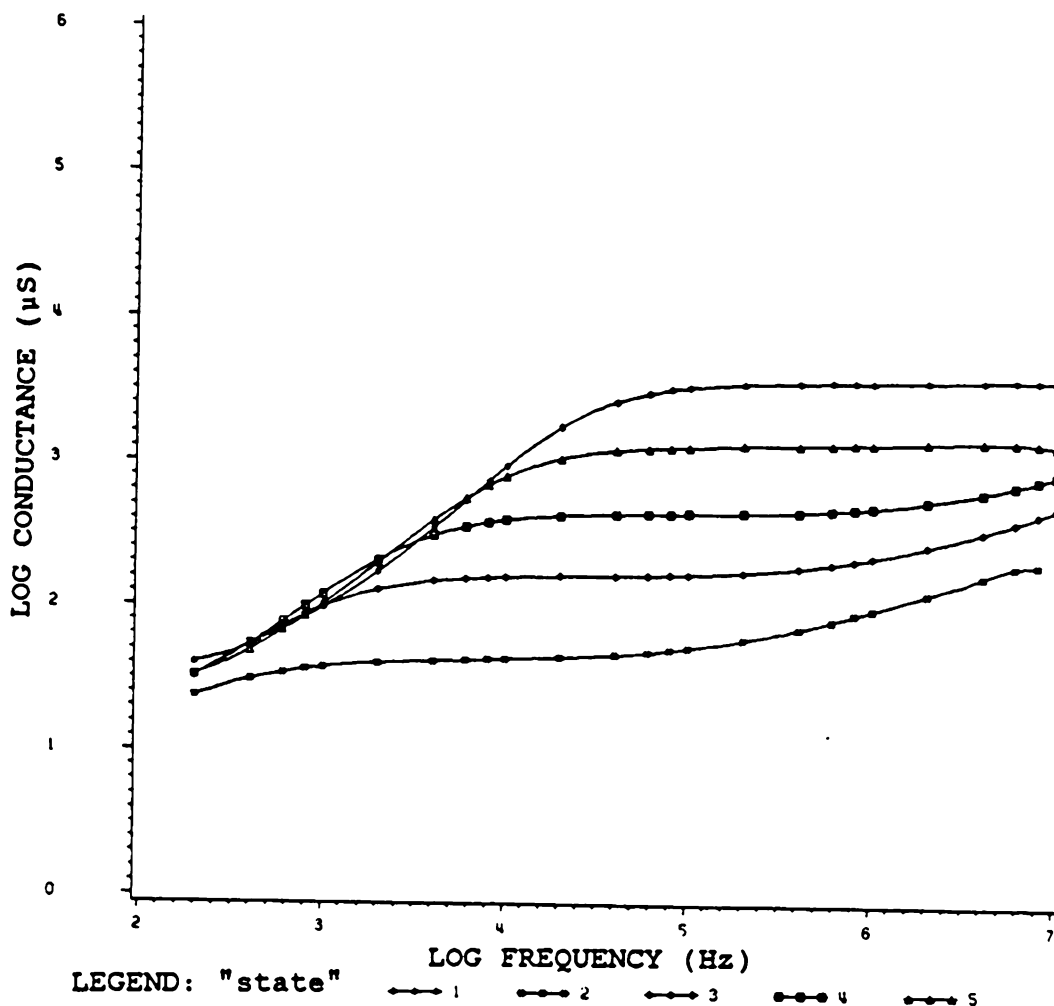
Figure 29. Conductance versus frequency for NAT15 in various "states"



"state"

- 1 - thermally relieved
- 2 - 10 min. after 150 psi compression and release
- 3 - after sitting overnight
- 4 - after 10 min. at 70°C and cooled to room temp.
- 5 - after 50 additional min. at 70°C and cooled to room temp.

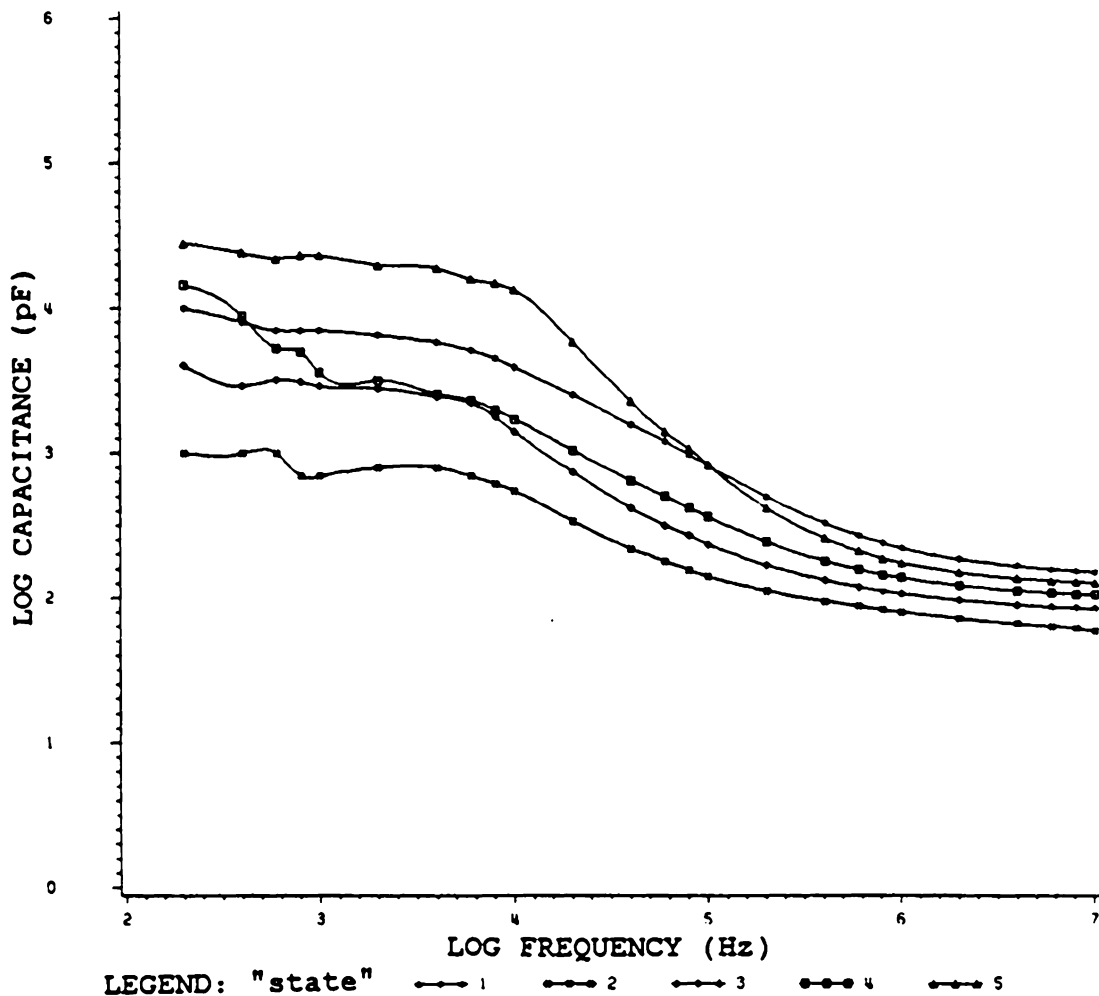
Figure 30. Capacitance versus frequency for NAT18 in various "states"



"state"

- 1 - thermally relieved
- 2 - 10 min. after 150 psi compression and release
- 3 - after sitting overnight
- 4 - after 10 min. at 70°C and cooled to room temp.
- 5 - after 50 additional min. at 70°C and cooled to room temp.

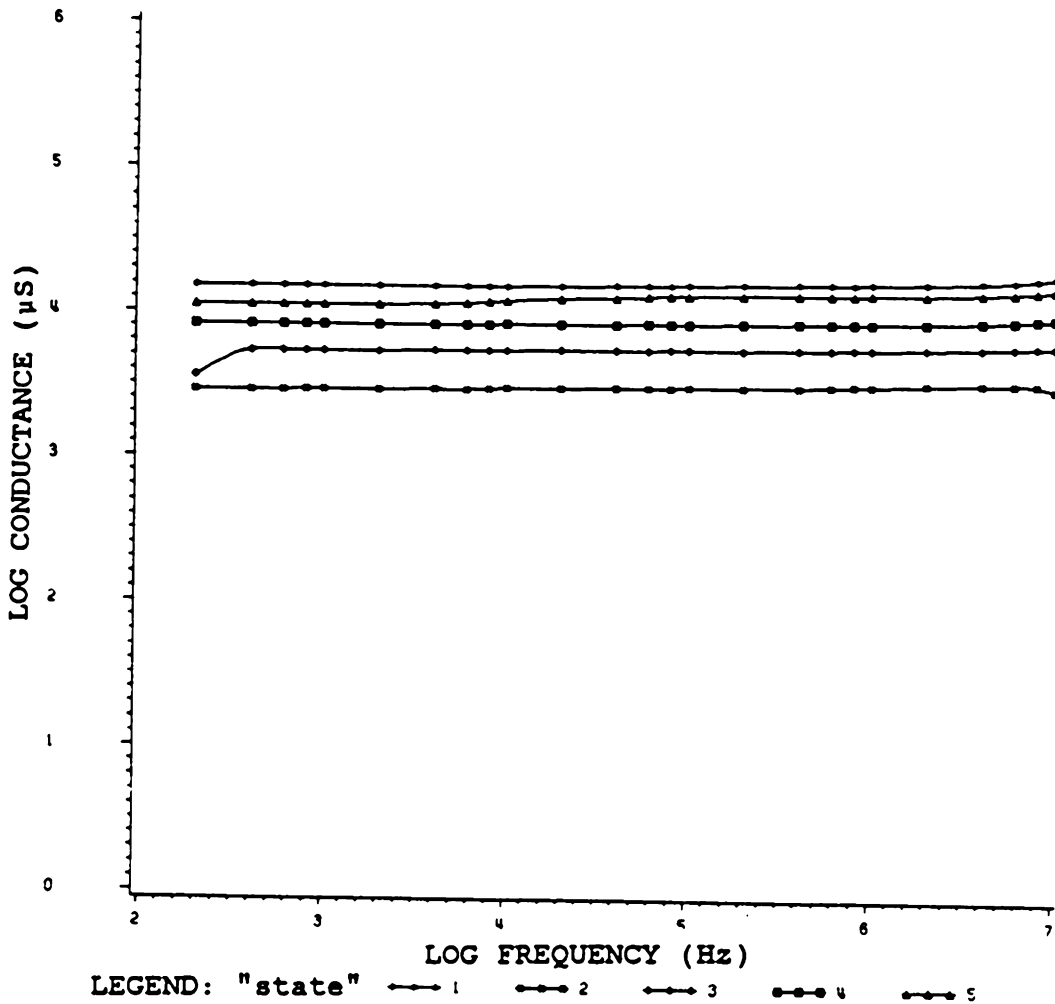
Figure 31. Conductance versus frequency for NAT18 in various "states"



"state"

- 1 - thermally relieved
- 2 - 10 min. after 150 psi compression and release
- 3 - after sitting overnight
- 4 - after 10 min. at 70°C and cooled to room temp.
- 5 - after 50 additional min. at 70°C and cooled to room temp.

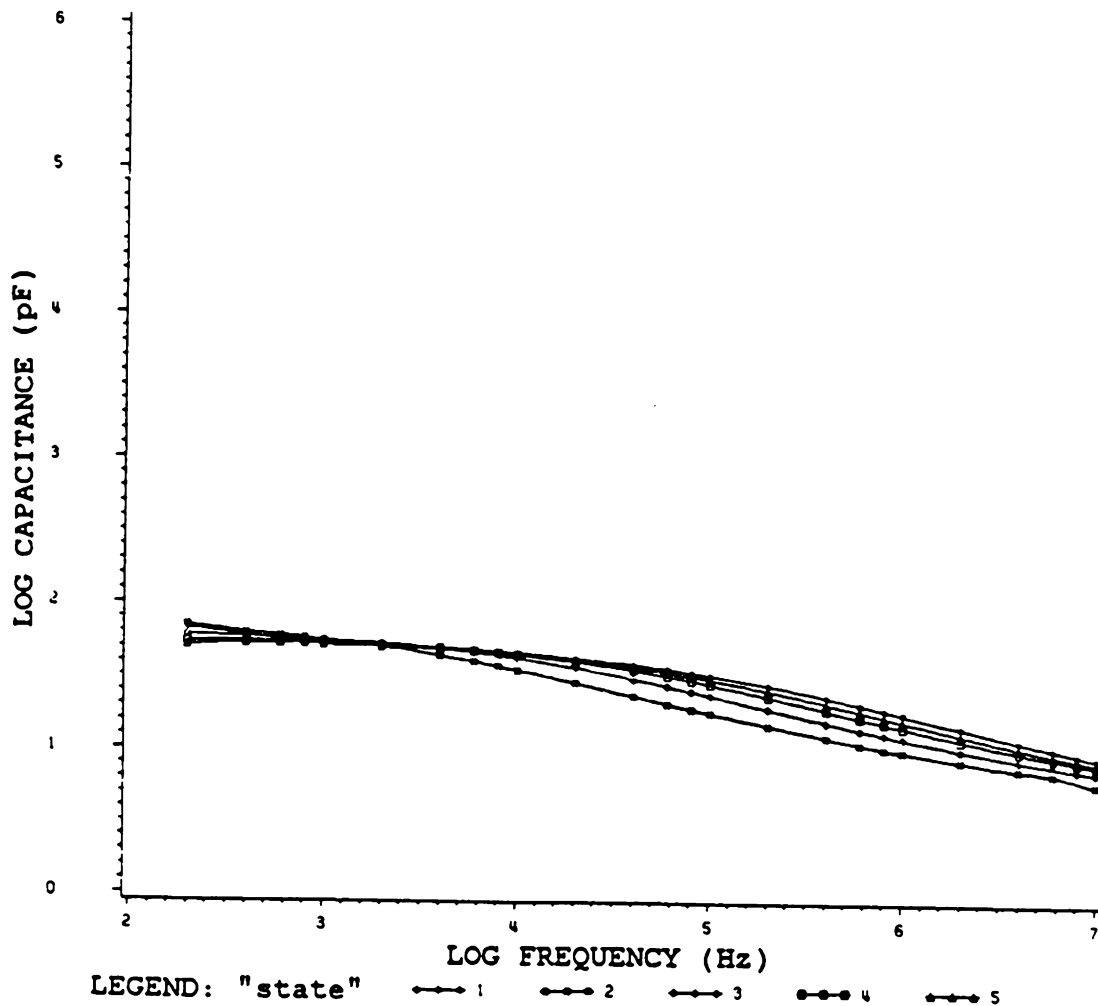
Figure 32. Capacitance versus frequency for NAT38 in various "states"



"state"

- 1 - thermally relieved
- 2 - 10 min. after 150 psi compression and release
- 3 - after sitting overnight
- 4 - after 10 min. at 70°C and cooled to room temp.
- 5 - after 50 additional min. at 70°C and cooled to room temp.

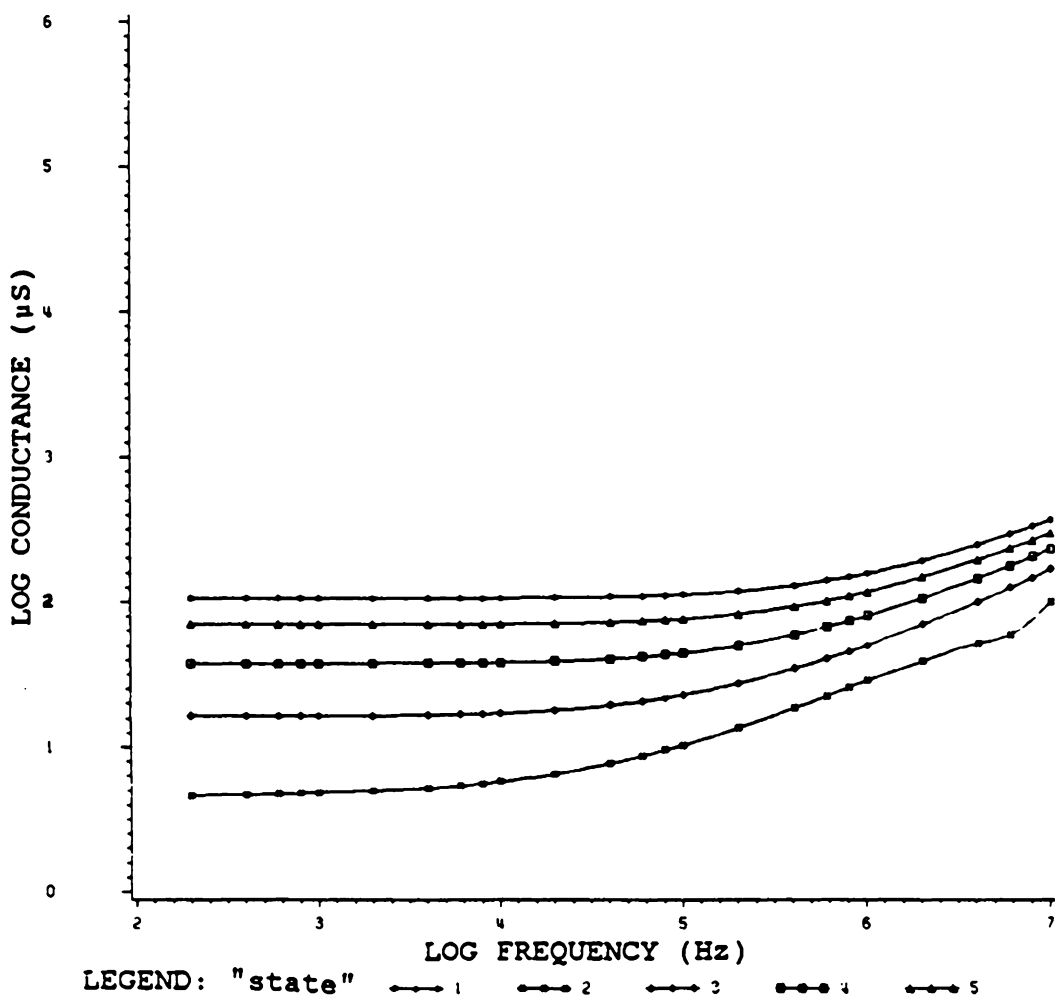
Figure 33. Conductance versus frequency for NAT38 in various "states"



"state"

- 1 - thermally relieved
- 2 - 10 min. after 150 psi compression and release
- 3 - after sitting overnight
- 4 - after 10 min. at 70°C and cooled to room temp.
- 5 - after 50 additional min. at 70°C and cooled to room temp.

Figure 34. Capacitance versus frequency for NAT42 in various "states"



"state"

- 1 - thermally relieved
- 2 - 10 min. after 150 psi compression and release
- 3 - after sitting overnight
- 4 - after 10 min. at 70°C and cooled to room temp.
- 5 - after 50 additional min. at 70°C and cooled to room temp.

Figure 35. Conductance versus frequency for NAT42 in various "states"

samples had been thermally cycled up to 5 times in previous tests but had never been mechanically tested. The degraded samples had been subjected to uniaxial compressive stresses of 60 to 200 psi several hundred times and had been thermally cycled up to 15 times. A trend of decreasing capacitance and conductance occurs with mechanical history.

4.10 EQUIVALENT CIRCUIT MODEL

Theories have been formulated for conductive network formation and its behavior. The results of this study add a new dimension to the previous theories in that the capacitive behavior is found to be a function of the same mechanism as the conductive behavior. Thus when one describes events that occur on the "micro" level to explain conductive responses, they must also now be able to account for the capacitive behavior.

It is known that

$$C = \epsilon_0 KA/d$$

and that, in these tests ϵ_0 and A are constants. The change in K of an elastomer or a carbon black particle upon small stress application can be considered to be negligible. Thus we can attribute changes in C to changes in d. The distance, d, for an insulator filled with conductive particles will not be the same as the macroscopic "d". Rather, this system

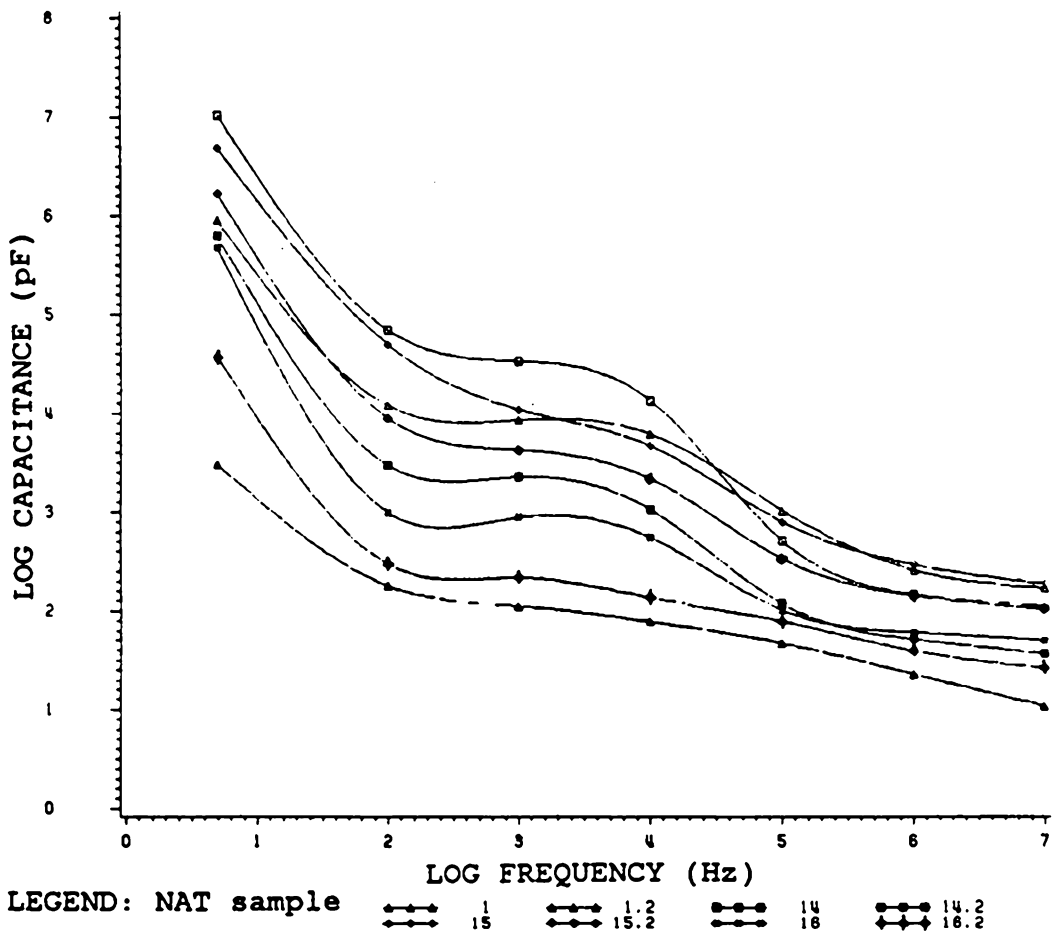


Figure 36. Capacitance versus frequency for "virgin" and degraded samples: (1, 14, 15 and 16 are "virgin", 1.2, 14.2, 15.2 and 16.2 are degraded)

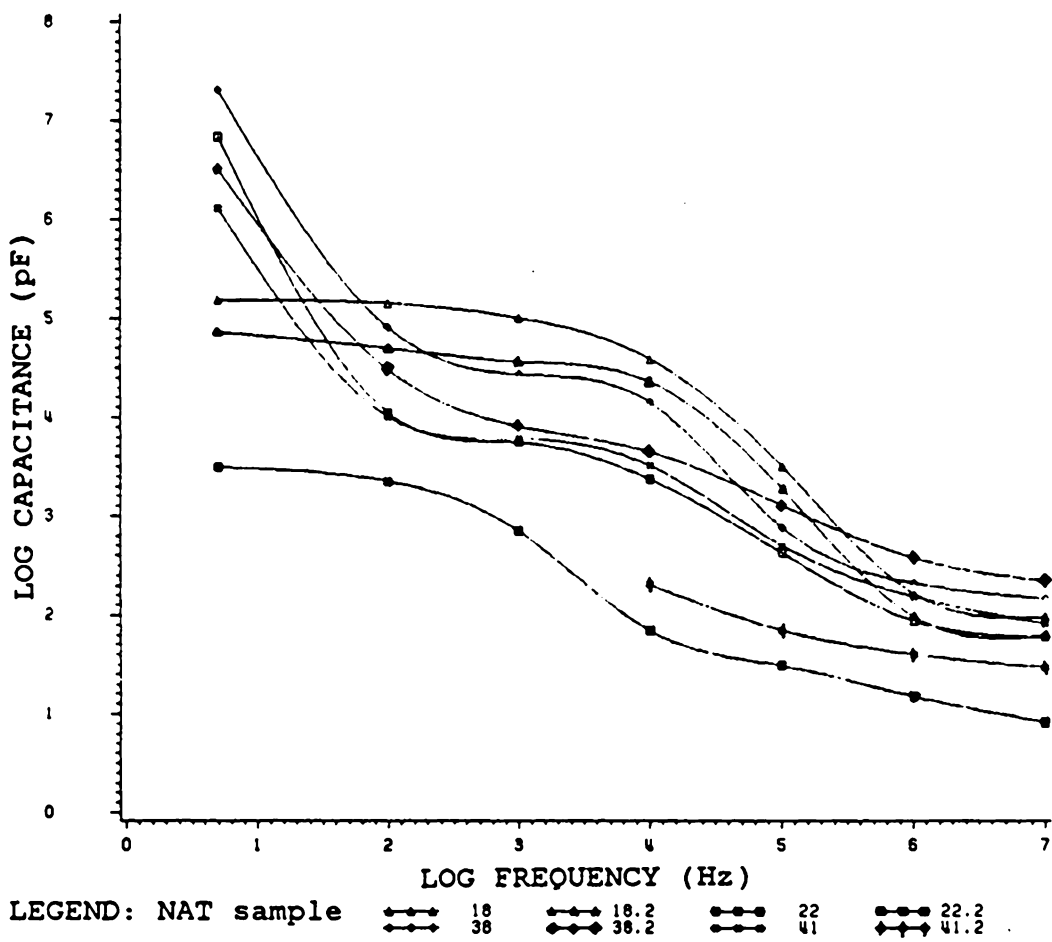


Figure 37. Capacitance versus frequency for "virgin" and degraded samples: (18, 22, 38 and 41 are "virgin", 18.2, 22.2, 38.2, and 41.2 are degraded)

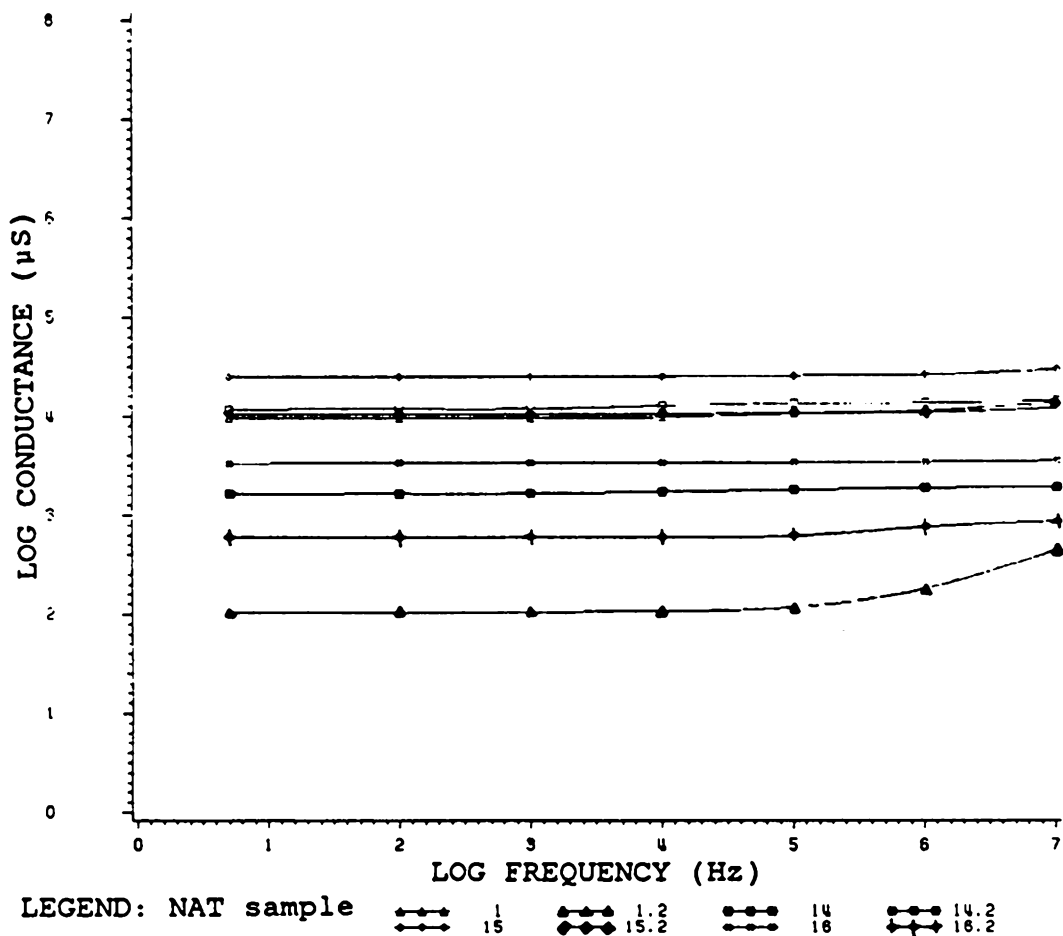


Figure 38. Conductance versus frequency for "virgin" and degraded samples: (1, 14, 15 and 16 are "virgin", 1.2, 14.2, 15.2, and 16.2 are degraded)

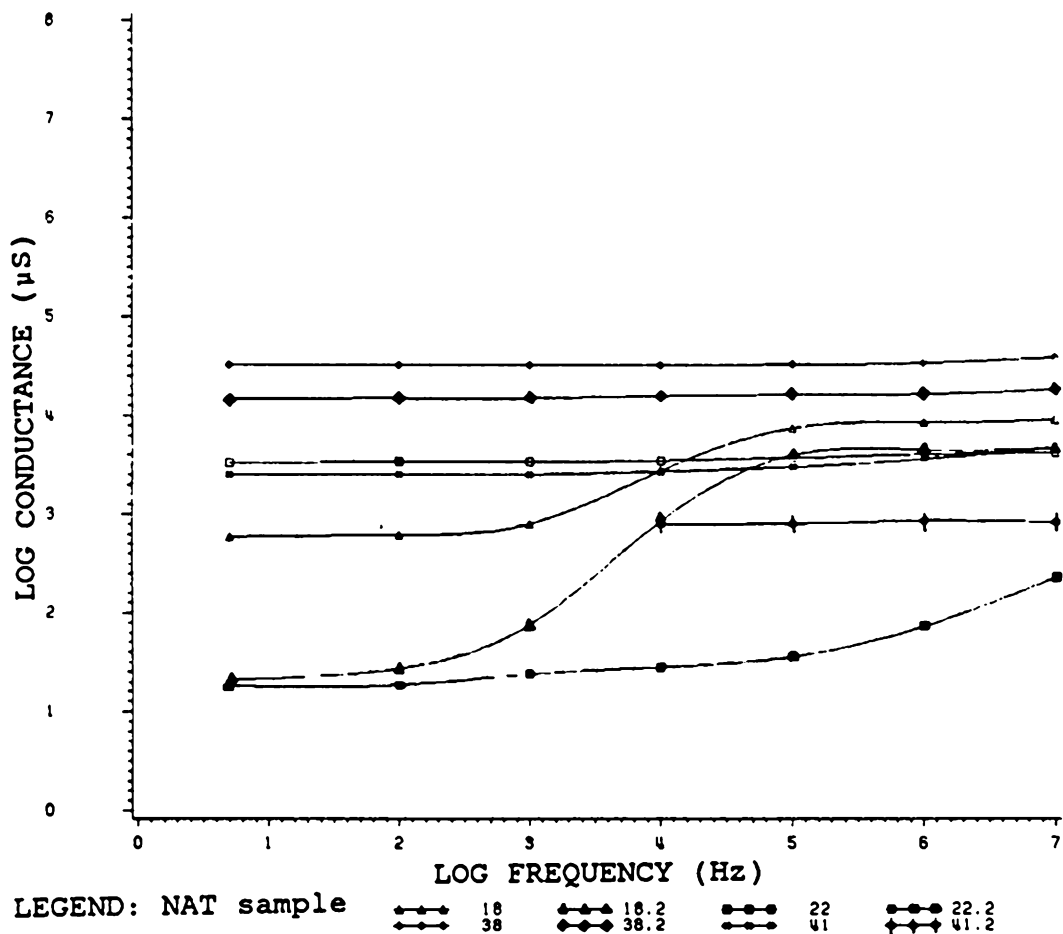


Figure 39. Capacitance versus frequency for "virgin" and degraded samples: (18, 22, 38 and 41 are "virgin", 18.2, 22.2, 38.2, and 41.2 are degraded)

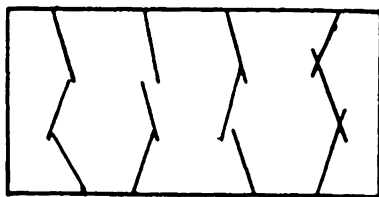
could be viewed as a network of "micro"capacitors, each with their own "d".

If one considers also that the carbon black network physically breaks down under pressure, then at each interparticle break point, another capacitor is created. Therefore one must also consider the possibility of the creation of many more capacitors which, when placed in series can serve to lower the macroscopic capacitance.

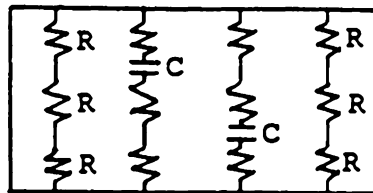
We can now describe an equivalent circuit of the composite. It will consist of a network of conductive carbon black particles (above the percolation threshold) and a separate network of "micro"capacitors. Stress can cause the dimensions of the "micro"capacitors to change and it can also cause part of the conductive network to break down creating new capacitors, thus reducing both the macroscopic capacitance and conductance. This equivalent circuit for an uncompressed and a compressed sample is drawn schematically in Figure 40.

4.11 THERMOELECTRIC EFFECT

All samples in this study responded to thermal stimulation in the same way. The electrode opposite the heat source registered a negative polarity within 2-3 seconds after heat application. This indicates that the charge carriers are either electrons or negative ions.



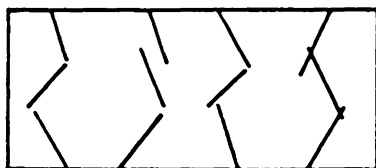
NETWORK



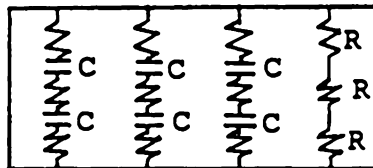
EQUIVALENT CIRCUIT

resistance = $1.5 R$
 capacitance = $2 C$

BEFORE COMPRESSIVE LOADING



NETWORK



EQUIVALENT CIRCUIT

resistance = $3 R$
 capacitance = $1.5 C$

AFTER COMPRESSIVE LOADING

Figure 40. Equivalent circuit for carbon black filled rubber

The quick time response of this measurement, and the absence of current drift during longer-term current measurements, indicates that the carrier is the electron.

4.12 THERMAL CONDUCTIVITY

Thermal conductivity, K , can be defined as;

$$K = Pt/A\Delta T$$

where P = power in

t = sample thickness

A = sample area

ΔT = change in temperature across the sample

In this experiment, the input power was measured as the power input into the heaters ($P=IV$). The heat generated can travel only in two directions, assuming that the sides of the copper blocks are perfectly insulated.

After initial experiments it was found that the ΔT across the lower rubber sample was always around 2°C less than the ΔT across the upper rubber sample. Assuming that the thermal conductivities for identical samples would not be significantly different, this difference in ΔT 's could be accounted for in that the power that each sample was apportioned was not equal. This was probably because the lab bench upon which the apparatus sat made the apparatus non-symmetric in heat conduction.

Thus assuming equal thermal conductivities for identical samples 1 & 2;

$$\begin{aligned}K &= t_1 P_1 / A_1 \Delta T_1 \\ &= t_2 P_2 / A_2 \Delta T_2\end{aligned}$$

$$t_1 = t_2$$

$$K_1 = K_2$$

$$A_1 = A_2$$

$$P_1 + P_2 = P(\text{total}) = P$$

$$K_1 A_1 / t_1 = P_1 / \Delta T_1$$

$$K_2 A_2 / t_2 = P_2 / \Delta T_2$$

therefore;

$$P_1 / P_2 = \Delta T_2 / \Delta T_1$$

and one can algebraically arrive at;

$$K = t P / A (\Delta T_1 + \Delta T_2)$$

Each of the 15 samples were measured for K then allowed to sit for at least one week and then remeasured for K again. All of the data was combined and the resulting K(average) values and their standard deviations are listed in Table 9.

Table 9. Thermal conductivity values for all samples

SAMPLE	K(AVERAGE) X.1000 (J/CM S K)	STANDARD DEVIATION X.1000 (J/CM S K)	NUMBER OF MEASUREMENTS
NAT25A	3.063	0.027	9
NAT14	2.866	0.008	7
NAT1	3.055	0.015	13
NAT15	2.950	0.012	7
NAT16	2.844	0.011	9
NAT18	2.926	0.023	8
NAT41	3.033	0.031	10
NAT42	2.962	0.035	8
NAT44	3.080	0.009	6
NAT43	3.022	0.010	8
NAT38	3.131	0.020	9
NAT57	3.118	0.027	8
NAT61	2.867	0.022	9
NAT60	3.351	0.028	8
NAT22A	3.088	0.015	8

The assumption that there is no heat loss at the sides of the apparatus is not true, however heat loss can be considered to be small and relatively constant over a small temperature range. Heat loss at the sides would cause the apparent thermal conductivity to be higher than the actual thermal conductivity because the total power, P , to the rubber samples would be less than the input power. The measured values for K have a very low standard deviation ($\pm 1\%$). This indicates that any heat losses are very consistent and that these values are at least relatively accurate.

Values for thermal conductivity for natural rubber filled with 40 phr carbon black have been reported as around .00250 J/cm sec K (67) which is exactly in the region of these results. (NOTE - Most of the samples in this experiment have only 45 phr carbon black.)

5.0 CONCLUSIONS AND RECOMMENDATIONS

Many experiments were performed in this study of carbon black filled rubber in search of characterization techniques and fundamental information. The original objectives of this investigation were met in that ;

1. A mechanical test was devised where the electrical resistance was simultaneously monitored and a unique response or "signature" was recorded for each sample type. Thus, all samples are electrically distinguishable.
2. Fundamental behavior was explored and new insights given to this system by establishing a "link" between the resistive and capacitive responses to mechanical and thermal stimulation. Because the resistive and capacitive responses are so similar for a given sample type under all conditions, the mechanisms for changes in each are likely to be the same. The electrical behavior has been explained in terms of the existence of a conductive network inside the composite and its response to thermal and mechanical stimulations.

The samples in this study were found to respond ohmically at voltages up to 100 volts. This indicates that the dominant mode of conduction is through carbon

black inter-agglomerate contacts from one electrode to the other. A capacitor exists anywhere there are two carbon black entities which are separated by a distance. When a carbon black filled rubber sample is compressed, in most all cases, its resistance increases and capacitance decreases. An analogous resistance response has been previously observed for samples tested in tension and explained as being due to disruption of the conductive network inside the composite. The results found in this study are consistent with the previous theories.

Capacitive behavior has previously not been monitored concurrent with resistive behavior. The conductive network is disrupted upon compression also, and the resistance increases. Additionally, the decrease in capacitance can be the result of only two mechanisms ; either the distance between the electrodes of the existing "micro"capacitors is increased or capacitors are added in series to the "network". Both mechanisms could reasonably occur. However, upon approximately 10% compression, the maximum change in the distance between electrodes of existing capacitors would be about 10% which could not account for the more than tenfold capacitance changes observed. Thus "micro"capacitors must be added in series to the network.

Temperature coefficients of resistivity were measured under load and no load conditions resulting in PTC and NTC resistance responses respectively. This is attributed to the "state" of the conductive network in both cases. The author believes that the most complete conductive network is formed at a high temperature during vulcanization and is somewhat disrupted with contraction upon cooling to room temperature. Thus, an increase in temperature under no load conditions allows the network to approach its most complete "state". When a sample is stressed at room temperature, its existing network is disrupted. When the temperature is additionally increased, the expansion of the sample being restricted in one direction only serves to cause further disruption of the network and thus a PTC response.

Thermal conductivities of all samples were recorded in the same temperature range and no correlation was found between these values and the room temperature resistance values. All values of thermal conductivity fell within an approximate 10% range and were only about twice that of unfilled natural rubber, whereas the range of electrical resistances was from 10^8 ohms to greater than 10^6 ohms.

A correlation exists between the magnitude of resistance response to the applied load profile and the modulus in the sample series that varies in sulfur content

(NAT25A,NAT14,NAT1,NAT15). This correlation could also be extended to other mechanical properties that are related to sulfur content. Other electrical-mechanical property correlations are not apparent between the electrical measurements performed in this study and the mechanical data provided by the U.S. Army. The range of values for most of the mechanical property data probably falls within the standard deviation for any one sample and thus correlations for such data are not postulated.

3. The electrical properties of any carbon black filled rubber have been shown to be very sensitive indicators of the "state" of the composite at any time. Certain mechanical properties of such composites, particularly time to fail under cyclic load, may also be functions of the "state" of the composite which can only be measured electrically. More information is needed to determine if electrical measurements can be used to help improve tank track pad reliability. Such information may be gained by performing relevant experiments to:

- a. see how resistance and capacitance change during vulcanization and upon cooling to room temperature;

- b. obtain carbon black filled samples that varied in their extent of mixing to record their resistance and capacitance as a function of mechanical degradation;
- c. obtain microstructural photographs of these composites to see if any differences can be seen and correlated with their electrical and/or mechanical behavior;
- d. obtain electrical and thermal conductivity data at the same temperature and look for correlations;
- e. determine the effect of humidity on electrical properties;
- f. measure the electrical response of samples to an applied standardized strain profile;
- g. and correlate measurements of these types performed on actual tank track pad material with the field performance of the same material.

APPENDIX A. RESISTANCE "SIGNATURES"

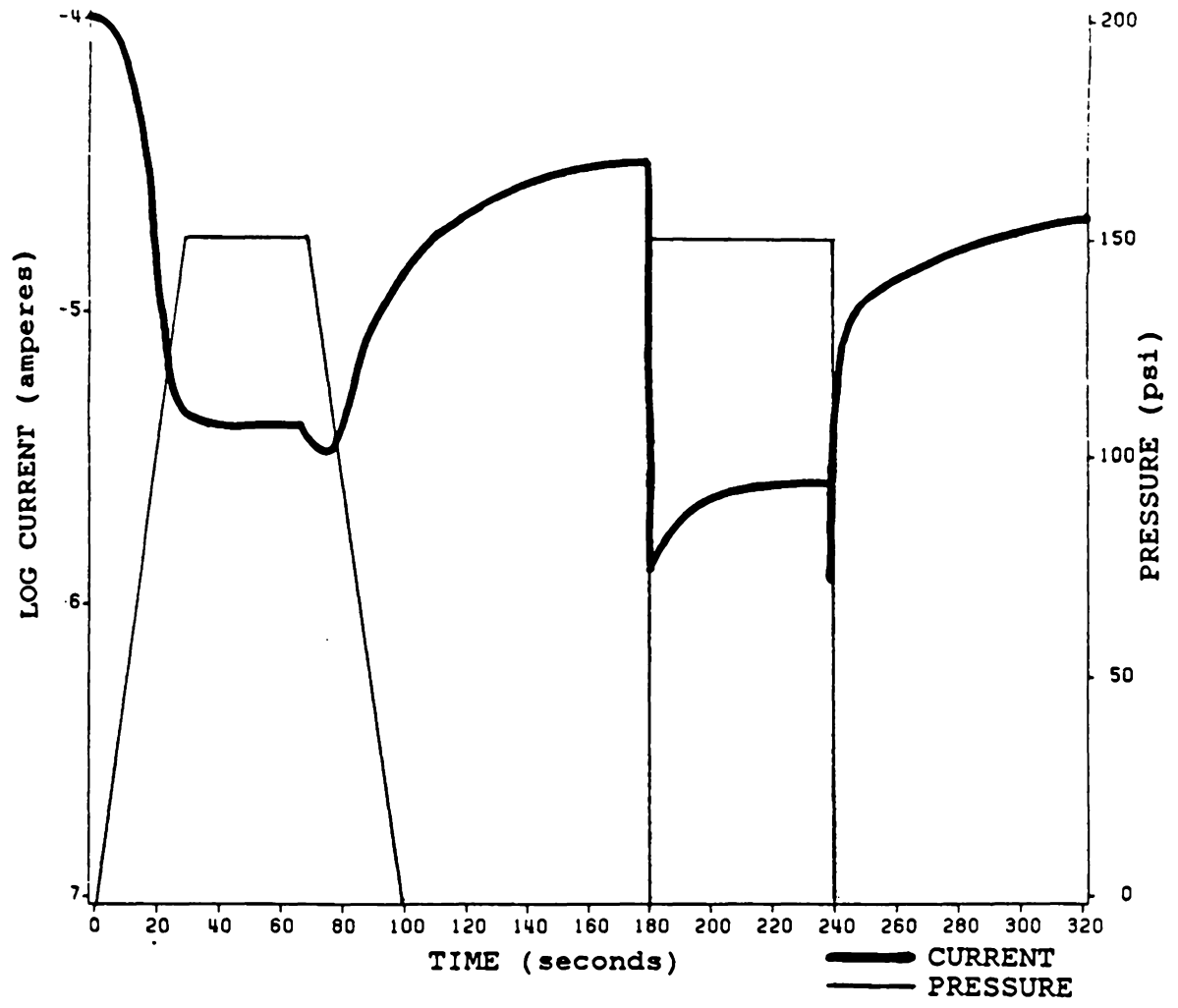


Figure 41. Resistance response to a standardized load profile (NAT25A)

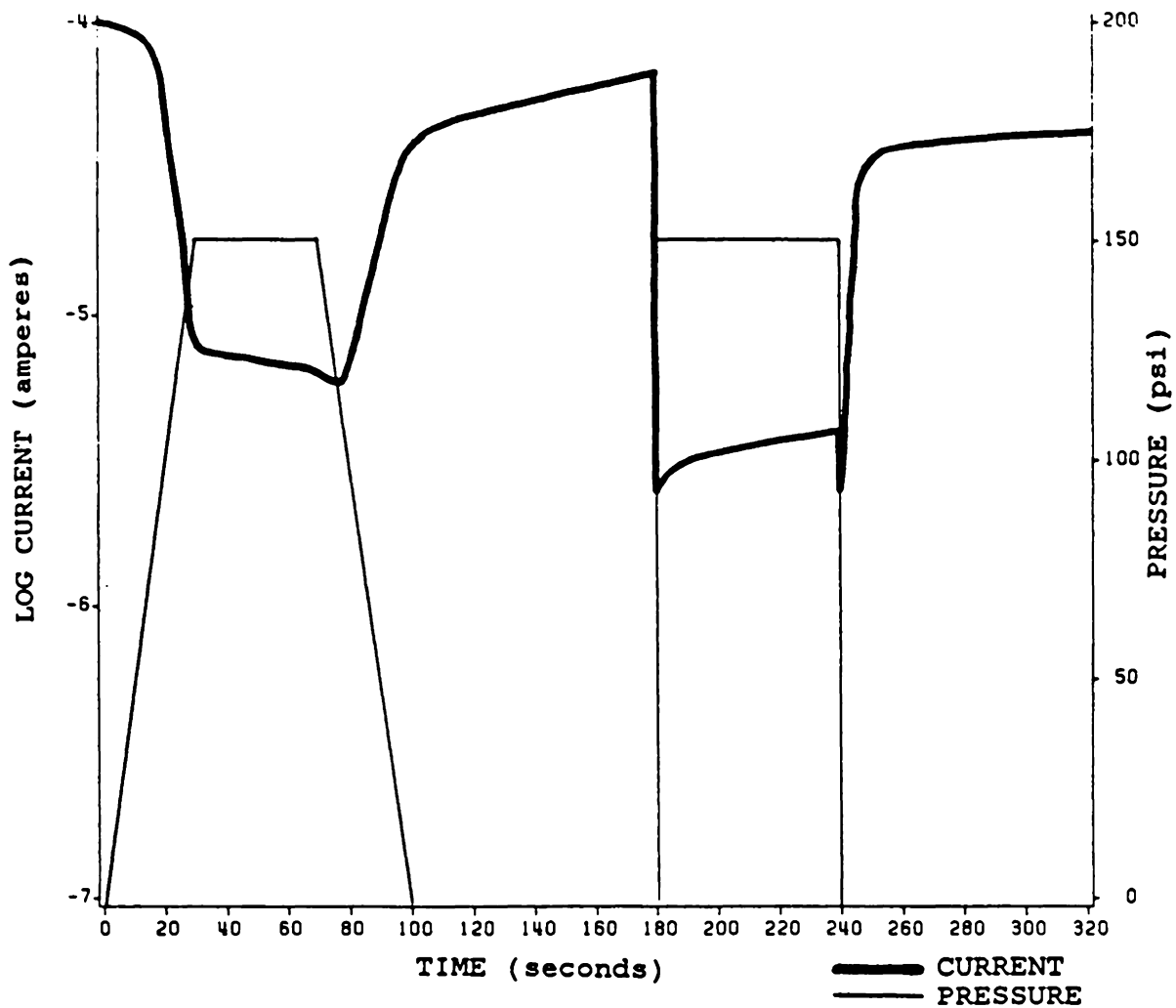


Figure 42. Resistance response to a standardized load profile (NAT1)

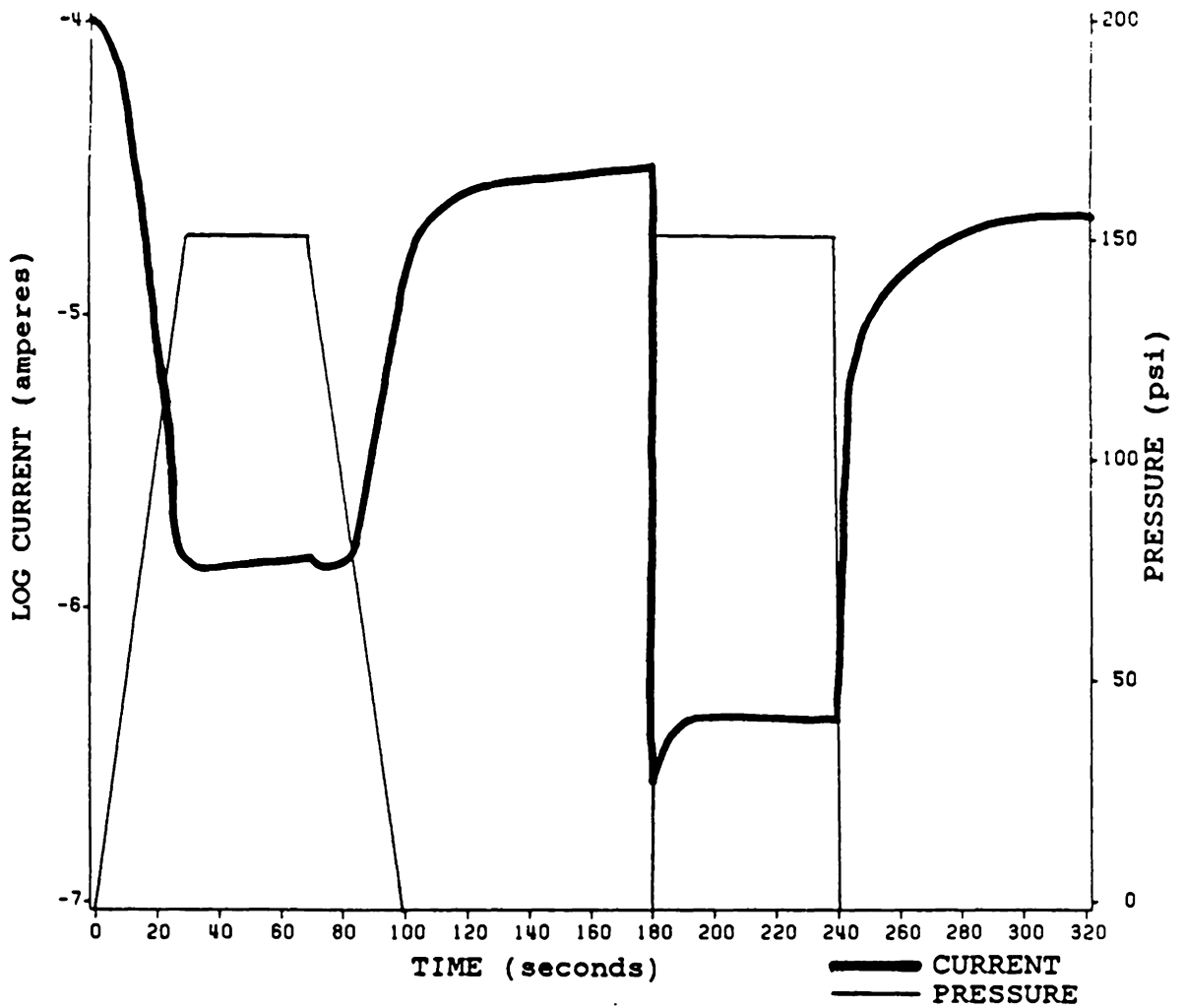


Figure 43. Resistance response to a standardized load profile (NAT16)

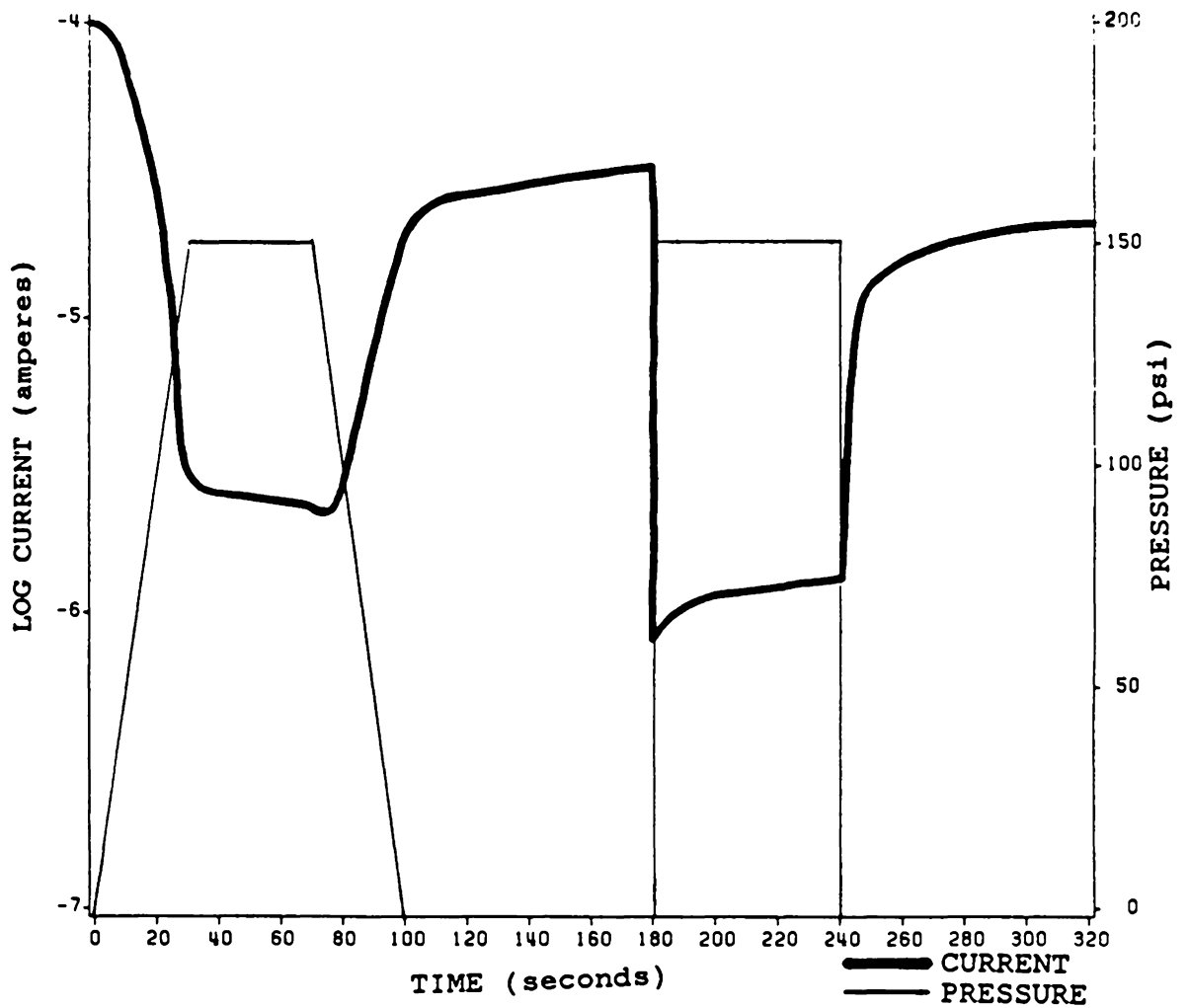


Figure 44. Resistance response to a standardized load profile (NAT41)

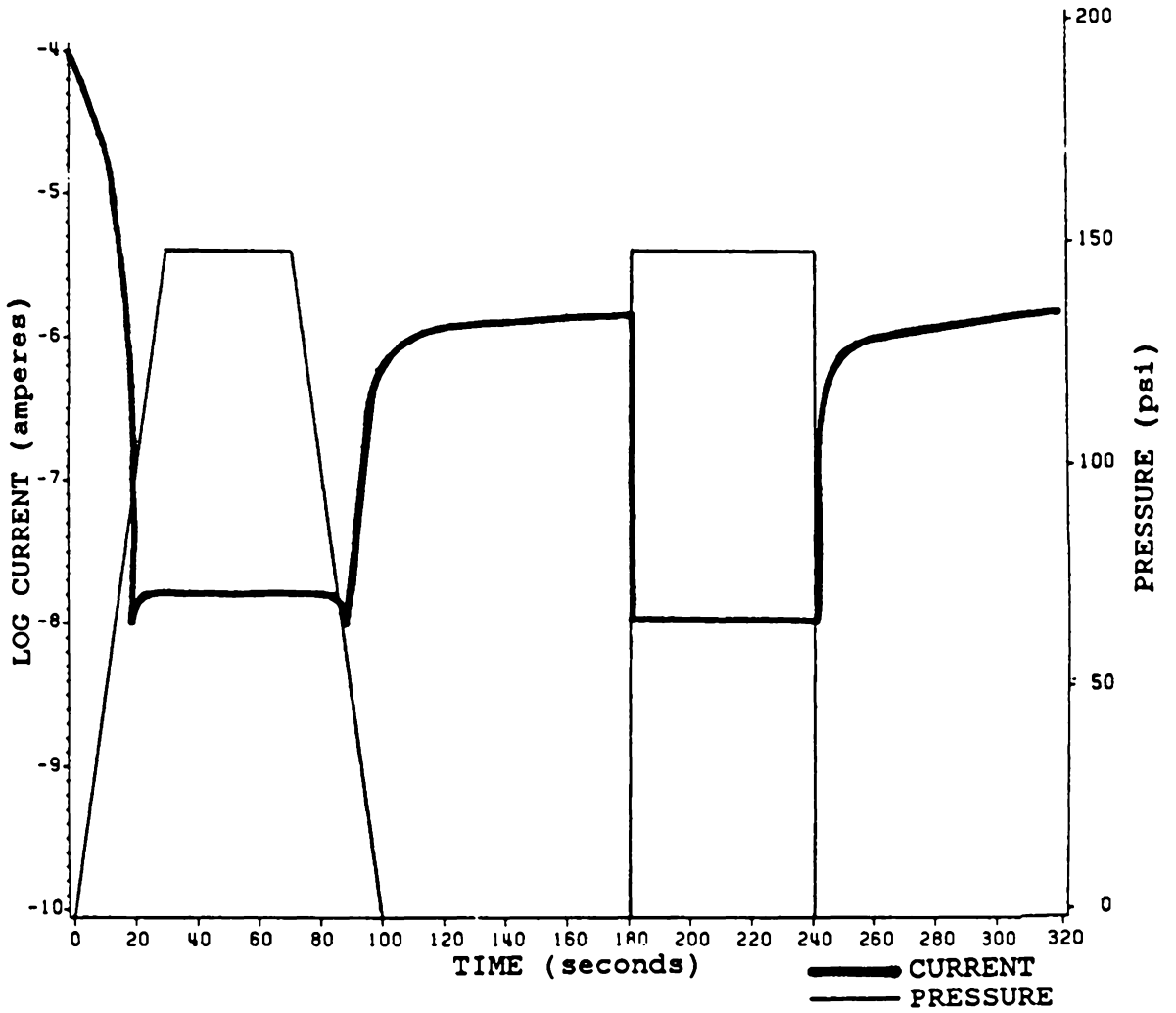


Figure 45. Resistance response to a standardized load profile (NAT44)

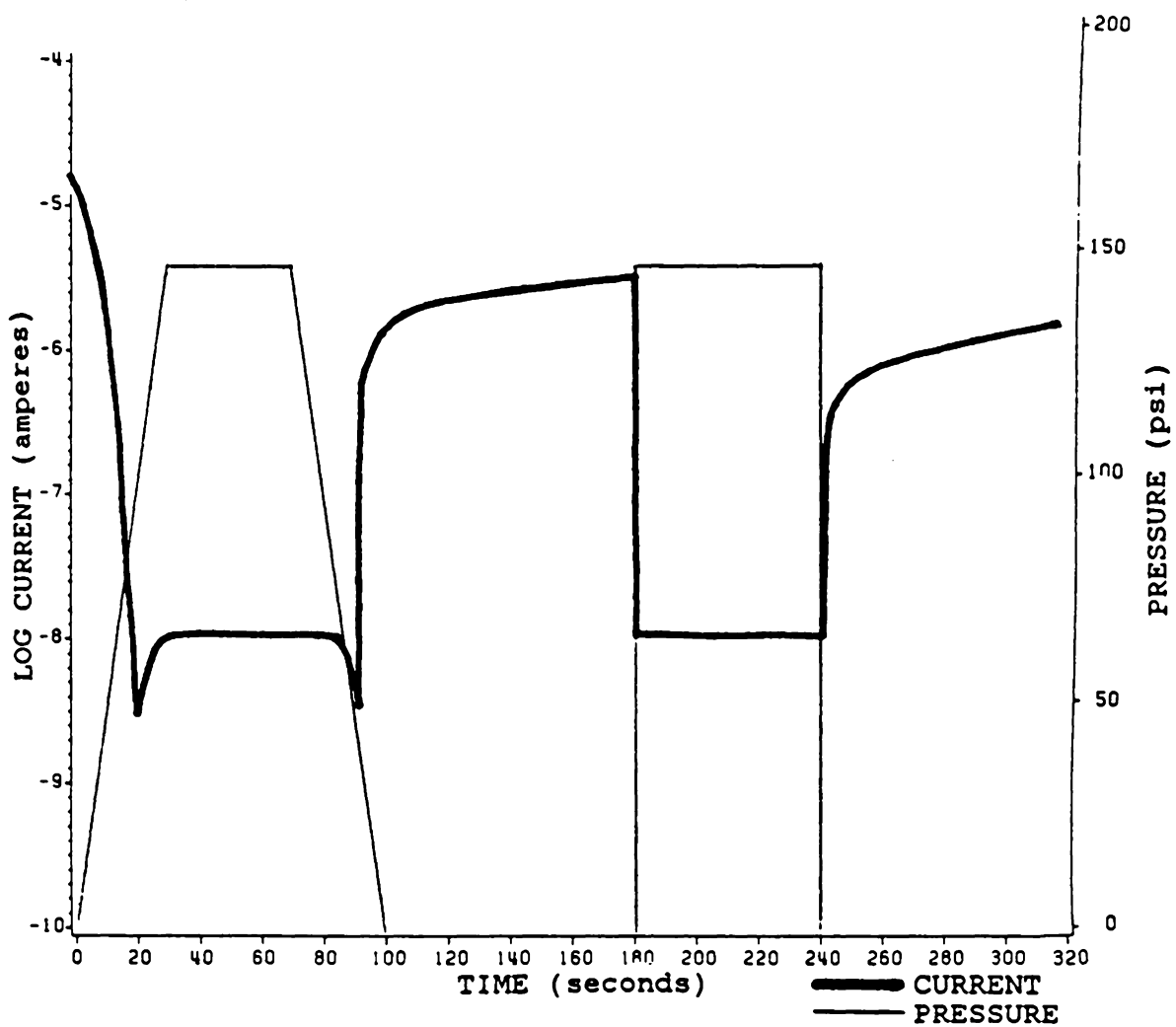


Figure 46. Resistance response to a standardized load profile (NAT43)

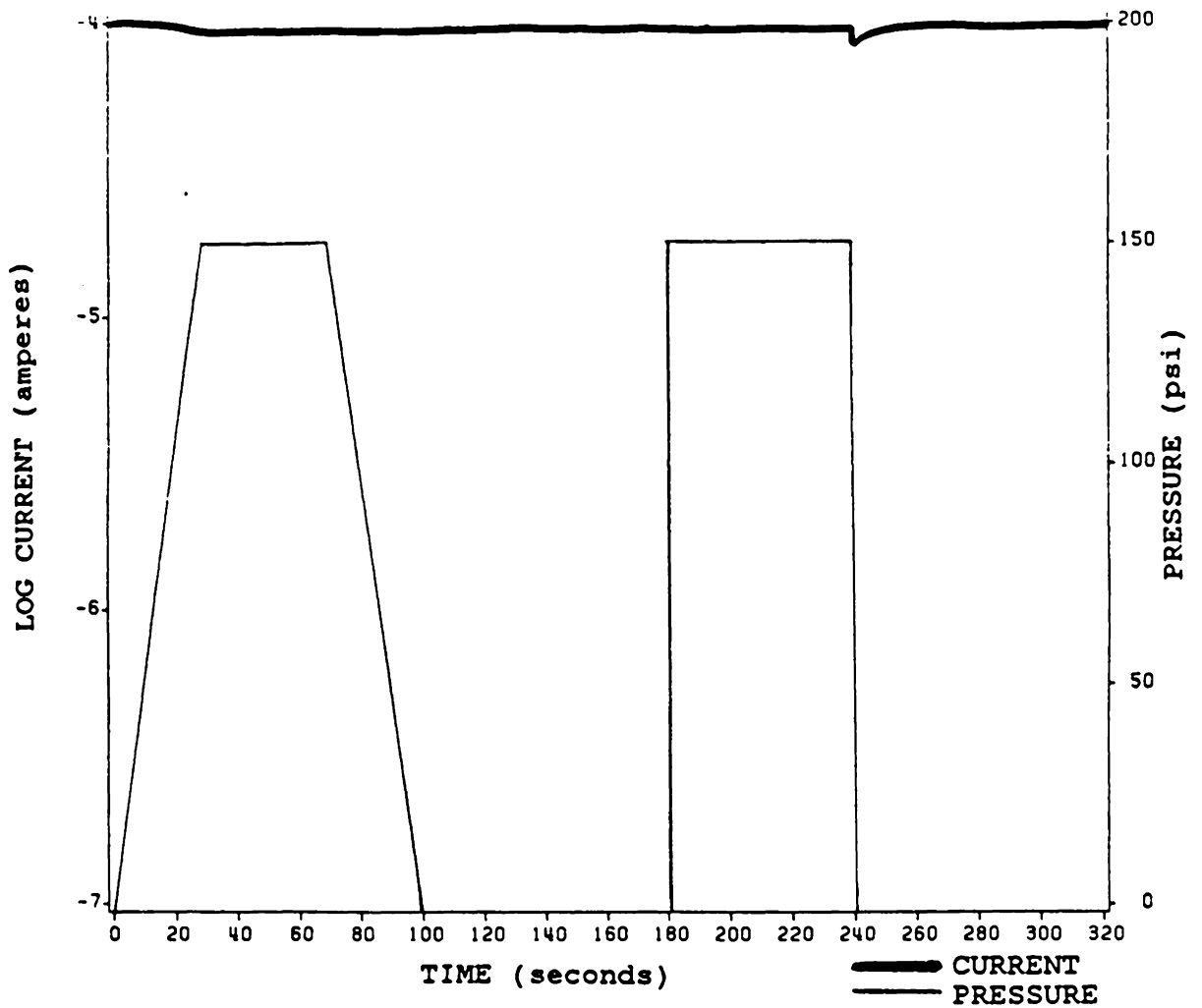


Figure 47. Resistance response to a standardized load profile (NAT57)

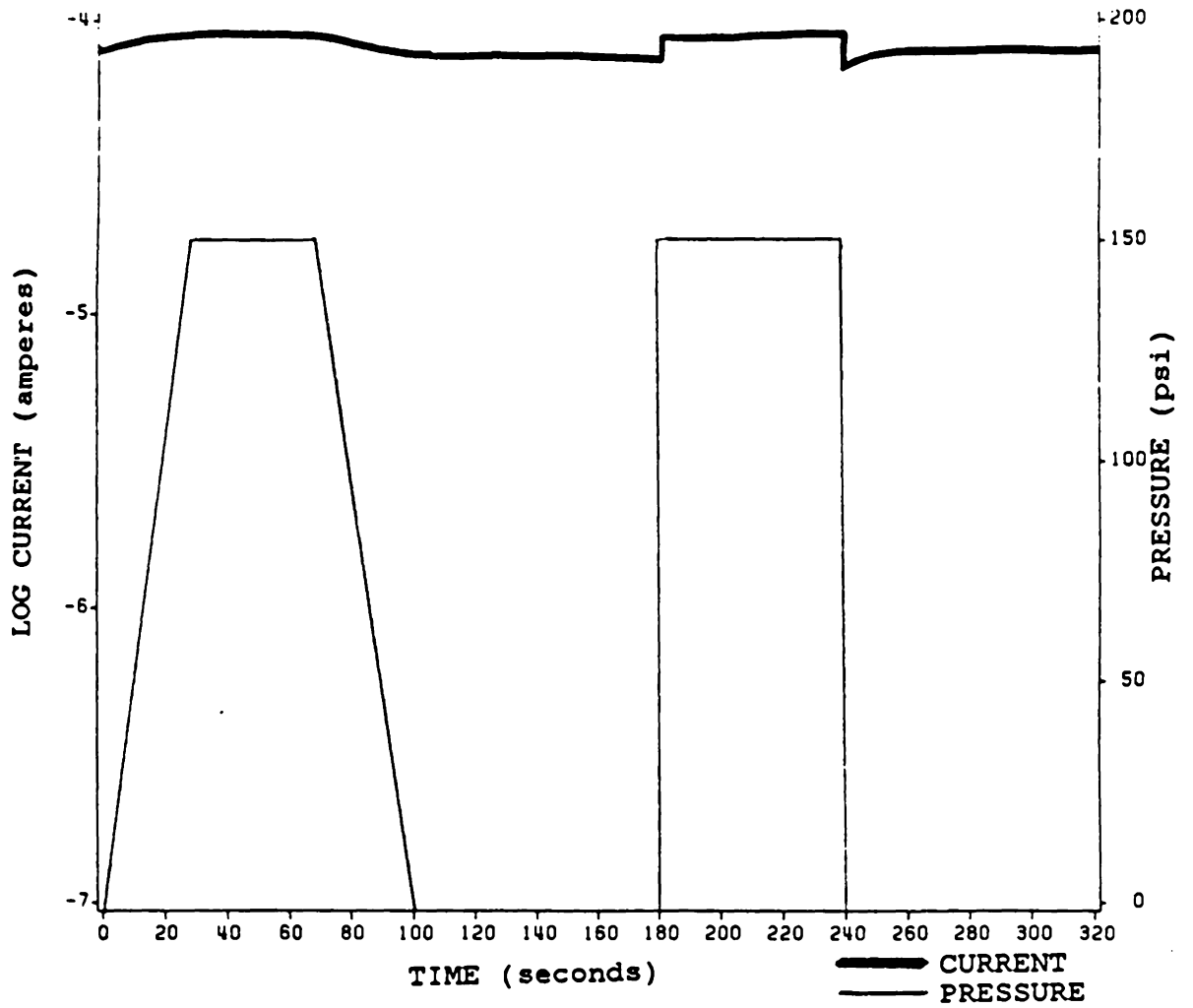


Figure 48. Resistance response to a standardized load profile (NAT60)

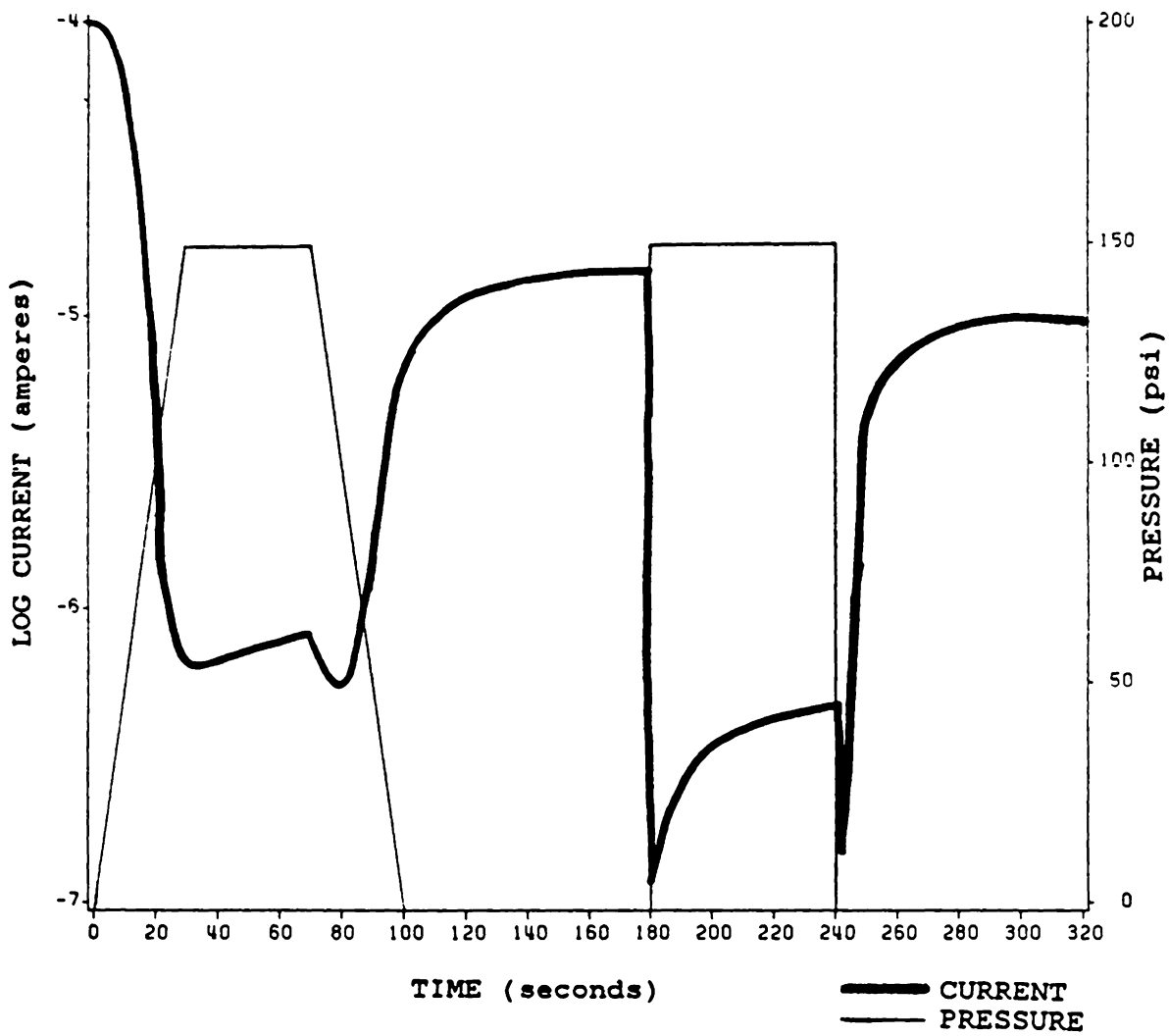


Figure 49. Resistance response to a standardized load profile (NAT61)

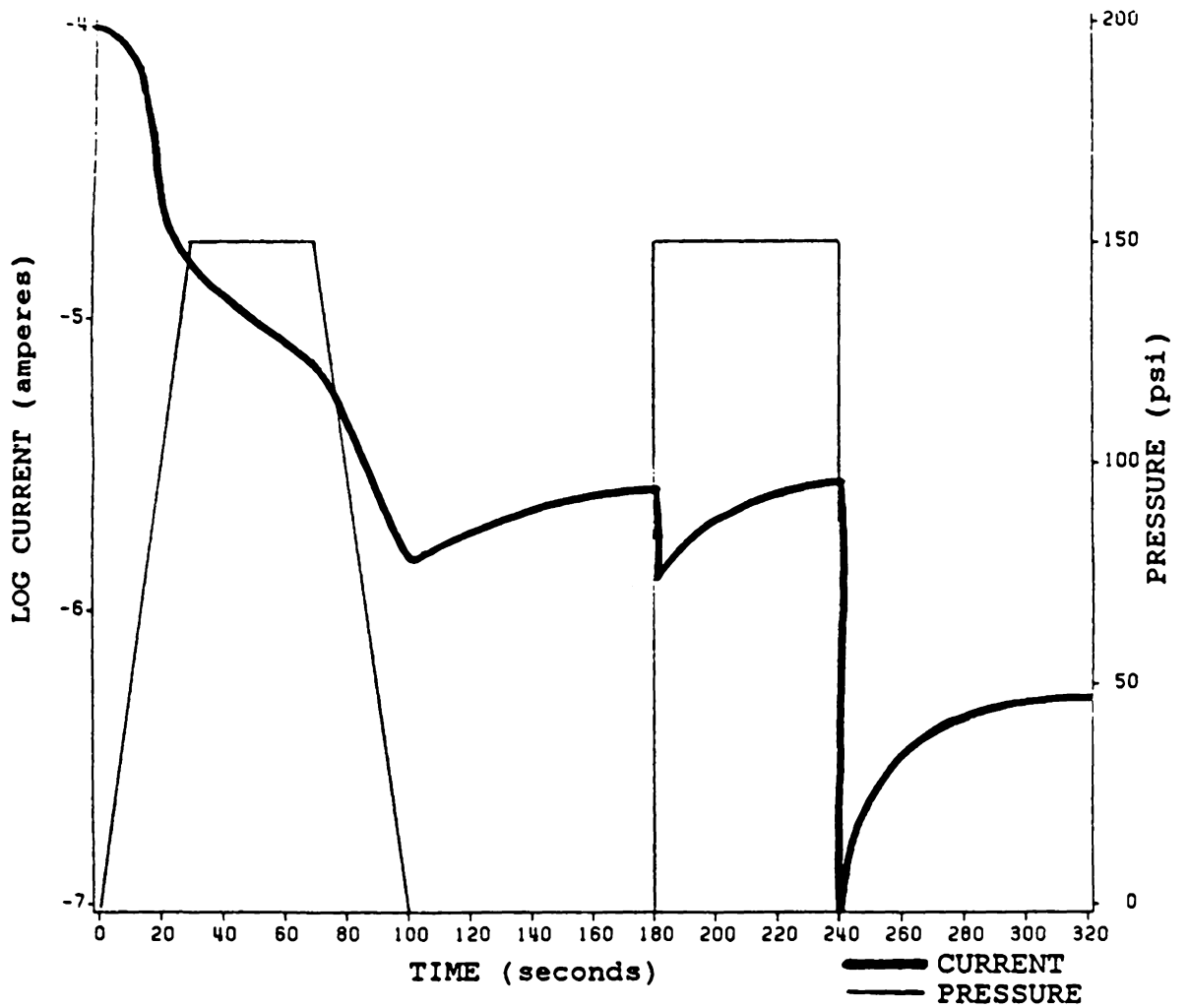


Figure 50. Resistance response to a standardized load profile (NAT22A)

BIBLIOGRAPHY

1. J.A. Manson and L.H. Sperling. Polymer Blends and Composites, chap.10, Plenum Press, N.Y., (1976).
2. J.B. Donnet and A. Voet. Carbon Black, Marcel Dekker, N.Y., (1976).
3. K. Evans. Materials and Design, 5, 43 (1984).
4. R.H. Norman. Conductive Rubbers and Plastics, Elsevier Publ. Co. Ltd., N.Y., (1970).
5. E.K. Sichel. Carbon Black-Polymer Composites, Marcel Dekker Inc., N.Y., (1982).
6. W.S. Stoy and M.D. Garret. Treatise on Coatings, vol. 3, Pigments, part 1, chap. 5, R.R. Meyers and J.S. Long, eds., Marcel Dekker, N.Y., (1975).
7. J. Janzen and G. Kraus., Rubber Chem. Technol. 44, 1287 (1971).
8. A.I. Medalia, E.M. Dannenberg, F.A. Heckman, and G.R. Cotten. Rubber Chem. Technol. 46, 1239 (1973).
9. ASTM Test D1510-76
10. ASTM Test D2414-76
11. A.I. Medalia. J. Colloid Interface Sci. 32, 115 (1970).
12. A. Voet. J. Chem. Phys., 61, 301, (1957).
13. A. Voet. Rubber Chem. Technol., 54, 42 (1981).
14. S. Kirkpatrick. Rev. of Mod. Phys., 45, 574, (1973).
15. F. Bueche. J. Appl. Phys., 43, 4837 (1972).
16. P.J. Flory. Principles of Polymer Chemistry, Cornell University Press, Ithica, N.Y., (1953).
17. F.A. Heckman and D.F. Harling. Rubber Chem. Technol., 39, 1 (1966).

18. W.F. Verhelst, K.G. Wolthuis, A. Voet, P. Ehrburger, and J.B. Donnet. Rubber Chem. Technol., 50, 735 (1977).
19. A. Malliaris and D.T. Turner. J. Appl. Phys., 42, 614 (1971).
20. A.K. Sircar and T.G. Lamond. Rubber Chem. Technol., 51, 126 (1978).
21. L.K.H. Van Beek and B.I.C.F. Van Pul. J. Appl. Polym. Sci., 6, 651 (1962).
22. R.D. Sherman, L.M. Middleman and S.M. Jacobs. Polym. Eng. Sci., 23, 36 (1983).
23. E.O. Forster. IEEE Trans. Power Appar. Syst., PAS-90, 913 (1971).
24. R. Oono. Rubber Chem Technol., 51, 278 (1978).
25. S. Kaufman, W.P. Slichter, and D. Davis. J. Polym. Sci., A-2, 9, 829 (1971).
26. N. Pliskin and L. Tokita. J. Applied Polym. Sci., 16, 473 (1972).
27. D. Bulgin. Trans. Inst. Rubber Ind., 21, 188 (1945).
28. E.M. Dannenberg. Ind. Eng. Chem., 44, 813 (1952).
29. B.B. Boonstra and A.I. Medalia. Rubber Age, 92, 892; 93, 82 (1963); Rubber Chem. Technol., 36, 115 (1963).
30. B.B. Boonstra. Rubber Chem. Technol., 50, 194 (1977).
31. R.J. Cembrola. Rubber Chem. Technol., 56, 233 (1983).
32. B.B. Boonstra, E.M. Dannenberg, and F.A. Heckman. Rubber Chem. Technol., 47, 1082 (1974).
33. L.L. Ban, W.M. Hess, and L.A. Papazian. Rubber Chem. Technol., 47, 859 (1974).
34. J. O'Brien, E. Cashell, G.E. Wardell, and V.J. McBrierty. Macromolecules, 9, 653 (1976); Rubber Chem. Technol., 50, 747 (1977).
35. G.E. Wardell, V.J. McBrierty and V. Marsland. Rubber Chem. Technol., 55, 1095 (1982).

36. E.M. Cashell, J.M.D. Coey, G.E. Wardell, D.C. Douglass, and V.J. McBrierty. *J. Appl. Phys.*, 52, 1542 (1981).
37. R.S. Hindmarch, G.M. Gale, and R.H. Norman. (paper from meeting of the Rubber Division, American Chem. Soc., Houston, Oct 24-28, 1983).
38. W.M. Hess, R.A. Swor and E.J. Micek. *Rubber Chem. Technol.*, 57, 959 (1984).
39. J.L. Thiele and R.E. Cohen. *Rubber Chem. Technol.*, 56, 465 (1983).
40. D.J. Hein and R.W. Wharlow. Research Report No.69, Croyden: RABRM (1952).
41. A. Voet, A. Sircar, and T. Mullens. *Rubber Chem. Technol.*, 42, 874 (1969).
42. P.E. Wack, R.L. Anthony, and E. Guth. *J. Appl. Phys.* 18, 456 (1947).
43. H. Sodolski, A. Szumilo and B. Jachym. *Acta Physica Polonica*, A51, 217 (1979).
44. A.N. Gent. *Rubber Chem. Technol.*, 36, 397, 697 (1963).
45. G.P. Cotten and B.B. Boonstra. *J. Appl. Polym. Sci.*, 9, 3395 (1965).
46. A. Voet, A.K. Sircar and F.R. Cook. *Rubber Chem. Technol.*, 44, 175, 185 (1971).
47. G.M. Bartenev. chap. 10 in Relaxation Phenomena in Polymers, G.M. Bartenev and Yu.V. Zelenev editors, Wiley and Sons, N.Y. (1974).
48. A.R. Payne. chap. 3 in Reinforcement of Elastomers, G. Kraus editor, Wiley Interscience (1965).
49. A.R. Payne. *J. Appl. Polym. Sci.*, 3, 127 (1960).
50. A.R. Payne. *J. Appl. Polym. Sci.*, 6, 57, 368 (1962).
51. C.I. MacKenzie and J. Scanlan. *Polymer*, 25, 559 (1984).
52. U. Meier, J. Kuster, and J.F. Mandell. *Rubber Chem. Technol.*, 57, 254 (1984).
53. G. Kraus and J.T. Gruver. *J. Polym. Sci.*, 8, 571 (1970).

54. D.R. Corson and P. Lorrain. Introduction to Electromagnetic Fields and Waves, chap.3, W.H. Freeman and Co., San Francisco (1962).
55. R. Plonsey and R.E. Collin. Principles and Applications of Electromagnetic Fields, chap.3, McGraw Hill Book Co., N.Y. (1961).
56. L. Solymar and D. Walsh. Lectures on the Electrical Properties of Materials, second edition, Oxford University Press, (1982).
57. P. Debye. Polar Molecules Chemical Catalog, New York, (1929).
58. H. Frohlich. Theory of Dielectrics Clarendon, Oxford, (1949).
59. A.I. Lukomskaya and B.A. Dogadkin. Kolloid Zhurnal, 22, 576 (1960).
60. Laboratory for Insulation Research, MIT in Dielectric Materials and Applications, A.R. Von Hippel, editor, John Wiley and Sons Inc., New York (1954).
61. O. Sandberg and G. Backstrom. J. Appl. Phys., 50, 4720 (1979).
62. Dept. of the Army. Elastomer Tank Track Pad Progress Report, U.S. Army Belvoir R & D Center, Fort Belvoir, Virginia 22060 (1984).
63. J.V. Schmitz. Testing of Polymers, Volume I, Interscience Publishers (1978).
64. R.O. Babbit, editor. The Vanderbilt Rubber Handbook, R.T. Vanderbilt Co. Inc., Norwalk, CT. (1978).
65. J. Reboul. J. Appl. Phys., 46, 2961 (1975).
66. J. Reboul and G. Moussalli. Intern. J. Polymeric Mater., 5, 133 (1976).
67. D. Hands. Rubber Chem. Technol., 53, 80 (1980).

**The vita has been removed from
the scanned document**